



Fakultät für Physik

Institut für Theorie der Kondensierten Materie

---

# **Quantentransport in Spindichtesystemen mit dem Memory-Matrix-Formalismus**

Masterthesis

von

Martin Lietz

27. Mai 2017 bis 27. Mai 2018

Referent: Prof. Dr. Jörg Schmalian  
Korreferent: Prof. Dr. Alexander Shnirman



Ich erkläre hiermit, dass die Arbeit selbstständig angefertigt, alle benutzten Quellen und Hilfsmittel vollständig und genau angegeben und alles kenntlich gemacht wurde, das aus Arbeiten anderer unverändert oder mit Abänderungen entnommen ist.

Karlsruhe, den 27. Mai 2018

.....  
(**Martin Lietz**)



# Acknowledgment



# Contents

<b>1</b>	<b>Introduction</b>	<b>1</b>
<b>2</b>	<b>Infinite Conductivity in Translation Invariant Systems</b>	<b>3</b>
2.1	An Overview over the Memory-Matrix-Formalism . . . . .	3
2.2	Electrical Conductivity in a Momentum Conserving System . . . . .	5
<b>3</b>	<b>Spin-Fermion-Model</b>	<b>9</b>
3.1	The Spin-Fermion-Model at the Onset of the Antiferromagnetic Quantum Phase Transition . . . . .	9
3.2	Momentum Conservation in the Spin-Fermion-Model and the Consequence of Umklapp Scattering . . . . .	14
<b>4</b>	<b>The Static Conductivity in the Spin Fermion Model including Umklapp Scattering</b>	<b>17</b>
<b>5</b>	<b>Memory-Matrix-Formalism</b>	<b>25</b>
5.1	Kubo relaxation function . . . . .	25
5.1.1	Spectral representation . . . . .	27
5.2	Deviation of the Memory-Matrix-Formalism . . . . .	28
5.2.1	Time Reversal Symmetry . . . . .	34
5.3	The Formula of the Static Conductivity . . . . .	37
<b>6</b>	<b>Conclusion</b>	<b>41</b>
<b>A</b>	<b>Computation of the Damped Spin Density Propagator</b>	<b>43</b>
A.1	Computation of the Free Propagator . . . . .	43
A.2	Consideration of Damping in the Spin Density Propagator . . . . .	44
A.3	Transformation into Matsubara Frequency Space . . . . .	50
<b>B</b>	<b>Time Derivative of momentum <math>\mathbf{P}</math> and current <math>\mathbf{J}</math></b>	<b>53</b>
<b>C</b>	<b>Computation of the Static Susceptibility</b>	<b>59</b>
<b>D</b>	<b>Finite Conductivity because of Breaking the Translation Symmetry via Umklapp Scattering</b>	<b>63</b>
<b>E</b>	<b>Properties of the Kubo Relaxation Function</b>	<b>69</b>





# 1 Introduction

The electrical conductivity or resistance is a fundamental characteristic and an accessible observable of metals. The response of electrons as a consequence of an external applied electrical field is measured by the conductivity and its magnitude is finite due to internal processes. A first physical explanation describing this circumstances was published by Drude [Dru00] in the year 1900. He supposed the electrons to be free particles moving around in the metal. As a consequence of scattering, the electrons are assumed to possess a finite relaxation time  $\tau$ . This characteristic variable denotes the passing time between to scattering events. At low temperatures, the electrical conductivity is determined by scattering between electrons and impurities. Drude's theory demonstrates the fact, that non-conservation of momentum due to relaxation and a finite electrical conductivity are directly associated. The results of this phenomenological theory are exactly confirmed by using the technique of quantum field theory without considering quantum correction to describe the electrons [BF10]. Landau's Fermi liquid theory is the well proven quantum mechanical description for metals. Electron-electron interaction and the consideration of umklapp scattering generates a quadratic temperature dependence of the resistance  $\rho(T) = \rho_0 + A \cdot T^2$ , where  $\rho_0$  is the saturation resistance from impurity scattering at low temperatures [Bab37; PYM12]. Quantum mechanical corrections, like weak localization [Alt+80] and the Kondo effect [Kon64], modify the temperature dependence. The latter describes a logarithmical increase of the resistance at small temperatures  $T < T_K \approx 1 - 10$  K [KG01] due to electron scattering with localized magnetic impurities. Landau's Fermi liquid theory can be described these modifications in the temperature dependence of the resistance. In contrast, alloys, like  $\text{CeCu}_{6-x}\text{Au}_x$  and  $\text{CeCu}_{6-x}\text{Ag}_x$  at a concentration of  $x = 0.1$  and  $x = 0.2$ , respectively, exhibit a non-Fermi liquid behaviour, that is characterized in a linear temperature dependence of the resistance  $\rho(T) = \rho_0 + A \cdot T$  [Löh+07]. The origin of this strange and unexpected behaviour is an antiferromagnetic quantum phase transition of second order. In comparison to normal phase transition, quantum phase transitions are governed by quantum fluctuations instead of thermal fluctuation. The spin-fermion-model describes those metals at the vicinity of an quantum critical point.



## 2 Infinite Conductivity in Translation Invariant Systems

Ever since Drude published his theory about the electrical conductivity in metals [Dru00] at the beginning of the last century, it is well known that non-conservation of electron momentum in a system is required for finite electrical conductivity. In Drude's model, the electrons possess a mean scattering time  $\tau_{el}$  representing the mean time between two scattering events of an electron and a lattice atom. At each scattering event, the electrons transfer momentum to the lattice atoms, which is the reason electron momentum is not a conserved quantity. In the case of conserved momentum, if an electrical field is exemplarily applied, it accelerates electrons up to an infinite velocity, causing infinite conductivity.

In the following section, a momentum conserving system is considered and the electrical conductivity is computed using the memory-matrix-formalism, where an infinite conductivity is expected. Beforehand, a short overview over the memory-matrix-formalism is given, followed by detailed and explicit deviations in chapter 5.

### 2.1 An Overview over the Memory-Matrix-Formalism

Let us assume a physical dynamical variable  $A(t)$  in an arbitrary system and an arbitrary perturbation too. Our interest is now the time evolution of  $A(t)$  depending on the perturbation. Completely general, a physical dynamical variable can be splitted into two parts, a secular one and a non-secular one, which is shown in [Mor65]. The latter represent processes like fluctuations or initial transient processes, which have in common a short lifetime comparing to the secular processes. The dynamic and time evolution of  $A(t)$  is therefore dominated by secular processes.

This separation enables a simple but clever geometrical interpretation, where dynamical variables are considered to be vectors in a vector space. The direction of the variable  $A(t)$  is denoted as the A-axis, considering an unperturbed system in equilibrium. Switching on a perturbation, the system is moved out of the equilibrium state and as a consequence the direction of  $A(t)$  is modified. The projection of  $A(t)$  onto the A-axis is identified with the secular part, while the non-secular part is the part perpendicular to the projection.

First of all, the mathematical framework for this vector space has to be established. In quantum mechanics, the Liouville space, also called as operator space, is the respective vector space of the memory-matrix-formalism. As indicated by the name *operator space*, the vectors of the Liouville space are operators, all of which being Hermitian. The basis of the Liouville space is signified as  $\{|A_i\rangle\}$ , where  $i = 1, 2, 3, \dots, n$ , and the

corresponding dual space basis is denoted as  $\{|A_i\rangle\}$ . To complete the definition of any vector space, a scalar product is required. The following one is chosen:

$$(A_i(t)|A_j(t')) = \frac{1}{\beta} \int_0^\beta d\lambda \left\langle A_i^\dagger(t) A_j(t' + i\lambda) \right\rangle. \quad (2.1)$$

The normal time evolution  $A_i(t) = e^{iHt/\hbar} A_i(0) e^{-iHt/\hbar}$  of an operator should be valid so that  $A_i(i\lambda) = e^{-\lambda H} A_i(0) e^{\lambda H}$  can be used. If secular processes are neglected, the choice of the scalar product is determined under the aspect that as a consequence the time evolution of  $A(t)$  given the most probably path, see [Mor65]. In quantum mechanics, the dynamic of an operator is ususally described by the Heisenberg equation of motion, which is transformed using the dyad product into the Liouville space

$$|\dot{A}_i(t)\rangle = \frac{i}{\hbar} [H, A_i(t)] = iL|A_i(t)\rangle. \quad (2.2)$$

Here the Hermitian Liouville operator,  $L = \hbar^{-1}[H, \bullet]$ , is introduced, which is defined by his action onto an arbitrary operator. The formal solution of this equation is given by  $|A_i(t)\rangle = \exp(itL) \cdot |A_i(0)\rangle$ , where the time evolution of an operator is therefore given by the Liouville operator. For our approach a further operator is required in the Liouville space, namely the projection operator. A set of arbitrary operators  $\{C_i\}$  is therefore defined. The choice of them is different for each observed problem and unimportant at the moment. The definition of the projection operator in Liouville space follows directly from the projection operator defined in the commonly used Hilbert space in quantum mechanics.

$$P = \sum_{i,j} \frac{|C_i(0)\rangle \langle C_j(0)|}{(C_i(0)|C_j(0))} \quad (2.3)$$

The projection operator acting on some vector in Liouville space yields the projection onto the subspace spanned by the operator  $C_i$ . Thus, the operator  $Q = 1 - P$  yields the corresponding part projected out of the subspace. Furthermore, the projection operator is Hermitian and fullfills the two properties  $P^2 = P$  and  $PQ = QP = 0$ . This completes the required mathematical basis of the memory-matrix formalism.

Correlation functions are the natural approach to describe the reaction of a dynamic variable on a perturbation. In quantum mechanics, the correlation function is defined in Kubo's linear response theory as an integral over an expectation value of two operators, one of them being the investigated operator, and the other one being the coupling operator from the perturbation Hamiltonian. In the Liouville space, the correlation function is defined as

$$c_{ij}(t) := (A_i(t)|A_j(0)) = \frac{1}{\beta} \int_0^\beta d\lambda \left\langle A_i^\dagger(t) A_j(i\lambda\hbar) \right\rangle, \quad (2.4)$$

## 2.2 Electrical Conductivity in a Momentum Conserving System

using the definition of the scalar product (2.1) in the second step. Expressing the time evolution of  $A_i(t)$  with the Liouville operator, using the Laplace transformation and a few conversions yields an algebraic matrix equation of the correlation function, which has the form

$$\sum_l \left[ \omega \delta_{il} - \Omega_{il} + i \Sigma_{il}(\omega) \right] C_{lj}(\omega) = \frac{i}{\beta} \chi_{ij}(0), \quad (2.5)$$

where the abbreviations

$$\Omega_{il} := i\beta \sum_k (\dot{A}_i | C_k) \chi_{kl}^{-1}(0) \quad \text{and} \quad \Sigma_{il}(\omega) := i\beta \sum_k (\dot{A}_i | Q \frac{1}{\omega - QLQ} Q | \dot{C}_k) \chi_{kl}^{-1}(0) \quad (2.6)$$

are introduced. Both sums over  $l$  and  $k$  run over the set of operators, defined by the projection operator. Similarly, the indices  $i$  and  $j$  have to be chosen from this set of operators so that (2.5) yields  $n^2$  equations, if  $n$  is the number of operators in the set. Both abbreviations can be combined to a function  $M_{il}(\omega) := \Sigma_{il}(\omega) + i\Omega_{il}$ , called the memory function. In this function,  $\Sigma_{il}(\omega)$  takes the role of the quantum mechanical self energy, while  $\Omega_{il}$  represents dissipative effects.  $\Omega_{il}$  vanishes under to conditions. The model Hamiltonian has to be invariant under time reversal symmetry. Furthermore, both operators,  $A_i$  and  $C_k$ , have to be the same sign with respect to time reversal symmetry. This assertion is proven in great detail in 5.2.1. It follows that the memory function is solely determined by  $\Sigma_{il}(\omega)$ .

The structure of  $\Sigma_{il}(\omega)$  resembles the one of the Laplace transformed correlation function, comparing equation (5.34), with two differences. The expectation value is performed with respect to the operators like  $Q|\dot{A}_i\rangle$  instead of  $|A_i\rangle$ , while only the reduced Liouville operator  $QLQ$  is considered. The latter projects at the part of the full Liouville operator, which causes the intrinsic fluctuations of the operator  $A$ . In other words, the operator  $QLQ$  describes the internal dynamics of all other degrees of freedom of the system, called the *bath*, excluded  $A$ . The coupling to the bath is characterized by the vector  $Q|\dot{A}_i\rangle$  and is clearly changing the dynamic behaviour of  $A$ .

## 2.2 Electrical Conductivity in a Momentum Conserving System

In the following section, the electrical conductivity is computed for a system, where momentum is conserved, using the memory-matrix-formalism. An infinite conductivity is expected due to the fact that electrons do not transfer any momentum to other degrees of freedom. Besides conserving momentum, the observed system has to satisfy some additional requirements. Firstly, the current has to be an unconserved quantity. Furthermore, the scalar product  $(J|P)$  of current and momentum has to be non-zero. In other words, both quantities possess a finite overlap. These two quantities should also generate the subspace into the projection operator projects. The sum in (2.3)

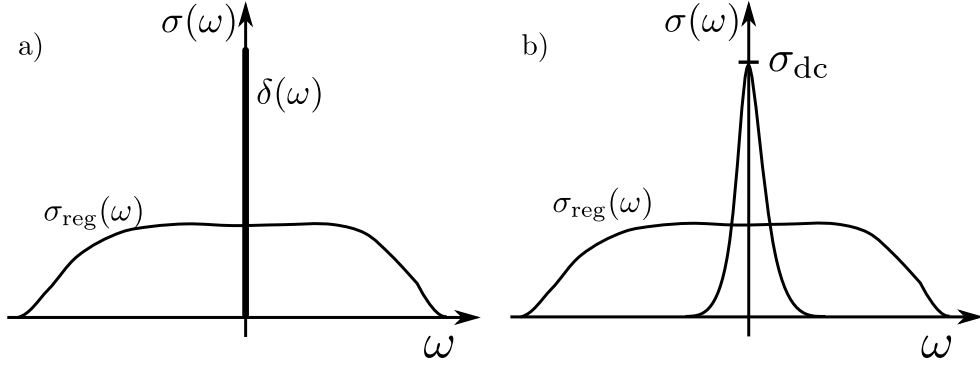


Figure 2.1: Figure a) and b) shown the static electrical conductivity in a unpertubated and pertubated system, respectively. In a system with unbroken translation symmetry, the relaxation of momentum is impossible to other degrees of freedom. As a consequence, the static conductivity is infinite. This is illustrated in a). Switching on a perturbation as umklapp scattering, the translation symmetry is broken. The static conductivity becomes finite due to the relaxation of momentum to other degrees of freedom. In both figures, the regular conductivity, caused by fluctuation e. g., is denoted as  $\sigma_{\text{dc}}$ .

summerizes over all operators  $C_i$ , where the choice has now to be done with respect to the electrical conductivity. As electrical conductivity is determined by momentum and current, these are chosen as operators. The last requirement is for the Hamiltonian to be invariant under time reversal symmetry, which is our last requirement.

Nevertheless, one remark has to be made for computing the conductivity. Due to the fact that the Hamiltonian is invariant under time reversal symmetry and the subspace is generated by  $J$  and  $P$ , which have same signature under time reversal symmetry, no dissipative effects exist. The quantity  $\Omega$ , defined in (2.6), is therefore zero.

In the strictly general sense, the electrical conductivity is given by the current-current correlation function  $\mathcal{C}_{JJ}(\omega)$  (see [Czy17]). The static case is obtained by taking the small frequency limit,  $\omega \rightarrow 0$ , of the conductivity.

$$\sigma_{\text{dc}} = \lim_{\omega \rightarrow 0} \sigma(\omega) = \lim_{\omega \rightarrow 0} \beta \mathcal{C}_{JJ}(\omega) \quad (2.7)$$

The current-current correlation function is given by equation (2.5), which is in the case of the J-P subspace a  $2 \times 2$  matrix equation. The quantity  $\Sigma$  is simplified by two aspects. Firstly, the momentum is conserved, which means the time derivative of  $P$  is zero and therefore all expectation values are trivially zero where  $\dot{P}$  is a taken vector. The remaining expectation values of  $\Sigma$  contains only the current  $J$ , but these ones are vanishing as well. The operator  $QLQ$  describes the intrinsic fluctuation of  $|J\rangle$ , which are assumed to be zero. Furthermore, the operator  $Q$  acting on  $|J\rangle$  yields the coupling to these intrinsic fluctuation and, leading to  $Q|J\rangle = 0$ . The obtained matrix equation has a very simple form and the current-current correlation function can be directly

## 2.2 Electrical Conductivity in a Momentum Conserving System

read out as

$$\mathcal{C}_{JJ}(z) = \frac{i}{\omega} \beta^{-1} \chi_{JJ}(\omega = 0) = \frac{i}{\omega} \mathcal{C}_{JJ}(t = 0), \quad (2.8)$$

where relation (5.31) is being used. The correlation function at time  $t = 0$  is given by the scalar product  $(J(0)|J(0))$  (see (2.4)). Due to the fact that current and momentum are two closely connected quantities, this is also valid for their correlation functions. For this reason, the current-current correlation function is expressed with respect to the momentum-momentum correlation function.

The vector operator  $|J(0)\rangle$  is separated into two pieces, one parallel and one perpendicular part, which are labeled as  $|J_{\parallel}\rangle$  and  $|J_{\perp}\rangle$ , respectively. As discussed above, every variable generally consists of a secular and non-secular part, which does not mean that both parts need to exist in the observing model. The non-secular part is represented by the perpendicular component of  $|J\rangle$ . In the experiment, these processes are observed as a constant slowly fluctuating background, known as noise. The secular part is represented by the parallel component of  $|J\rangle$ , which is responsible for the electrical conductivity and is visible as a peak in the measurement, depicted in figure 2.1.

Drude's theory of conductivity yields a direct proportionality between  $J$  and  $P$  (see for example [GM14]). Since momentum is conserved and current is unconserved, in the investigated system this proportionality can't be valid. Nevertheless, both quantities possess a finite overlap, which means that a part of the current is conserved and therefore parallel to the momentum. This part is the parallel component of  $J$  and given by the projection von  $|J\rangle$  onto  $|P\rangle$ .

$$|J_{\parallel}\rangle = \mathcal{P}|J\rangle = \frac{|P\rangle\langle P|}{\langle P|P\rangle} |J\rangle = \frac{\chi_{PJ}}{\chi_{PP}} |P\rangle \quad (2.9)$$

Separating both current operator in  $(J(0)|J(0))$  yields four new correlation functions, where the mixed ones are zero, since  $|J_{\parallel}\rangle$  and  $|J_{\perp}\rangle$  are perpendicular to each other by construction. For the operators in the parallel correlation function,  $(J_{\parallel}(0)|J_{\parallel}(0))$  equation (2.9) is used. In this equation, the correlation function of the parallel components is represented as a momentum-momentum correlation function. Inserting the obtained expression for the current-current correlation function in (2.8) the conductivity is given by

$$\sigma(\omega) = \frac{|\chi_{PJ}|^2}{|\chi_{PP}|} \frac{i}{\omega} + \sigma_{\text{reg}}(\omega), \quad (2.10)$$

where the momentum-momentum correlation function is expressed as static susceptibility (see (5.31)), and the regular conductivity  $\sigma_{\text{reg}}(\omega) = i(\omega\beta)^{-1}(J_{\perp}|J_{\perp})$  is introduced, which represents the noise (see figure 2.1).

In the above equation the quantity  $\omega$  is a complex number. Since  $\omega$  has to be a real number for a physical interpretation, it is transformed on the real axis using analytical continuation. The conductivity is then given by

$$\sigma(\omega) = \frac{|\chi_{PJ}|^2}{|\chi_{PP}|} \left( \text{P.V.} \frac{i}{\omega} + \pi \delta(\omega) \right) + \sigma_{\text{reg}}(\omega) \quad (2.11)$$

## 2 Infinite Conductivity in Translation Invariant Systems

where  $\frac{1}{\omega+i\eta} = \text{P.V.} \frac{1}{\omega} - i\pi\delta(\omega)$  is used and P.V. symbolizes the prinzipel value. Taking now the small frequency limit  $\omega \rightarrow 0$  the  $\delta$ -distribution is the dominant term and the static conductivity becomes infinite, which is the exactly expected result. The static electrical conductivity is infinite in a momentum conserving system, thus conductivity is getting finite if the momentum is not a conserved quantity any more. The respective underlying symmetry is translation symmetry. For breaking this symmerty, many possibilities are available, but in the following computation only one of them, namely umklapp scattering, is considered.

In the next chapter, the observed spin-fermion model is introduced. Beforehand, quantum phase transitions are reviewed. The conservation of momentum and non-conservation of current is further constituted. Finally, umklapp scattering is introduced for breaking translation symmetry and unconserving momentum.



## 3 Spin-Fermion-Model

The spin-fermion-model, as introduced in [ACS03], for a metal exhibiting an antiferromagnetic quantum phase transition is presented in following chapter. Bosonic spin fluctuations arise in the vicinity of the quantum critical point due to fermionic particle-hole-excitations, enabling an attractive interaction between electrons. This chapter does not intend to give a detailed mathematical and microscopic derivation of the spin-fermion-model. It rather provides a qualitative description to justified the form of the model. A short overview over quantum phase transitions is previously established, as suggested in [Sac11]. In particular focus lies on the arising spin fluctuations and why these fluctuations carry large momentum  $\mathbf{Q}$ . The damped spin density propagator and its periodicity is finally introduced. The basic concepts of the hot-spot theory are additionally presented. The proof of momentum and current conservation is shown for cases: excluded and included umklapp scattering.

### 3.1 The Spin-Fermion-Model at the Onset of the Antiferromagnetic Quantum Phase Transition

An antiferromagnetic phase transition is observed in many metals at a characteristic temperature  $T_N$ , the so-called Néel-temperature. This temperature can be changed by tuning a certain parameter like the pressure in the system or doping in the material. The spins of lattice atoms are generally randomly ordered at  $T > T_N$ . When temperature comes below  $T_N$ , spins are being ordered due to thermal fluctuations in such a way that nearest neighbours always point to the opposite directions. A schematic and simplified phase diagram is depicted in figure 3.1. The magnetic phase line ends at a certain value  $g_c$  of the tuning parameter by decreasing the temperature up to  $T = 0$ . This point is called quantum critical point due to the fact that the phase transition is originated by quantum fluctuation instead of thermal fluctuations.

A short description of quantum phase transitions is given and is continued by a qualitative derivation of the spin-fermion-model. This overview is needed to understand the analytical discussion of our computation in chapter 4. The origin of phase transitions is always level crossing between the ground and an excited state. A band gap  $\Delta$  arises due to the fact that level crossing is forbidden. This band gap is therefore a characteristic energy scale for the quantum phase transition. The characteristic energy scale  $\Delta$  is proportional to the tuning parameter

$$\Delta \sim J|g - g_c|^{z\nu}, \quad (3.1)$$

considering only phase transitions of second order. Here,  $z\nu$  is a critical exponent and  $J$  an energy scale of a microscopic coupling [Sac11]. A characteristic length scale  $\xi$

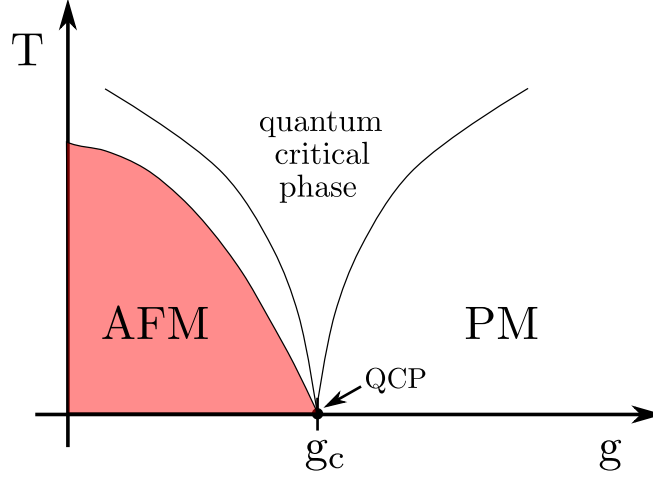


Figure 3.1: A schematic and simplified phase diagram is shown for metals transition from a paramagnetic (PM) into an antiferrmagnetic (AFM) phase depending on a tuning parameter  $g$ . The phase line of the AFM phase ends in a quantum critical point (QCP) at  $g = g_c$ , decreasing temperature down to  $T = 0$ . At this point, the phase transition is only caused by quantum fluctuations. At  $T > 0$ , thermal fluctuations more and more dominates the phase transition. Nevertheless, the physical behaviour is influenced due to quantum fluctuations in a large regime, labeled as quantum critical phase.

is also required for quantum phase transitions. This length scale is called correlation length, which diverges right at the quantum critical point.

$$\xi^{-1} \sim \Lambda |g - g_c|^\nu, \quad (3.2)$$

where  $\nu$  is again a critical exponent and  $\Lambda$  an arbitrary inverse length scale as a momentum cut-off. A directly relation between both characteristic quantities can be obtained when (3.2) is inserted in (3.1). For finite temperatures,  $T > 0$ , a second energy scale is given by  $k_B T$ , where  $k_B$  is the Boltzmann constant. A proportionality between temperature and correlation length is

$$T \sim \xi^{-z}. \quad (3.3)$$

The curved conical boundary phase lines of the quantum critical phase can be explained with this relation. Figure 3.1 shows this phase: In the case of small temperatures, the critical exponent  $z$  attains the value  $z = 2$ , so that the phase lines are shaped like a square root. At higher temperatures the phase boundary lines are linear, since the critical exponent is changed to  $z = 1$  [PS14]. In this regime the physical behaviour of metals is determined by quantum fluctuations.

Now that the physical origin of quantum phase transitions is known, the spin-fermion-model is introduced. Instead of a microscopic and detailed mathematical description,

### 3.1 The Spin-Fermion-Model at the Onset of the Antiferromagnetic Quantum Phase Transition

an introduction with qualitative arguments motivating the model is presented. Metals in the vicinity of a magnetic quantum critical point are described with the spin-fermion-model, considering fermionic quasi-particles and bosonic spin density waves. The fermionic propagator is determined by the usual free fermionic Green function. Spin fluctuations are collective modes and their propagator is characterized by the dynamical magnetic susceptibility.

$$\mathcal{D}_\mu(\mathbf{q}, \omega) = \sum_{\mathbf{Q}} \frac{1}{(\mathbf{q} + \mathbf{Q})^2 + \xi^{-2} - (\omega/v_S)^2}, \quad (3.4)$$

where  $\mu$  is the spatial direction of the spin density wave,  $\xi$  is the magnetic correlation length and  $v_S$  is the spin wave velocity. The latter is of the same order as the Fermi velocity since spin fluctuations are originated due to fermions in the vicinity of the Fermi surface. Furthermore, a peak at the momentum vector  $\mathbf{Q} = (\pi, \pi)$  is exhibit in the magnetic susceptibility. A strong coupling interaction is therefore implicated between momentum vectors  $\mathbf{k}$  and  $\mathbf{k} + \mathbf{Q}$ .

Phase transitions are generally characterized by an order parameter. In the case of the investigated antiferromagnetic phase transition this also holds true. The corresponding order parameter here is the local magnetization and can be measured by the spin expectation value  $\langle \mathbf{S}(\mathbf{r}_i) \rangle$ . Naturally, it is a sum over all spins located at a certain position  $\mathbf{r}_i$ . The order parameter is finite in the antiferromagnetic ordered phase and vanishes in the paramagnetic disordered phase. The expectation value of the spin operator is spatially modulated according to  $\langle S_\mu \rangle \sim \exp(i\mathbf{Q}\mathbf{R})$ , where  $\mathbf{R}$  is a lattice vector [Wei15]. As a consequence, the order parameter and equally the propagator are therefore periodic quantities. This is reflected in the periodicity of the magnetic Brillouin zone, spanned by the vector  $\mathbf{Q}$ .

The presented description of the antiferromagnetic quantum phase transition in the spin-fermion-model is based on [ACS03]. It is assumed that spin fluctuations are generated over a large range of the tuning parameter  $g$ . Other low-energy collective degrees of freedom that are independent of spin excitations are neglected. At large values of the tuning parameter  $g$  in the paramagnetic phase, the physical behaviour is described by Landau's Fermi liquid theory. Decreasing the tuning parameter and getting closer to the quantum critical point the behaviour is changed to a Non-Fermi liquid behaviour. Only one type of fermions is assumed to exist and the arising collective modes are originated from permanent interaction between particles and holes. The physics in the vicinity of the quantum critical point is determined by spin excitations that are turning into smooth modes. One dominant channel containing fermion-fermion interaction with energies smaller than a certain energy cut-off  $\Lambda$  is assumed.

In the vicinity of the quantum critical point the (magnetic) correlation length  $\xi$  and the coupling constant  $\lambda$  is divergent. The correlation length is therefore much larger than the lattice constant,  $\xi \gg a$ , and the coupling constant is much larger than the band gap,  $\lambda \gg \Delta$ . The band gap is associated with the energy of spin excitations. In the limit of large distance and small energies or temperatures a microscopic consideration of the lattice Hamiltonian is unnecessary. In this low-energy theory, spin fluctuations

### 3 Spin-Fermion-Model

are described as a three component bosonic field  $\Phi_\mu(\mathbf{x}, \tau)$ . The field is defined as a sum over all spin operators analysed in the neighbourhood of the spin's position  $i$ . It is formally written as  $\Phi_\mu(\mathbf{x}, \tau) \sim \sum_{i \in \Gamma(\mathbf{r}_i)} S_\mu(\mathbf{r}_i)$ , where  $\mu$  is the spatial direction of the field and  $\Gamma(\mathbf{r}_i)$  represented the neighbourhood around the spin position  $\mathbf{r}_i$  [Sac11]. The magnitude of the bosonic field is chosen arbitrary and the field itself is considered as a real field. The bosonic field plays the role of an order parameter, since the spin fluctuations only emerge near the phase transition. In the low-energy theory, the obtained effective Hamiltonian for spin fluctuations is then given by

$$H_\Phi = \sum_\mu \int_{\mathbf{k}} \left[ -\frac{\mathbf{k}^2}{2} - \frac{r_0}{2} \right] \Phi_\mu(\mathbf{k}, \tau) \Phi_\mu(-\mathbf{k}, \tau) + \frac{v_S^2}{2} \pi_\mu(\mathbf{k}, \tau) \pi_\mu(-\mathbf{k}, \tau), \quad (3.5)$$

where  $r$  is a control parameter and corresponds to the squared inverse correlation length,  $r = \xi^{-2}$ . The integral is extended over the first Brillouin zone and the sum runs over the spatial direction of the bosonic field.

It should be noted that the spin density waves are damped in consequence of the interaction with fermions. The spin itself does not possess an own damping source. The whole damping is governed by the decay of particle-holes-pairs. As a consequence, the full renormalized particle-hole bubble corresponds to the inverse lifetime of spin fluctuations. The interaction Hamiltonian between spin density waves and fermions is given by

$$H_{\Psi\Phi} = -\lambda \sum_\mu \int_{\mathbf{k}} \int_{\mathbf{q}} \Phi_\mu(\mathbf{k} - \mathbf{q}, \tau) \left[ \Psi_a^\dagger(\mathbf{k}, \tau) \cdot \sigma_\mu \cdot \Psi_b(\mathbf{q}, \tau) + \Psi_b^\dagger(\mathbf{k}, \tau) \cdot \sigma_\mu \cdot \Psi_a(\mathbf{q}, \tau) \right], \quad (3.6)$$

where  $\lambda$  is the coupling constant. Both integrals are extended over the first Brillouin zone and the sum runs over the spatial directions of the bosonic field.  $\sigma_\mu$  is the Pauli matrix with respect to the spatial direction. The two different Fermi surfaces in the obtained model are represented by the indices a and b at the fermionic fields  $\Psi$ . The imaginary part of the susceptibility has to be computed in the low-energy limit with tools of the quantum field perturbation theory. An explicit calculation is presented in the appendix A. Furthermore, the dynamic of the spin fluctuations is assumed to be governed by the low-energy fermions. The  $\omega^2$ -term in the susceptibility (3.4) can be neglected [ACS03] and at the vicinity of the quantum critical point the correlation length diverges, implying  $\xi^{-2} \rightarrow 0$ . The damped magnetic susceptibility is then given by

$$\mathcal{D}_\mu(\mathbf{q}, i\omega_n) = \sum_{\mathbf{Q}} \frac{1}{(\mathbf{q} + \mathbf{Q})^2 + \gamma|\omega_n|}, \quad (3.7)$$

where  $\omega_n$  represent the bosonic Matsubara frequency. Spin fluctuations are no independent degrees of freedom due to the fact that their damping is strongly connected to fermions. The interaction between fermions on the Fermi surface separated by the large vector  $\mathbf{Q}$  constitutes in the damped susceptibility. These points separated by

### 3.1 The Spin-Fermion-Model at the Onset of the Antiferromagnetic Quantum Phase Transition

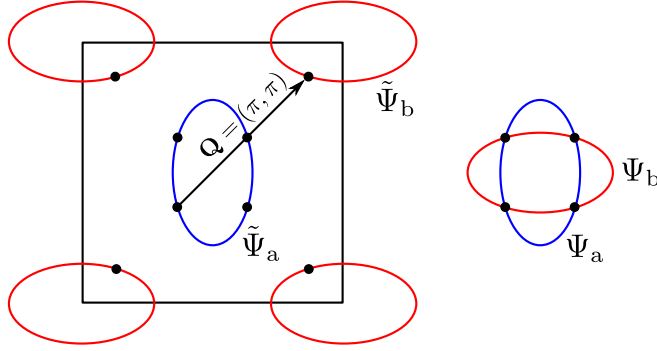


Figure 3.2: On the left hand side the Brillouin zone is depicted containing the Fermi surface of both species of fermions,  $\tilde{\Psi}_a$  and  $\tilde{\Psi}_b$ . While the fermions  $\tilde{\Psi}_a$  are located with an anisotropic parabolic dispersion at the origin  $(0,0)$ , the fermions  $\tilde{\Psi}_b$  are located with a  $\pi/2$ -rotated anisotropic parabolic dispersion at the corners of the Brillouin zone,  $(\pi, \pi)$  for example. The vector  $\mathbf{Q}$  connects certain points on the Fermi surface, called hotspots and represented with dots. As a result of this an attraction between these fermions occurs. On the right hand side the fermions  $\tilde{\Psi}_a$  are shifted to the corner at  $(\pi, \pi)$ . The convenience of this representation is that the coupling between fermions and spin fluctuations is local and independent of the position.

$\mathbf{Q}$  on the Fermi surface are called hot-spots in two dimensions and their theory is discussed next. In comparison to a normal metals, the new interaction of spin fluctuations separates the Fermi surface in *hot* and *cold* manifolds. A point  $\mathbf{k}$  is considered on the Fermi surface of a  $d$ -dimensional system and, there, the fermion is assumed to has zero energy. This point is connected to another point  $\mathbf{k} + \mathbf{Q}$  via the spin density wave and is required to be also on the Fermi surface. A  $d - 2$ -dimension manifold is yielded for a  $d$ -dimensional system due to both constraints. In the case of  $d = 2$  the *hot* manifold is therefore called a hot-spot. Another visualization of *hot* manifolds is offered by the magnetic Brillouin zone spanned by the vector  $\mathbf{Q}$ . The intersections of the magnetic Brillouin zone and the Fermi surface are equivalent to the *hot* manifolds.

In our investigated model the fermions are considered as free, up to the interaction with the spin fluctuations. Two species of fermions are assumed,  $\tilde{\Psi}_a$  and  $\tilde{\Psi}_b$ . Their dispersion is anisotropic and parabolic, as suggested in [PS14]. The anisotropic parabolic Fermi surface are depicted on the left hand side in figure 3.2. This is not a discrepancy to our previous constraint, assuming one fermion, since both species of fermions are electrons and differ only in their dispersion. The fermions  $\tilde{\Psi}_a$  and  $\tilde{\Psi}_b$  are located on an ellipse around the origin  $(0,0)$  and  $(\pi, \pi)$ , respectively. Both ellipses are separated by the vector  $\mathbf{Q} = (\pi, \pi)$  and rotated by  $\pi/2$  to each other. For achieving a continuum theory the ellipse centered around  $(\pi, \pi)$  is shifted by the vector  $\mathbf{Q}$  to the origin. New fermionic fields,  $\tilde{\Psi}_a(\mathbf{r}) = \Psi_a(\mathbf{r})$  and  $\tilde{\Psi}_b(\mathbf{r}) = \Psi_b(\mathbf{r}) \exp(i\mathbf{Q}\mathbf{r})$ , are therefore intro-

duced. The new Fermi surfaces of the fermions  $\Psi_a(\mathbf{r})$  and  $\Psi_b(\mathbf{r})$  are depicted on the right hand side in figure 3.2. The enormous advantage of the continuum theory is that the coupling between the fermions, caused by spin density waves, is now local and independent of the position. In reciprocal space, the Hamiltonian of the free fermions  $\Psi_a(\mathbf{r})$  and  $\Psi_b(\mathbf{r})$  is given by

$$H_\Psi = \int_{\mathbf{k}} \left[ \epsilon_a(\mathbf{k}) \psi_a^\dagger(\mathbf{k}, \tau) \psi_a(\mathbf{k}, \tau) + \epsilon_b(\mathbf{k}) \psi_b^\dagger(\mathbf{k}, \tau) \psi_b(\mathbf{k}, \tau) \right], \quad (3.8)$$

where the integral is extended over the first Brillouin zone.  $\epsilon_a(\mathbf{k})$  and  $\epsilon_b(\mathbf{k})$  are the anisotropic parabolical dispersions, corresponding to the fermion species a and b, and are given by

$$\epsilon_a(\mathbf{k}) = \frac{k_x^2}{2m_1} + \frac{k_y^2}{2m_2} - \mu_0 \quad \text{and} \quad \epsilon_b(\mathbf{k}) = \frac{p_x^2}{2m_2} + \frac{p_y^2}{2m_1} - \mu_0, \quad (3.9)$$

where  $\mu_0$  is the chemical potential.

## 3.2 Momentum Conservation in the Spin-Fermion-Model and the Consequence of Umklapp Scattering

In the low-energy theory, our investigated 2D-model is described by the continuum Hamiltonian  $H_\Psi$  for free fermions on the Fermi surface, the effective Hamiltonian  $H_\Phi$  for spin fluctuations and by the interaction Hamiltonian  $H_{\Psi\Phi}$  between both. Directly at the quantum critical point the control parameter  $r$  in (3.5) is zero, due to  $r = \xi^{-2}$  and the correlation length  $\xi$  is divergent.  $r$  is thus set to zero in the Hamiltonian  $H_\Phi$ . The obtained model Hamiltonian is given by  $H = H_\Psi + H_\Phi + H_{\Psi\Phi}$ . In the next step, the conservation of momentum and current for this model Hamiltonian will be proved. A perturbation Hamiltonian is then introduced to consider umklapp scattering, since translation symmetry is broken by this perturbation and momentum is not a conserved quantity any more.

A physical quantity is conserved, if its time derivative vanishes. In quantum mechanics the time derivative is given by Heisenberg equation of motion,  $\dot{A}(t) = i[H, A(t)]_-$ , where  $A(t)$  is an arbitrary operator. The momentum operator is given by

$$P_j = \int_{\mathbf{k}} k_j \left[ \Psi_a^\dagger(\mathbf{k}, \tau) \Psi_a(\mathbf{k}, \tau) + \Psi_b^\dagger(\mathbf{k}, \tau) \Psi_b(\mathbf{k}, \tau) - \pi_\mu(\mathbf{k}, \tau) \Phi_\mu(-\mathbf{k}, \tau) \right], \quad (3.10)$$

where the spatial direction is indicated by  $j$ . The integral is extended over the first Brillouin zone and the sum over  $\mu$  is implied in the last term. The energy-momentum-tensor, as suggested in [Ili02], is used for the computation, shown in appendix B. Further the x-component of current operator is given by

$$J_x = - \int_{\mathbf{k}} \left[ \frac{k_x}{m_1} \Psi_a^\dagger(\mathbf{k}, \tau) \Psi_a(\mathbf{k}, \tau) + \frac{k_x}{m_2} \Psi_b^\dagger(\mathbf{k}, \tau) \Psi_b(\mathbf{k}, \tau) \right], \quad (3.11)$$

### 3.2 Momentum Conservation in the Spin-Fermion-Model and the Consequence of Umklapp Scattering

where the integral is also extended over the first Brillouin zone. The y-component of the current operator is obtained by changing the index x to y and interchanging the index a and b of the fermionic field operators. Now, the time derivative of both quantities is computed by using the basic bosonic and fermionic commutator relations. An explicit calculation is also represented in the appendix B. This yields a vanishing time derivative for the the momentum,

$$\dot{P}_j = 0, \quad (3.12)$$

and the following expression for the time derivative of the x-component of the current

$$\begin{aligned} \dot{J}_x = \lambda \sum_{\mu} \int_{\mathbf{k}} \int_{\mathbf{q}} \Phi_{\mu}(\mathbf{k} - \mathbf{q}, \tau) & \left[ \left( \frac{q_x}{m_1} - \frac{k_x}{m_2} \right) \Psi_b^{\dagger}(\mathbf{k}, \tau) \cdot \sigma_{\mu} \cdot \Psi_a(\mathbf{q}, \tau) \right. \\ & \left. + \left( \frac{q_x}{m_2} - \frac{k_x}{m_1} \right) \Psi_a^{\dagger}(\mathbf{k}, \tau) \cdot \sigma_{\mu} \cdot \Psi_b(\mathbf{q}, \tau) \right]. \end{aligned} \quad (3.13)$$

The y-component of the current is obtained by changing again the index x to y and interchanging the index a and b of the fermionic field operators. In the spin-fermion-model, described by the Hamiltonian  $H$ , momentum is a conserved quantity, whereas the current is not. The Hamiltonian is further invariant with respect to time reversal symmetry and a finite overlap is possessed between both quantities. An infinite static electrical conductivity is obtained, compared to the discussion in chapter 2. A finite conductivity is only obtained when translation symmetry is broken. This corresponds to an unconserved momentum. Therefore, the model Hamiltonian  $H$  is pertubated by umklapp scattering via the Hamiltonian

$$H_{\text{umklapp}} = \sum_{\mu, \mathbf{G}} J_{\mathbf{G}} \int_{\mathbf{k}} \Phi_{\mu}(\mathbf{k}, \tau) \Phi_{\mu}(-\mathbf{k} + \mathbf{G}, \tau), \quad (3.14)$$

where the integral extends over the first Brillouin zone and the sum over  $\mathbf{G}$  includes all reciprocal lattice vectors. The quantity  $J_{\mathbf{G}}$  is a coupling parameter depending on reciprocal lattice vectors. It is assumed that the coupling is decreasing fast to zero in the limit of large reciprocal lattice vectors ( $|\mathbf{G}| \rightarrow \infty$ ). The time derivative of the momentum is given by

$$\dot{P}_j(\tau) = i \sum_{\mathbf{G}} J_{\mathbf{G}} \int_{\mathbf{k}} G_j \Phi_{\mu}(\mathbf{k}, \tau) \Phi_{\mu}(-\mathbf{k} - \mathbf{G}, \tau) \quad (3.15)$$

with respect to the new model Hamiltonian  $H' = H + H_{\text{umklapp}}$ . The time derivative of the current is persisted, since the current and pertubation Hamiltonian depends on different types of field operators and the commutator is therefore trivially zero. The static electrical conductivity has become finite due to the unconserved momentum. In the next chapter, the static electrical conductivity is computed using diagrammatic perturbation theory and the results are analysed.





## 4 The Static Conductivity in the Spin Fermion Model including Umklapp Scattering

The static electrical conductivity  $\sigma_{\text{dc}}$  is computed in this chapter, using the memory-matrix-formalism. The underlying model is the spin-fermion-model (see chapter 3), including umklapp scattering that breaks translation symmetry. In this chapter, our focus lies on the physical analysis of the obtained expression for the conductivity. An explicit computation is demonstrated in appendix C and D.

Two physical objects, fermions near the Fermi surface and spin fluctuations, are considered in the spin-fermion-model as introduced in the previous chapter. Spin fluctuations are generated at the vicinity of an antiferromagnetic quantum critical point due to particle-holes-excitations. Fermions, located at the point  $\mathbf{k}$  and  $\mathbf{k} + \mathbf{Q}$  on the Fermi surface, are connected to each other because of these fluctuations. The momentum conservation of the spin-fermion-model Hamiltonian has been shown in the previous chapter. The static electrical conductivity is thus infinite as it is proven in chapter 2. Considering umklapp scattering, the translation symmetry is broken and the momentum is unconserved. As a consequence the static conductivity becomes finite. This calculation is presented here.

The memory-matrix-formalism is used in chapter 5 to derive the following formula for the static electrical conductivity, including the spin-fermion-model as well as umklapp scattering.

$$\sigma_{\text{dc}} = - \lim_{z \rightarrow 0} \frac{z \cdot |\chi_{\text{JP}}(\omega = 0)|^2}{\mathcal{G}_{\dot{\mathbf{P}}\dot{\mathbf{P}}}(\mathbf{k}, z)} \quad (4.1)$$

Here,  $z$  is a complex frequency and  $\chi_{\text{JP}}(\omega = 0)$  is the static susceptibility between current and momentum. The Green function in the denominator is given by

$$\mathcal{G}_{\dot{\mathbf{P}}\dot{\mathbf{P}}}(\mathbf{k}, z) = \int_0^\infty dt e^{izt} \left\langle \left[ \dot{\mathbf{P}}(t), \dot{\mathbf{P}}(0) \right]_- \right\rangle_0, \quad (4.2)$$

where the usual quantum mechanical commutator is used, indicated with the minus sign at the squared brackets. The expectation value is evaluated with respect to the unperturbative Hamiltonian  $H$ , visualized with the index 0. The interaction between fermions and spin fluctuations is included in the Hamiltonian  $H$ . The time derivative of momentum is given by equation (3.15).

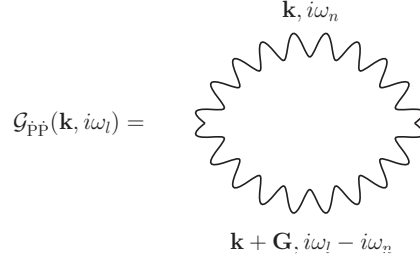


Figure 4.1: The zeroth order bubble diagram is shown for spin density fluctuations. The wavy lines symbolizes the spin density wave, denoted as  $\mathcal{D}_\mu(\mathbf{k}, i\omega_n)$ . The momentum of lower line is modified by the vector  $\mathbf{G}$ , originated from umklapp scattering.

The possible temperature dependence of the Green function  $\mathcal{G}_{\dot{P}\dot{P}}(\mathbf{k}, z)$  and the static susceptibility  $\chi_{JP}(\omega = 0)$  is investigated. The latter is expected to be temperature independent, since both quantities are not explicitly time dependent. This calculation is shown in detail in the appendix C, using the diagrammatic perturbation technique. The considered diagrams are the electron-pair bubble for each species of fermions, depicted in figure C.1. Therefore, the obtained expression of the susceptibility is given by

$$\chi_{PJ}(\omega = 0) = \frac{\sqrt{m_1 m_2}}{\pi} T \cdot \ln(e^{\mu/T} + 1), \quad (4.3)$$

where the chemical potential is denoted as  $\mu$ . The logarithm is approximated in the limit of small temperatures ( $\mu \gg T$ ) to  $\ln(e^{\mu/T} + 1) \rightarrow \mu/T$ . The temperature cancels when this expression is inserted and the static susceptibility is given by constant parameters,  $\chi_{PJ}(\omega = 0) = \mu \sqrt{m_1 m_2} / \pi$ . The chemical potential is assumed to be temperature independent in the observed regime.

The only temperature dependence of the static electrical conductivity emerges hence by the Green function  $\mathcal{G}_{\dot{P}\dot{P}}(\mathbf{k}, z)$ . Only the free bubble diagram is considered when calculating the Green function with diagrammatic perturbation theory, which is depicted in figure 4.1. Higher order terms in the diagrammatic treatment are corrections of the bubble diagram. Therefore the conductivity or resistance is only determined by spin fluctuations. Resistance is a consequence of fermionic coupling to other degrees of freedom, obtained as finite fermionic lifetime. It is thus proportional to the imaginary part of the retarded Green function  $\mathcal{G}_{\dot{P}\dot{P}}^{\text{ret}}(\mathbf{k}, z)$ . Appendix D shows the detailed computation of the expression of the retarded Green function.

$$\begin{aligned} \text{Im}\left\{\mathcal{G}_{\dot{P}\dot{P}}^{\text{ret}}(\mathbf{k}, \omega)\right\} &= -\frac{4\gamma^2\beta\omega}{\pi} \sum_{\mathbf{Q}_1, \mathbf{Q}_2} \sum_{\mathbf{G}} |\mathbf{J}\mathbf{G}|^2 \int_0^\infty d\epsilon \frac{\epsilon^2 e^{\beta\epsilon}}{(e^{\beta\epsilon} - 1)^2} \\ &\times \int_{\mathbf{k}} G_j^2 \cdot \frac{1}{(\mathbf{k} + \mathbf{G} - \mathbf{Q}_1)^4 + \gamma^2 \epsilon^2} \cdot \frac{1}{(\mathbf{k} + \mathbf{Q}_2)^4 + \gamma^2 \epsilon^2} \end{aligned} \quad (4.4)$$

The integral is extended over the first Brillouin zone. The periodicity of the spin susceptibility and perturbation is considered by the sums over  $\mathbf{Q}_i$  ( $i = 1, 2$ ) and  $\mathbf{G}$ , respectively. In both cases these are reciprocal lattice vectors. Spatial direction of the momentum is represented by the index  $j$  and  $\beta^{-1} = T$ . The obtained integrals are now investigated with respect to different cases since their are not exactly solvable.

The integral converges if the magnitude of one of the momentum terms,  $\mathbf{k} + \mathbf{G} - \mathbf{Q}_1$  or  $\mathbf{k} + \mathbf{Q}_2$ , is large. Since both terms are of the power of four, the integral is a fast decreasing function in the large momentum limit. The integral diverges, if these terms are zero and this happens in many constellations. One of the most divergent one is assumed in the following approach. The vector  $\mathbf{k}$  is limited to the first Brillouin zone and the reciprocal lattice vectors are set to  $\mathbf{G} = \mathbf{Q}_1$  and  $\mathbf{Q}_2 = 0$ . The choice of the reciprocal lattice vectors is arbitrary and it is therefore possible that the  $j$ -component of  $\mathbf{G}$  is large. This divergence is killed by the coupling parameter  $J_{\mathbf{G}}$  that is assumed to be fast decreasing for large  $|\mathbf{G}|$ .

The remaining momentum integral is now exactly integrable. First of all, the momentum and frequency variables are transformed into dimensionless variables, using the transformation rules  $\mathbf{k} = \mathbf{y} \cdot \sqrt{\gamma T}$  and  $\epsilon = x \cdot T$ , respectively. The new variable  $\mathbf{y}$  is further transformed into plane polar coordinates. The upper limit of the radius  $|\mathbf{y}|$  is set to infinity, since the integrand is decreasing fast to zero for  $|\mathbf{y}| \rightarrow \infty$ . As a consequence the angular integral is easily evaluated, yielding the factor  $2\pi$ . The remaining integral is given by the following expression.

$$\text{Im}\left\{\mathcal{G}_{\text{PP}}^{\text{ret}}(\mathbf{k}, z)\right\} = -\frac{2 \cdot G_j^2 \cdot |J_{\mathbf{K}}|^2}{\gamma \cdot \pi^2} \cdot \frac{\omega}{T} \int_0^\infty dx \frac{x^2 e^x}{(e^x - 1)^2} \int_0^\infty dy \frac{y}{(y^4 + x^2)^2} \quad (4.5)$$

The  $y$ -integral is substituted one last time, using the transformation rule  $y^2 = z \cdot x$ . The obtained integral is evaluated to  $\pi/4$ , using the integral formula (??). Both limits,  $x \rightarrow 0$  and  $x \rightarrow \infty$ , of the integral over  $x$  are investigated. In the case of large  $x$ , the integral is decreasing fast to zero due to the ratio of the exponential functions. The upper limit is thus set to one and the integrand is expanded for small values of  $x$ . In first order the integrand is approximated to  $1/x^3$ . This is a highly divergent function in the limit  $x \rightarrow 0$  and as a consequence the static conductivity is divergent as well.

The result of a divergent conductivity is surely incorrect in a system with broken translation symmetry. In chapter 2, it is shown that translation symmetry and the consequent conserved momentum causes an infinite conductivity in the static limit. Chapter 3 shows, that momentum is conserved in the unpertubated spin-fermion-model (3.12), while it is unconserved considering umklapp scattering 3.15. As a consequence, a finite static conductivity is expected instead of divergence.

The origin of this discrepancy is supposed to be in the choice of the control parameter  $r$ . The parameter  $r$  is assumed to be zero, since its proportional to  $\xi^{-2}$  and the correlation length  $\xi$  diverges at the quantum critical point. This assumption is incorrect in the sense that the system is not directly at the quantum critical point, but rather in the vicinity of him. The system is supposed to be in the quantum critical phase, see figure 3.1, at a point with tuning parameter  $g = g_c$  and temperature  $T > 0$ . While

the temperature is decreased to get closer to the quantum critical point, the tuning parameter is fixed. Considering a finite value of the control parameter  $r$ , the imaginary part of the retarded Green function is given by

$$\begin{aligned} \text{Im}\left\{\mathcal{G}_{\text{PP}}^{\text{ret}}(\mathbf{k}, z)\right\} &= -\frac{4\gamma^2\beta\omega}{\pi} \sum_{\mathbf{Q}_1, \mathbf{Q}_2} \sum_{\mathbf{G}} |\mathbf{J}_{\mathbf{G}}|^2 \int_0^\infty d\epsilon \frac{\epsilon^2 e^{\beta\epsilon}}{(e^{\beta\epsilon} - 1)^2} \\ &\times \int_{\mathbf{k}} G_j^2 \cdot \frac{1}{((\mathbf{k} + \mathbf{G} - \mathbf{Q}_1)^2 + r)^2 + \gamma^2\epsilon^2} \cdot \frac{1}{((\mathbf{k} + \mathbf{Q}_2)^2 + r)^2 + \gamma^2\epsilon^2} \end{aligned} \quad (4.6)$$

The approach to solve the integrals is nearly the same as above. Firstly, the convergence of large values of momenta is not changed, because of considering  $r$ . One of the most divergent constellations is still  $\mathbf{G} = \mathbf{Q}_1$  and  $\mathbf{Q}_2 = 0$ . The divergence, generated by large values of  $G_j$ , is still killed since the coupling parameter  $\mathbf{J}_{\mathbf{G}}$  decreases fast in the limit  $|\mathbf{G}| \rightarrow \infty$ . The remaining momentum integral is of the same structure as above and exactly solvable. Therefore, the momentum integral is firstly transformed into plane polar coordinates,  $\mathbf{k} = (k \cos \phi, k \sin \phi)$ . The upper limit of  $k$  is again set to infinity, since the integrand decreases fast to zero for  $k \rightarrow \infty$  and the contributions are neglected.

$$\text{Im}\left\{\mathcal{G}_{\text{PP}}^{\text{ret}}(\mathbf{k}, z)\right\} = -\frac{|\mathbf{J}_{\mathbf{G}}|^2 \cdot G_j^2}{\gamma\pi^2} \cdot \frac{\omega}{T} \int_0^\infty d\epsilon \frac{\epsilon^2 e^{\beta\epsilon}}{(e^{\beta\epsilon} - 1)^2} \int_0^\infty dk \frac{k}{((r + k^2)^2 + \gamma^2\epsilon^2)^2} \quad (4.7)$$

The angular integral is already performed and the obtained momentum integral is substituted using  $z = (r + k^2)/\gamma\epsilon$ . In comparison to the case above, the lower limit is changed to  $r/\gamma\epsilon$ . Both cases are equivalent in the limit  $r \rightarrow 0$ . The finite lower boundary guarantees the convergence of the remaining integral over  $\epsilon$ . The integral over  $z$  is performed, utilizing the integral formula (??) again. The dimensionless variable are introduced, using  $x = \beta\epsilon$ . The obtained expression is given by

$$\begin{aligned} \text{Im}\left\{\mathcal{G}_{\text{PP}}^{\text{ret}}(\mathbf{k}, z)\right\} &= -\frac{|\mathbf{J}_{\mathbf{G}}|^2 \cdot G_j^2}{4\gamma\pi^2} \cdot \frac{\omega}{T} \\ &\times \int_0^\infty dx \frac{1}{x} \frac{e^x}{(e^x - 1)^2} \cdot \left[ \pi - \frac{2\tilde{r}/x}{(\tilde{r}/x)^2 + 1} - 2 \arctan(\tilde{r}/x) \right], \end{aligned} \quad (4.8)$$

where the abbreviation  $\tilde{r} = r/\gamma T$  is introduced. The integral over  $x$  is not analytical exactly solvable. However, the integral is finite in both limits,  $x \rightarrow 0$  and  $x \rightarrow \infty$ . The latter is surely satisfied due to the ratio of exponential functions is fast decreasing to zero and no other term is divergent. In the limit  $x \rightarrow 0$ , the integrand is limited by  $4/3\tilde{r}^3$ , which is only divergent for  $\tilde{r} \rightarrow 0$ . The behaviour of the integrand is depicted on left hand side in figure 4.2, where  $\tilde{r} = 2$ . A solution of the integral is evaluated determining the behaviour of the expression in squared brackets. For large values of  $x$ , a linear  $r$ -dependence is given by the power of  $-3/2$ . This is depicted in the

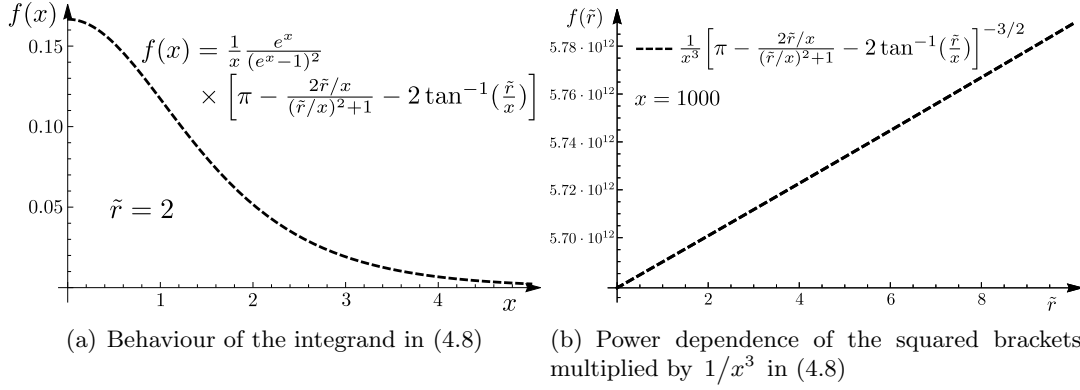


Figure 4.2: On the left hand side, the behaviour of the integrand in equation (4.8) is depicted for large und small values of  $x$ , where the factor  $\tilde{r} = r/\gamma T$  is set to 2. The integrand function is convergent for large values due to the function decreases fast for large values of  $x$ . For small values of  $x$ , the function takes a constanst value of  $4/3\tilde{r}^3$ . The integrand gets more divergent for small  $x$ , if the value  $\tilde{r}$  decrease to zero. The power dependence of the obtained momentum integral in (4.8) is depicted on the right hand side, where  $x = 1000$ . Since the behaviour is linear, the investigated expression has the power of  $-3/2$ .

right hand side of figure 4.2, where  $x$  is set to 1000. An approximated expression is generated for the interand using the method of power counting. The initial point of this approach is the momentum integral in euqtion (4.7). Numerator and differential yield in total the power of two, while the denominator generates the power of eight. The integrand is a function proportional to  $k^{-6}$  combing both powers. The further approach is to investigate singularities of the integrand. The limit  $r \rightarrow 0$  or  $\epsilon \rightarrow 0$  is seperately generated singularities in the function. Both are considered with the power of three, since the power of them is half in comparison to the power of  $k$  in equation (4.7). The integrand is therefore approximated by the following expression.

$$\text{Im}\left\{\mathcal{G}_{\text{PP}}^{\text{ret}}(\mathbf{k}, z)\right\} \approx -\frac{2|\mathbf{J}_{\mathbf{G}}|^2 \cdot G_j^2}{\gamma\pi^2} \cdot \frac{\omega}{T} \int_0^\infty dx \frac{x^2 e^x}{(e^x - 1)^2} \frac{1}{(\tilde{r}^2 + x^2)^{3/2}} \quad (4.9)$$

In figure 4.3, the approximated expression is illustrated against the exact one. The behaviour of both are nearly identical and the estimation is inspected to be valid. The integrand decreases still fast to zero for  $x \rightarrow \infty$ , while the upper limit is set to some arbitrary cut-off  $\Lambda$ . The ratio of the exponential functions are then expanded for small values of  $x$  up to the first non-vanishing order. The remained integral is solved exactly while the solution of its is expanded for small  $\tilde{r}/\Lambda$ .

$$\text{Im}\left\{\mathcal{G}_{\text{PP}}^{\text{ret}}(\mathbf{k}, z)\right\} \approx -\frac{2\gamma|\mathbf{J}_{\mathbf{G}}|^2 \cdot G_j^2}{\pi^2\Lambda} \cdot \frac{\omega T}{r^2} \quad (4.10)$$

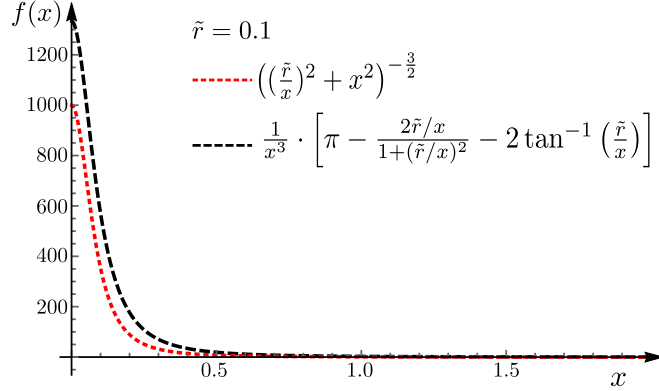


Figure 4.3: This figure shows the obtained expression of the momentum integral calculation (black curve, large strokes) in contrast to the obtained approximation using power counting technique (red curve, small strokes). The used approximation is considered as good, since the characteristic of both curves is quite similar. The value of  $\tilde{r}$  is set to 0.1.

To get the static electrical conductivity, this expression and the approximated value of (4.3) is inserted into equation (4.1).

$$\sigma_{\text{dc}}(T) = \frac{\mu m_1 m_2 \Lambda}{2 \gamma |\mathbf{J}_{\mathbf{G}}|^2 G_j^2} \cdot \frac{r^2}{T} \quad (4.11)$$

Beside the temperature itself, the only temperature dependent parameter is the control parameter  $r$ , which is proportional to the squared inverse correlation length,  $r = \xi^{-2}$ . The correlation length is originated due to the fact that the system possesses a quantum phase transition and is temperature dependent is given by  $\xi = T^{-1/z}$ , as shown in chapter 3.  $z$  is a critical exponent and it is chosen in dependence of the temperature distance to the quantum critical point. The corresponding temperature dependence of the control parameter is provided to  $r = T^{2/z}$ . The resistance is determined by the inverse of the conductivity. Considering only the temperature dependent parameters, the static resistance is given by

$$\rho_{\text{dc}}(T) \sim T^{1-4/z}. \quad (4.12)$$

Two possible choices are mentioned for the critical exponent  $z$ . In the vicinity of the quantum critical point at higher temperatures,  $z$  is chosen to be one. The  $T$ -dependence of the resistance is then given by  $T^{-3}$ . In the limit  $T \rightarrow 0$ , this is highly divergent.  $z$  can be chosen to be 2 for lower temperatures. Nevertheless, the  $T$ -dependence is evaluated to  $T^{-1}$ , which is still divergent in the limit  $T \rightarrow 0$ .

Our physical expectation is not confirmed with this divergent behaviour of the resistance. Experiments of observed metals [Löh+07] are shown a linear temperature dependence of the resistance,  $\rho(T) = \rho_0 + A T$ . The behaviour of the resistance is therefore described incorrect using the obtained solution (4.12). A possible origin of

this discrepancy between experiment and theory is maybe the diagrammatic perturbation theory. In equation (4.2), the time evolution operator is expanded up to the first non-vanishing order. This yields the free bubble diagram, while correction to the bubble are considered if the time evolution operator is expanded up to the next order.





## 5 Memory-Matrix-Formalism

The memory-matrix-formalism is a technique to determine the correlation function between two observables. In difference to other methods the Liouville space is considered. The derivation of the memory-matrix-formalism is exhaustively demonstrated in this chapter, as suggested in [For90]. At the beginning Kubo's relaxation function is introduced, since the correlation function is based on it in memory-matrix-formalism. After the derivation the formula for the static electrical conductivity is determined for the spin-fermion-model pertubated by umklapp scattering.

### 5.1 Kubo relaxation function

A system in equilibrium, represented by the Hamiltonian  $H_0$ , is considered. The perturbation  $H_1 = -B \cdot F(t)$  is switched on at an arbitrary time  $t'$ . The coupling to the system is determined by the operator  $B$  and the time evolution of the perturbation is described by  $F(t)$ , where  $F(t)$  is assumed to be zero for times  $t < t'$ . Our interest is now focused on the reaction of an operator  $A$  due to the perturbation. The deviation in comparing to the equilibrium value is given by

$$\delta \langle A(t) \rangle := \langle A \rangle(t) - \langle A(t) \rangle_{H_0} \approx \int_{-\infty}^{\infty} dt' \chi_{AB}(t-t') F(t') \quad (5.1)$$

where  $\chi_{AB}(t-t')$  is called the retarded susceptibility and is given by

$$\chi_{AB}(t-t') = i\Theta(t-t') \langle [A_I(t-t'), B_I(0)] \rangle_{H_0} \quad (5.2)$$

The above equation for  $\delta \langle A(t) \rangle$  is denoted as the Kubo formula. In the following, a certain type of perturbations is considered. The time evolution of the perturbation is assumed to be  $F(t) = \Theta(-t) \cdot F \cdot e^{-s\tau}$ . The perturbation is switched on adiabatically at  $t = -\infty$  and is switched off at  $t = 0$ . This time evolution is inserted into the Kubo formula and  $t-t'$  is substituted by  $\tau$ . The deviation of  $A(t)$  is then given by  $\delta \langle A(t) \rangle = \Phi_{AB}(t) \cdot F e^{st}$ . The arising function  $\Phi_{AB}(t)$  is called Kubo relaxation function and is given by

$$\Phi_{AB}(t) = \frac{i}{\hbar} \lim_{s \rightarrow 0} \int_t^{\infty} d\tau \langle [A_I(\tau), B_I(0)] \rangle_0 e^{-s\tau}. \quad (5.3)$$

The lower limit of the integral is determined to  $t$  due to the  $\theta$ -distribution. For a more detailed derivation of the Kubo relaxation function see [Sch08] or [Sch06]. Between

the Kubo relaxation function and the Kubo formula exist three very important relations used during the derivation of the correlation function and the formula of the conductivity.

$$1. \quad \chi_{AB}(t) = -\Theta(t) \frac{d}{dt} \Phi_{AB}(t) \quad (5.4)$$

$$2. \quad \Phi_{AB}(t=0) = \chi_{AB}(\omega=0) \quad (5.5)$$

$$3. \quad \Phi_{AB}(\omega) = \frac{1}{i\omega} [\chi_{AB}(\omega) - \chi_{AB}(\omega=0)]. \quad (5.6)$$

The evidence of these three relations are shown in the appendix E. The Kubo relaxation function is now transferred into a commutator independent form, using two identities. The first identity is given by

$$\langle [A(t), B(t')] \rangle = \frac{1}{Z} \text{Tr} \{ [\rho, A(t)] B(t') \}, \quad (5.7)$$

where the invariance of the trace with respect to cycling permutation is used. The second identity is denoted as the Kubo-identity.

$$\begin{aligned} i[\rho, A(t)] &= i \left[ \rho A(t) - e^{-\beta H} e^{\beta H} A(t) e^{-\beta H} \right] \\ \Leftrightarrow i[\rho, A(t)] &= -i\rho \int_0^\beta d\lambda \frac{d}{d\lambda} e^{\lambda H} A(t) e^{-\lambda H} \\ \Leftrightarrow i[\rho, A(t)] &= -i\rho \int_0^\beta d\lambda [H, A(t - i\lambda)] \\ \Leftrightarrow i[\rho, A(t)] &= -\rho \int_0^\beta d\lambda \dot{A}(t - i\lambda) \end{aligned} \quad (5.8)$$

Here the analogy between the time evolution of an operator and the exponential function is used in the second step. Furthermore, Heisenberg equation of motion is utilized in the third step. The time derivative of the operator  $A$  is symbolized with the dot above the operator.

$$\begin{aligned} \Phi_{AB}(t) &= -\lim_{s \rightarrow 0} \int_0^\beta d\lambda \int_t^\infty d\tau \langle \dot{A}_I(\tau - i\lambda\hbar) B_I(0) \rangle_0 e^{-s\tau} \\ \stackrel{\text{PI}}{\Leftrightarrow} \Phi_{AB}(t) &= \int_0^\beta d\lambda \langle A_I(t - i\lambda\hbar) B_I(0) \rangle_0 = \int_0^\beta d\lambda \langle A_I(t) B_I(i\lambda\hbar) \rangle_0 \end{aligned} \quad (5.9)$$

The first line is obtained, inserting both identities. On the right hand side the integral is evaluated using integration by parts (PI). Afterwards, the limit  $s \rightarrow 0$  is performed, which yields the obtained result for  $\Phi_{AB}(t)$ . This structure of the Kubo relaxation function is similar to the later chosen scalar product in the memory matrix formalism.

### 5.1.1 Spectral representation

In the previous section, the dynamical susceptibility  $\chi_{AB}$  is introduced deviating the Kubo-formula (5.1). The evolution of a operator is described by this function, while a perturbation is acting to the system. The dynamic susceptibility is separated into two types, non-dissipative and dissipative processes. In the following, dissipative processes are investigated. The dissipative susceptibility of the form

$$\chi''_{AB}(t-t') = \frac{1}{2\hbar} \langle [A(t), B(t')] \rangle \quad (5.10)$$

is considered, where the operators A and B are Hermitian. The property

$$(\chi''_{AB}(t-t'))^* = -\chi''_{AB}(t-t') \quad (5.11)$$

is valid, since the commutator of two Hermitian operators is anti-Hermitian. In the following, the dynamic susceptibility is expressed using (5.10). The obtained equation is multiplied with  $e^{i\omega t}$  and is integrated over time  $t$ .

$$\begin{aligned} \chi_{AB}(t) &= \frac{i}{\hbar} \Theta(t) \langle [A(t), B(0)] \rangle = 2i\Theta(t)\chi''_{AB}(t) \\ \Leftrightarrow \chi_{AB}(\omega) &= 2i \int_{-\infty}^{\infty} dt e^{i\omega t} \Theta(t) \chi''_{AB}(t) \\ \Leftrightarrow \chi_{AB}(\omega) &= -\frac{1}{\pi} \lim_{\eta \rightarrow 0} \int_{-\infty}^{\infty} d\omega' \frac{1}{\omega' + i\eta} \int_{-\infty}^{\infty} dt e^{i(\omega - \omega')t} \chi''_{AB}(t) \\ \Leftrightarrow \chi_{AB}(\omega) &= \frac{1}{\pi} \lim_{\eta \rightarrow 0} \int_{-\infty}^{\infty} d\omega' \frac{\chi''_{AB}(\omega')}{\omega' - \omega - i\eta} \\ \Leftrightarrow \chi_{AB}(\omega) &= \frac{1}{\pi} \text{PV} \int_{-\infty}^{\infty} d\omega' \frac{\chi''_{AB}(\omega')}{\omega' - \omega} + i \int_{-\infty}^{\infty} d\omega' \delta(\omega' - \omega) \chi''_{AB}(\omega') \\ \Leftrightarrow \chi_{AB}(\omega) &= \chi'_{AB}(\omega) + i\chi''_{AB}(\omega) \end{aligned} \quad (5.12)$$

On the left hand side the definition of the Fourier transformation is used, while on the right hand side the following definition of the  $\Theta$ -function is inserted.

$$\Theta_{\eta}(t) = i \lim_{\eta \rightarrow 0} \int_{-\infty}^{\infty} \frac{d\omega'}{2\pi} \frac{e^{-i\omega' t}}{\omega' + i\eta} \quad (5.13)$$

The dynamical susceptibility  $\chi_{AB}(\omega)$  is separated into two parts  $\chi'_{AB}(\omega)$  and  $\chi''_{AB}(\omega)$ , where the latter is the dissipative susceptibility. Assuming the dissipative susceptibility is a real number, then this is also valid for  $\chi'_{AB}(\omega)$  and the both functions  $\chi'_{AB}(\omega)$  and  $\chi''_{AB}(\omega)$  represent real and imaginary part of  $\chi_{AB}(\omega)$ , respectively. After this introduction about the Kubo relaxation function, the next chapter is illustrated the derivation of the memory matrix formalism.

## 5.2 Deviation of the Memory-Matrix-Formalism

In order to determine transport properties of many-body-systems, the time evolution of an observable has to be investigated. The memory-matrix-formalism is historically introduced to describe the Brownian motion under the consideration of dissipation and fluctuations. In [Mor65] is demonstrated the separation of a dynamical variable  $A(t)$  into two parts, one secular and one non-secular one. The starting point of this approach is based on the Langevin equation, considering damping of the variable, the coupling to some external force and a random force. To get a linearized form of the Langevin equation, it is assumed to separate the dynamical variable into a part considering its history and a part containing all effects of other degrees of freedom. The first part is now expanded up to the linear order. The obtained differential equation is solved using the Laplace transformation. The dynamical variable is then given by

$$A(t) = \Xi(t) \cdot A(0) + A'(t) \quad \text{with} \quad A'(t) = \int_0^t dt' \Xi(t-t') F(t'). \quad (5.14)$$

The function  $\Xi(t)$  is defined by the Laplace transformation of  $\Xi(s) = [s - \mathcal{C}(s)]^{-1}$  and  $\mathcal{C}(s)$  is the Laplace transformation of the correlation function  $\mathcal{C}(t)$ . Our further derivation of the memory-matrix-formalism is motivated by this short historical review. It shows, that a dynamical variable is separated into two parts. The first term includes the linear contributions of  $A(t)$ , while the second term contains non-linear effects and fluctuations, for example. Both terms are identified with secular and non-secular effects, respectively, while the dynamics of  $A(t)$  are dominated by the secular ones. The separation of  $A(t)$  offers the opportunity to a simple geometrical interpretation. The variable  $A(t)$  is assumed as a vector in a vector space. The direction of  $A(t)$  is labeled as the A-axis, if the system is in equilibrium. If now the system moves out of equilibrium caused by a perturbation, also the direction of  $A(t)$  changes. The part parallel to the A-axis is identified with the secular part, while the part perpendicular to the A-axis corresponds to the non-secular part.

A mathematical vector space has to be defined, for using this geometrical interpretation to determine the time evolution of an observable. Afterwards we define a correlation function in this vector space and bring it in much usefuller form. Our starting point is the usual Hilbert space in quantum mechanics. A short review based in [Aud05] is given in the following.

The  $d$ -dimensional Hilbert-space is linear, complex and has a defined scalar product. The vectors  $|\phi\rangle$ , usually denoted in the Dirac-notation, are identified with all possible states of the system. Since we are always interested in observables, linear Hermitian operators are defined in the Hilbert-space. The eigenvalues of them conform to observables. Using the dyad product  $\sum_i |i\rangle\langle i|$ , any linear operator can be written as a dyad decomposition

$$A = \sum_{i,j} |i\rangle\langle i| A |j\rangle\langle j| = \sum_{i,j} A_{ij} |i\rangle\langle j|, \quad (5.15)$$

where  $A_{ij} := \langle i | A | j \rangle$  is the matrix element of the corresponding linear operator. The dyad product of an operator is now used to introduce a new vector space of all linear operators acting on the  $d$ -dimensional Hilbert-space, called the Liouville-space  $\mathbb{L}$  or operator space.

The Liouville-space is a linear and complex vector space equally to the Hilbert-space. The difference between both are the vectors or elements living in the space. In the Liouville-space the vectors are linear operators  $A, B, \dots$  which are acting on a Hilbert-space. In other words this means that the dyad decomposition of an vector in the  $d$ -dimensional Hilbert-space is the new vector in the Liouville-space. A vector in the Liouville-space is notated as

$$|A\rangle := \sum_{ij}^d A_{ij} |i\rangle\langle j|. \quad (5.16)$$

Similiarly to the quantum mechanic the Dirac notation is used with the difference that round brackets are used instead of angle brackets to distinguish both spaces. Out of the definition (5.16) it is clear, that the basis in the Liouville-space is build by the  $d^2$  dyads of the Hilbert-space. The dimension of the Liouville-space is therefore  $d^2$ . Equally to a Hilbert-space, there are many other opportunities to choose the basis in the Liouville space  $\mathbb{L}$ , but the definition in (5.16) is the one which we choose in the following.

The basis of our Liouville space is denoted with  $\{|A_i\rangle\}$  where  $i = 1, 2, 3, \dots, n$  and  $A_i$  is an operator. The corresponding basis of the dual space is given by  $\langle A_i|$ , similarly to the Hilbert space. The last needed element of our Liouville space is a scalar product which has to fulfil the following three conditions.

$$1. \quad \langle A_i | A_j \rangle = \langle A_j | A_i \rangle^* \quad (5.17)$$

$$2. \quad \langle A_i | B \rangle = c_1 \langle A_i | A_j \rangle + c_2 \langle A_i | A_k \rangle, \\ \text{where } B = c_1 A_j + c_2 A_k \quad \text{and} \quad c_1, c_2 \in \mathbb{C} \quad (5.18)$$

$$3. \quad \langle A_i | A_i \rangle \geq 0, \quad \text{where equality is fulfilled if } A_i = 0. \quad (5.19)$$

Beside these the choice of the scalar product is arbitrary. For the moment let us choose

$$\langle A_i(t) | A_j(t') \rangle = \frac{1}{\beta} \int_0^\beta d\lambda \langle A_i^\dagger(t) A_j(t' + i\lambda\hbar) \rangle \quad (5.20)$$

as our scalar product, where the normal time evolution of an operator  $A_i(t) = e^{iHt/\hbar} A_i(0) e^{-iHt/\hbar}$  is valid, so that  $A_i(i\lambda\hbar) = e^{-\lambda H} A_i(0) e^{\lambda H}$  is possible to use. Now we have to prove, if the conditions are fulfilled by the choice of our scalar product. The second condition is shown transforming the expectation value into the trace representation and using the properties of the trace.

$$\langle A_i(t) | B(t') \rangle = \frac{1}{\beta} \int_0^\beta d\lambda \frac{1}{Z} \text{Tr} \left\{ \rho A_i^\dagger(t) \left[ c_1 A_j(t' + i\lambda\hbar) + c_2 A_k(t' + i\lambda\hbar) \right] \right\}$$

$$\Leftrightarrow (A_i(t)|B(t')) = c_1(A_i(t)|A_j(t')) + c_2(A_i(t)|A_k(t')) \quad (5.21)$$

The first and third condition can be shown by transforming the scalar product in the spectral representation. The trace is written explicitly as a sum over all states and the unity operator,  $1 = \sum_m |m\rangle \langle m|$ , is inserted between both operators  $A_i$  and  $A_j$ .

$$\begin{aligned} (A_i(t)|A_j(t')) &= \frac{1}{\beta \cdot Z} \int_0^\beta d\lambda \sum_{n,m} \langle n| e^{-\beta H} A_i^\dagger(t) |m\rangle \langle m| e^{-\lambda H} A_j(t') e^{\lambda H} |n\rangle \\ \Leftrightarrow (A_i(t)|A_j(t')) &= \frac{1}{\beta \cdot Z} \sum_{n,m} \langle n| A_i^\dagger(t) |m\rangle \langle m| A_j(t') |n\rangle e^{-\beta E_n} \int_0^\beta d\lambda e^{\lambda(E_n - E_m)} \\ \Leftrightarrow (A_i(t)|A_j(t')) &= \frac{1}{\beta \cdot Z} \sum_{n,m} \langle n| A_i^\dagger(t) |m\rangle \langle m| A_j(t') |n\rangle \frac{e^{-\beta E_m} - e^{-\beta E_n}}{E_n - E_m} \end{aligned} \quad (5.22)$$

The complex conjugated of the expectation value is considered in the Liouville space and the first condition is instantly proven, using  $\langle n| A_j^\dagger(t) |m\rangle^* = \langle m| A_j(t) |n\rangle$ . Notice that on the right hand side of equation (5.22) only the expectation values are complex quantities. The complex conjugated of them yields

$$\left( \langle n| A_i^\dagger(t) |m\rangle \langle m| A_j(t') |n\rangle \right)^* = \langle n| A_j^\dagger(t') |m\rangle \langle m| A_i(t) |n\rangle. \quad (5.23)$$

If this is inserted back in  $(A_i(t)|A_j(t'))^*$ , equation (5.22) is found.. To prove the third condition  $A_j(t')$  is set to  $A_i(t)$  in equation (5.22) On the right hand side of this equation we obtain

$$\frac{1}{\beta \cdot Z} \sum_{n,m} \left| \langle m| A_i(t) |n\rangle \right|^2 \frac{e^{-\beta E_m} - e^{-\beta E_n}}{E_n - E_m}. \quad (5.24)$$

The squared expectation value is always non-negative and the fraction is positive too. This is proven investigating the two cases  $E_n > E_m$  and  $E_n < E_m$ . Therefore, the expectation value  $(A_i(t)|A_i(t)) \geq 0$  and equality is only possible if  $A_i = 0$ . All three conditions are well proven and the choice of our scalar product is valid. At this point the definition of our used vector space is complete. We know the description of the vectors and scalar product in the Liouville space

To describe the results of measurements, we need a definition of a correlation function. In the following, a correlation function is derivated in the Liouville space. The natural starting point to determine the time evolution of an operator  $A_i$  is the Heisenberg equation of motion in quantum mechanics.

$$\frac{d}{dt} A_i(t) = \dot{A}_i(t) = \frac{i}{\hbar} [H, A_i(t)] = iL A_i(t) \quad (5.25)$$

The operators are in the Heisenberg representation and the Hermitian Liouville operator  $L = \hbar^{-1} [H, \bullet]$  is introduced, which is defined by its action on an operator. The formal solution of equation (5.25) is given by

$$A_i(t) = e^{itL} A_i(0) = e^{itH/\hbar} A_i(0) e^{-itH/\hbar}. \quad (5.26)$$

In the second step, the definition of the Liouville operator and some algebraic transformations are used. In this notation, it is more clearly that the time evolution of an operator is given by the Liouville operator. The same result is obtained in the Liouville space if the Liouville operator is acting on the basis vectors. The following equation is obtained inserting the dyad product in equation (5.25).

$$|\dot{A}_i(t)\rangle = \frac{i}{\hbar} [H, A_i(t)] = iL|A_i(t)\rangle \quad (5.27)$$

There formal solution is given by

$$|A_i(t)\rangle = e^{itL}|A_i(0)\rangle. \quad (5.28)$$

Beside the Liouville operator, one more operator, called the projection operator, is introduced for the derivation of the correlation function. Therefore, we define a set of operators  $\{C_i\}$ , where the choice of these operators are differently depending on the investigated system and correlation function. The choice of these operators is discussed in chapter 2 and later at the derivation of the formula of the static conductivity. For the moment it is sufficient to know that the set of operators exists. Directly following from the definition of the projection operator in quantum mechanics the projection operator in the Liouville space possesses the form

$$P = \sum_{i,j} |C_i(0)\rangle (C_i(0)|C_j(0)\rangle)^{-1} (C_j(0)|. \quad (5.29)$$

The action of  $P$  on a vector  $|A(t)\rangle$  in the Liouville space yields the parallel components to the chosen operators  $C_i$ , which is the projection from  $|A(t)\rangle$  into the vector subspace spanned by  $C_i$ . The corresponding vertical component of  $|A(t)\rangle$  is given by  $Q = 1 - P$ , which is the projection out of the vector subspace. Naturally the projection operator is fulfilled the two properties  $P^2 = P$  and  $PQ = QP = 0$  of a projection operator, which follows immediately from the definition of  $P$ .

After we know the time evolution of an operator and the projection operator the correlation function is defined as

$$C_{ij}(t) = (A_i(t)|A_j(0)) \stackrel{(5.20)}{=} \frac{1}{\beta} \int_0^\beta d\lambda \langle A_i^\dagger(t) A_j(i\lambda\hbar) \rangle, \quad (5.30)$$

where in the last step the definition of the scalar product is inserted. Comparing equation (5.30) with (5.9) our choice of the correlation function is more clear. The defined correlation function is proportional to the Kubo relaxation function. In the memory-matrix-formalism we want to describe the reaction of an operator as a consequence of a switched off perturbation. This is exactly describes by the Kubo relaxation function, introduced in section 5.1 For  $t = 0$  the correlation function is also proportional to the Fourier transformed susceptibility

$$C_{ij}(t = 0) = \frac{1}{\beta} \Phi_{ij}(t = 0) = \frac{1}{\beta} \chi_{ij}(\omega = 0). \quad (5.31)$$

Equation (5.28) is used to bring the time evolution of the correlation function in more suitable expression.

$$\mathcal{C}_{ij}(t) = (A_i(0)|A_j(-t)) = (A_i(0)|e^{-itL}|A_j(0)) \quad (5.32)$$

The obtained relation is transformed into frequency space using the Laplace transformation. The used Laplace transformation is given by

$$f(\omega) = \int_0^{\infty} dt e^{-i\omega t} f(t) \quad (5.33)$$

Equation for  $\mathcal{C}_{ij}(t)$  is multiplied with  $e^{i\omega t}$  and is integrated from zero to infinity with respect to  $t$ . The Laplace transformed correlation function is given by

$$\mathcal{C}_{ij}(\omega) = (A_i| \int_0^{\infty} dt e^{i(\omega-L)t} |A_j) = (A_i| \frac{i}{\omega-L} |A_j). \quad (5.34)$$

For reasons of clarity the argument  $t = 0$  is not written at the basis vectors any more. Now, the relation  $L = LQ + LP$  which follows immediatly using the definition of  $P$  and  $Q$  together with the identity  $(X + Y)^{-1} = X^{-1} - X^{-1}Y(X + Y)^{-1}$  is used to simplify the correlation function. We chose  $X = \omega - LQ$  and  $Y = -LP$ .

$$\begin{aligned} \mathcal{C}_{ij}(\omega) &= (A_i| \frac{i}{\omega - LQ - LP} |A_j) \\ \Leftrightarrow \mathcal{C}_{ij}(\omega) &= (A_i| \frac{i}{\omega - LQ} |A_j) + (A_i| \frac{1}{\omega - LQ} LP \frac{i}{\omega - L} |A_j) \end{aligned} \quad (5.35)$$

Both terms on the right hand side are considered seperatly. The fraction of the first term is written as the geometric series. It is assumed that  $\frac{LQ}{\omega} < 1$ , which means that the pertubation is assumed to be small.

$$\frac{i}{\omega - LQ} = \frac{i}{\omega} \left[ 1 + \frac{LQ}{\omega} + \left( \frac{LQ}{\omega} \right)^2 + \dots \right] \quad (5.36)$$

Each term of the series in the squard brackets acting on the operator  $|A_j)$ . This is the operator at time  $t = 0$ , which means that no vertical component exists and therefore  $Q|A_j) = 0$ . Every term contains an operator  $Q$ , except of the first one. The first term of the correlation function yields

$$(A_i| \frac{i}{\omega - LQ} |A_j) = \frac{i}{\omega} (A_i|A_j) = \frac{i}{\omega} \mathcal{C}_{ij}(0). \quad (5.37)$$

At the second term only the back is considered. Here the explicit expression of the projection operator 5.29 is inserted. This yields the definition of the Laplace transformed correlation function.

$$P \frac{i}{\omega - L} |A_j) = \sum_{k,l} |C_k)(C_k|C_l)^{-1} (C_l| \frac{i}{\omega - L} |A_j) = \sum_{k,l} |C_k) \mathcal{C}_{kl}^{-1}(0) \mathcal{C}_{lj}(\omega) \quad (5.38)$$



Both simplifications are inserted back and the correlation function is get the formal expression:

$$\mathcal{C}_{ij}(\omega) = \frac{i}{\omega} \mathcal{C}_{ij}(0) + \sum_{k,l} (A_i | \frac{1}{\omega - \text{LQ}} \text{L} | C_k) \mathcal{C}_{kl}^{-1}(0) \mathcal{C}_{lj}(\omega). \quad (5.39)$$

In a last step, the fraction in the second term is more simplified. Therefore, our expression is multiplied with  $\omega$  and the null  $\text{LQ} - \text{LQ}$  is added in the nominator at the fraction. The rearrangement of the fractions yields the following algebraic matrix equation for the correlation function.

$$\begin{aligned} \omega \mathcal{C}_{ij}(\omega) &= i \mathcal{C}_{ij}(0) + \sum_{k,l} (A_i | \frac{\omega}{\omega - \text{LQ}} \text{L} | C_k) \mathcal{C}_{kl}^{-1}(0) \mathcal{C}_{lj}(\omega) \\ \Leftrightarrow \omega \mathcal{C}_{ij}(\omega) &= i \mathcal{C}_{ij}(0) + \sum_{k,l} (A_i | 1 + \frac{\text{LQ}}{\omega - \text{LQ}} \text{L} | C_k) \mathcal{C}_{kl}^{-1}(0) \mathcal{C}_{lj}(\omega) \\ \Leftrightarrow \omega \sum_l \delta_{il} \mathcal{C}_{lj}(\omega) &= i \frac{1}{\beta} \chi_{ij}(0) + \sum_l [\Omega_{il} - i \Sigma_{il}(\omega)] \mathcal{C}_{lj}(\omega) \\ \Leftrightarrow \sum_l [\omega \delta_{il} - \Omega_{il} + i \Sigma_{il}(\omega)] \mathcal{C}_{lj}(\omega) &= i \frac{1}{\beta} \chi_{ij}(0) \end{aligned} \quad (5.40)$$

where equation (5.5) is used and the abbreviations

$$\Omega_{il} := \beta \sum_k (A_i | \text{L} | C_k) \chi_{kl}^{-1}(0) \quad \text{and} \quad \Sigma_{il}(\omega) := i \beta \sum_k (A_i | \frac{\text{LQ}}{\omega - \text{LQ}} \text{L} | C_k) \chi_{kl}^{-1}(0) \quad (5.41)$$

are defined. Equation (5.40) is mostly the final form of our correlation function. This expression is an exact formula to determine the correlation function between two variables in a system. Only in the explicite computation, using diagrammatic perturbation theory for example, assumptions and approximations are made. The sums over  $k$  and  $l$  are originated from the utilization of the projection operator. Therefore, each sum is summarized over all operators included in the set  $\{C_i\}$  of selected operators. The indices  $i$  and  $j$  are chosen out of this set as well. Equation (5.40) yields therefore a  $n^2$  algebraic equations, if  $n$  is the number of operators in  $\{C_i\}$ .

It is useful to write the even defined abbreviations in another form for our later computations. For  $\Omega_{il}$ , we use equation (5.27) to write the time derivative of an operator instead of the Liouville operator.

$$\Omega_{il} = i \beta \sum_k (\dot{A}_i | C_k) \chi_{kl}^{-1}(0). \quad (5.42)$$

For the rearrangement of the second abbreviation, equation (5.27) is used as well. Furthermore, the fraction is written as the geometric series. In every term the relation

$Q = Q^2$  is inserted. After factorizing one  $Q$  to each vector operator the geometric series is written back as a fraction.

$$\begin{aligned}
 \Sigma_{il}(\omega) &= \frac{i\beta}{\omega} \sum_k (\dot{A}_i | Q \left[ 1 + \frac{LQ}{\omega} + \left( \frac{LQ}{\omega} \right)^2 + \dots \right] | \dot{C}_k) \chi_{kl}^{-1}(0) \\
 \Leftrightarrow \Sigma_{il}(\omega) &= \frac{i\beta}{\omega} \sum_k (\dot{A}_i | Q^2 + \frac{Q^2 L Q^2}{\omega} + \frac{Q^2 L Q^2 L Q^2}{\omega^2} + \dots | \dot{C}_k) \chi_{kl}^{-1}(0) \\
 \Leftrightarrow \Sigma_{il}(\omega) &= \frac{i\beta}{\omega} \sum_k (\dot{A}_i | Q \left[ 1 + \frac{QLQ}{\omega} + \left( \frac{QLQ}{\omega} \right)^2 + \dots \right] Q | \dot{C}_k) \chi_{kl}^{-1}(0) \\
 \Leftrightarrow \Sigma_{il}(\omega) &= i\beta \sum_k (\dot{A}_i | Q \frac{1}{\omega - QLQ} Q | \dot{C}_k) \chi_{kl}^{-1}(0)
 \end{aligned} \tag{5.43}$$

After all this exhausting mathematical and algebraical conversions the correlation function in the memory matrix formalism is in a useful and workable form. In equation (5.40) the abbreviations is combined to one function  $M_{il}(\omega) := \Sigma_{il}(\omega) + i\Omega_{il}$ . The symbol  $\Sigma$  is selected in dependence on the quantum mechanical self energy. The function  $M(\omega)$  is called the mass operator in quantum field theory and the memory function in non-equilibrium physics.

Let us discuss the physical meaning of  $\Omega$  and  $\Sigma(\omega)$  in more detail. The quantity  $\Omega$  always vanishes in the case, if the considered Hamiltonian possesses time reversal symmetry and if the operators  $A_i$  and  $A_k$  transform with the same sign under time reversal symmetry. Under these conditions  $(\dot{A}_i | A_k) = 0$ . This assertion is immediatly proven extensivly in the section below. In this case, the memory function is solely given by the function  $\Sigma(\omega)$ . If we compare equation (5.43) with the definition of the correlation function (5.30) the string analogy is visable.  $\Sigma(\omega)$  is different in two aspects.  $Q | \dot{A}$  forms the basis vectors of the expectation value, which is perpendicular to  $|A\rangle$ . On the other hand only the reduced Liouville operator  $QLQ$  contribute to the expectation value.

The latter one projects at the part of the full Liouville operator  $L$ , which causes the intrinsic fluctuations of the operator  $A$ . This means that the function  $\Sigma(\omega)$  describes the dynamic of the operators. In other words the operators  $QLQ$  describes the internal dynamics of all other degrees of freedom of the system excluded  $A$ . This is called the *bath*. The coupling to the bath is characterised by  $Q | \dot{A}$  and is clearly changed the dynamics of  $A$ .

### 5.2.1 Time Reversal Symmetry

Even above the assertion is postulated that the quantity  $\Omega_{il}$  vanishes, if the considered Hamiltonian is symmetric and if the operators  $\dot{A}$  and  $A$  have different sign under time reversal symmetry. In the following section the evidence of this statement is proven. Our starting point is the introduction of the time reversal operator  $T$  by the transformation rule

$$A(t) \rightarrow A'(t) = TA(t)T^{-1} = \epsilon_A A(-t), \tag{5.44}$$

where  $\epsilon_A$  supposes two different values, +1 or -1. The first one is taken by the physical quantity as position or electrical field, while the latter is taken by physical quantity as momentum, angular momentum or magnetic field. The action of T with respect to the time evolution of an operator is investigated firstly.

$$T e^{iHt/\hbar} T^{-1} = e^{-iHt/\hbar} \quad (5.45)$$

The Hamiltonian is assumed to be invariant under time reversal symmetry. The only changed quantity is therefore the explicit time argument  $t$ . The action of the time reversal operator on the time derivative of the time evolution of an operator is given by

$$T \frac{\partial}{\partial t} e^{iHt/\hbar} T^{-1} = \frac{i}{\hbar} T H e^{iHt/\hbar} T^{-1} = \frac{i}{\hbar} T H T^{-1} T e^{iHt/\hbar} T^{-1} = \frac{i}{\hbar} H e^{-iHt/\hbar}. \quad (5.46)$$

In the second step, the unit element  $\mathbb{1} = T T^{-1}$  is inserted. To get the commutator relation between T and H, the time variable  $t$  is set to zero and the equation is multiplied by T from the right.

$$[H, T] = 0. \quad (5.47)$$

This is equivalent to the assumption of an invariant Hamiltonian with respect to time reversal symmetry. The expectation value of a Hermitian operator is manipulated with the time reversal operator T.

$$\langle B \rangle = \frac{1}{Z} \text{Tr} \left\{ e^{-\beta H} T B T^{-1} \right\} = \left\langle (T B T^{-1})^\dagger \right\rangle \quad (5.48)$$

Here the invariance of the trace with respect to cycling permutation and the commutator relation between T and H is used. The anti-unitarity of the time reversal operator and the hermiticity of B is further utilized. The same is done with the commutator between two Hermitian operators.

$$\left( T [A(t), B(t')] T^{-1} \right)^\dagger = \epsilon_A \epsilon_B \left( [A(-t), B(-t')] \right)^\dagger = -\epsilon_A \epsilon_B [A(-t), B(-t')] \quad (5.49)$$

As seen in equation (5.42),  $\Omega_{il}$  is proportional to the correlation function  $(\dot{A}_i | A_k)$  between a time derivative quantity  $\dot{A}_i$  and the quantity  $A_k$ . The use of equation (5.12) yields

$$i\beta (\dot{A}_i | A_k) = i\chi_{\dot{A}_i A_k}(\omega = 0) = i \text{P.V.} \int_{-\infty}^{\infty} \frac{d\omega'}{\pi} \frac{\chi''_{\dot{A}_i A_k}(\omega')}{\omega'} - \lim_{\omega \rightarrow 0} \chi''_{\dot{A}_i A_k}(\omega). \quad (5.50)$$

Here the dissipative susceptibility  $\chi''_{\dot{A}_i A_k}(\omega)$  occurs. The difference to  $\chi''_{A_i A_k}(\omega)$  is the time derivative of an operator. Nevertheless, the one dissipative susceptibilities

is achieved from the other one. To find the relation between both the derivative of (5.10) is evaluated.

$$\frac{d}{dt}\chi''_{A_i A_k}(t) = \frac{1}{2} \left\langle \left[ \dot{A}_i(t), A_k(0) \right] \right\rangle = \chi''_{\dot{A}_i A_k}(t) \quad (5.51)$$

We express both susceptibilities by their Fourier transformions and we obtain

$$\chi''_{\dot{A}_i A_k}(\omega) = -i\omega \chi''_{A_i A_k}(\omega) \quad (5.52)$$

This is inserted into (5.50), which yields

$$i\beta(\dot{A}_i|A_k) = \text{P.V.} \int_{-\infty}^{\infty} \frac{d\omega'}{\pi} \chi''_{A_i A_k}(\omega'), \quad (5.53)$$

where the limit  $\omega$  is evaluated. This result entails two very important advantages. The physical meaning of the quantity  $\Omega_{il}$  becomes clearer, since  $\Omega_{il}$  is associated with dissipative processes by  $\chi''_{A_i A_k}(\omega')$ . On the other hand the founded expression establishes the possibility to analyse the behaviour of  $\Omega_{il}$  under time reversal symmetry. The dissipative susceptibility in equation (5.10) is now observed. The expectation value is rewritten using equation (5.48) and (5.49).

$$\chi''_{A_i A_k}(t - t') = \frac{1}{2} \left\langle [A_i(t), A_k(t')] \right\rangle = -\epsilon_{A_i} \epsilon_{A_k} \chi''_{A_i A_k}(t' - t), \quad (5.54)$$

where the relation (5.11) is used. The Laplace transformation of this equation yields

$$\chi''_{A_i A_k}(\omega) = -\epsilon_{A_i} \epsilon_{A_k} \chi''_{A_i A_k}(-\omega) = \epsilon_{A_i} \epsilon_{A_k} \chi''_{A_i A_k}(\omega), \quad (5.55)$$

where the antisymmetry of the commutator with respect of interchanging both operators is utilized. Two cases has to be investigated analyzing the analytical properties of  $\chi''_{A_i A_k}(\omega)$ , which are  $\epsilon_{A_i} = \epsilon_{A_k}$  and  $\epsilon_{A_i} \neq \epsilon_{A_k}$ . The analysis gives the required properties to compute the integral over the dissipative susceptibility.

**1. case:**  $\epsilon_{A_i} = \epsilon_{A_k}$

This yields  $\chi''_{A_i A_k}(\omega) = \chi''_{A_k A_i}(\omega)$ , which means that the dissipative susceptibility is symmetrical under interchanging  $A_i$  and  $A_k$ . The dissipative susceptibility is further an antisymmetrical function with respect to  $\omega$ , since  $\chi''_{A_i A_k}(\omega) = -\chi''_{A_i A_k}(-\omega)$ . The complex conjugated of  $\chi''_{A_i A_k}(\omega)$  yields, that the dynamical susceptibility is a real number.

$$\left( \chi''_{A_i A_k}(\omega) \right)^* = - \int_{-\infty}^{\infty} dt e^{-i\omega(t-t')} \chi''_{A_i A_k}(t - t') = -\chi_{A_i A_k}(-\omega) = \chi_{A_i A_k}(\omega) \quad (5.56)$$

Here equation (5.11) is used.

**2. case:**  $\epsilon_{A_i} \neq \epsilon_{A_k}$

If the sign of  $A_i$  and  $A_k$  is different under time reversal symmetry, the dissipative susceptibility is antisymmetric under the interchange of both operators. This yields  $\chi''_{A_i A_k}(\omega) = -\chi''_{A_k A_i}(\omega)$ . For the same reason  $\chi''_{A_i A_k}(\omega)$  is a symmetrical function with respect to  $\omega$ , since  $\chi''_{A_i A_k}(\omega) = \chi''_{A_i A_k}(-\omega)$ . Towards the first case, the dissipative susceptibility is an imaginary number, ensuring by the complex conjugation of  $\chi''_{A_i A_k}(\omega)$ .

$$\left(\chi''_{A_i A_k}(\omega)\right)^* = - \int_{-\infty}^{\infty} dt e^{-i\omega(t-t')} \chi''_{A_i A_k}(t-t') = -\chi_{A_i A_k}(-\omega) = -\chi_{A_i A_k}(\omega) \quad (5.57)$$

The integral in equation (5.53) is now solvable for one of these cases. We see that the integral vanishes in the first case, since the susceptibility is an odd function. This means that  $i\beta(\dot{A}_i|A_k)$  is always zero, if the operators  $A_i$  and  $A_k$  have the same signature with respect to time reversal symmetry and the Hamiltonian is invariant under time reversal symmetry.

### 5.3 The Formula of the Static Conductivity

In this section, the formula for the static electrical conductivity is derived. The considered system is the spin-fermion-model, described by the Hamiltonian  $H$ , perturbed by umklapp scattering  $H_{\text{umklapp}}$ . Both Hamiltonians are denoted in 3. The static electrical conductivity is given by the current current correlation function, as shown in (2.7). To get the correlation function in the memory-matrix-formalism, equation (2.5) has to be solved.

Equally to the discussion in chapter 2, momentum  $P$  and current  $J$  are chosen as the subspace operators of the projection operator. Again,  $J$  and  $P$  possess the same sign and the Hamiltonian is still invariant under time reversal symmetry. As a consequence the quantity  $\Omega_{il}$  in equation (2.5) vanishes. In comparison to the discussion in chapter 2, momentum is now unconserved. The time derivatives with respect to  $P$  in  $\Sigma_{il}(\omega)$  do not vanish. The condition that  $Q|\dot{J})$  vanishes is still valid as discussed in chapter 2. Since the time derivative of  $P$  does not vanish, the object  $Q|\dot{P})$  occurs. The  $J$ - $P$  subspace is defined with respect to the unperturbed Hamiltonian  $H$ , where momentum is conserved. The value of the time derivative of  $P$  is only determined by the perturbation and lies completely out of the  $J$ - $P$  subspace. Therefore,  $Q|\dot{P}) = |\dot{P})$  is valid. For the same reason, the reduced Liouville operator  $QLQ$  is assumed to be as  $L$ . All other discussed conditions in chapter 2 are still valid. The algebraic matrix equation for the correlation function is given by

$$\begin{pmatrix} \omega & 0 \\ -i\Sigma_{PJ}(\omega) & \omega - i\Sigma_{PP}(\omega) \end{pmatrix} \cdot \begin{pmatrix} C_{JJ}(\omega) & C_{JP}(\omega) \\ C_{PJ}(\omega) & C_{PP}(\omega) \end{pmatrix} = \frac{i}{\beta} \begin{pmatrix} \chi_{JJ}(0) & \chi_{JP}(0) \\ \chi_{PJ}(0) & \chi_{PP}(0) \end{pmatrix} \quad (5.58)$$

The current current correlation function is needed for computing the electrical conductivity. In the memory-matrix-formalism, the definition of this correlation function

is given by the following formula in frequency space.

$$\mathcal{C}_{JJ}(\omega) = \langle J | \frac{i}{\omega - L} | J \rangle \quad (5.59)$$

Equally to the procedure in chapter 2 the current operator is expressed as an parallel and perpendicular component. The parallel component is still identified with the projection from  $|J\rangle$  onto  $|P\rangle$ . The current operator is seperated in the expression above, producing for new correlation functions. Two of them are zero, since  $|J_{||}\rangle$  and  $|J_{\perp}\rangle$  are orthogonal. As discussed in chapter 2, the correlation function containing the perpendicular part represents the noisy background. In the further calculation this term is dropped, since the origin is chosen at this value. A detailed discussion is given in [Jun07]. The current curent correlation function is therefore given by

$$\mathcal{C}_{JJ}(\omega) = \langle J_{||} | \frac{i}{\omega - L} | J_{||} \rangle = \frac{|\chi_{PJ}|^2}{|\chi_{PP}|^2} \mathcal{C}_{PP}(\omega) \quad (5.60)$$

Equation (2.9) is used in the second step. The momentum momentum correlation function is readed out of equation (5.58). Therefore the inverse of the memory matrix is multiplied from the left. The following expression is obtained for the momentum momentum correlation function

$$\mathcal{C}_{PP}(\omega) = \frac{i}{\beta} \cdot \frac{i\Sigma_{PJ}(\omega)\chi_{JP}(0)}{\omega(\omega - i\Sigma_{PP}(\omega))} + \frac{i}{\beta} \cdot \frac{\chi_{PP}(0)}{\omega - i\Sigma_{PP}(\omega)} \approx \frac{i}{\beta} \cdot \frac{i\chi_{PP}(0)}{\Sigma_{PP}(\omega)} \quad (5.61)$$

In the last step, the limit of small frequencies  $\omega$  is made. The first term is proportional to  $\omega^{-2}$  and is therefore assmued to be small, comparing to the second one. This equation is inserted in (5.60), while this one is then again inserted in (2.7). This yields the following formula for the static electrical conductivity:

$$\sigma_{dc} = \lim_{\omega \rightarrow 0} \beta \mathcal{C}_{JJ}(\omega) = \frac{i}{\beta} \lim_{\omega \rightarrow 0} |\chi_{PJ}|^2 \left( \dot{P} | \frac{1}{\omega - L_0} | \dot{P} \right)^{-1} = -\beta^{-1} \lim_{\omega \rightarrow 0} |\chi_{PJ}|^2 \mathcal{C}_{PP}^{-1}(\omega). \quad (5.62)$$

Here the definition (5.43) of the memory function  $\Sigma_{PP}(\omega)$  and the definition of the correlation function in fequency space (5.34) is used. Above, it is discussed that the replacing of QLQ by L is valid. The  $\dot{P}$ - $\dot{P}$  correlation function is now transformed in an integral equation. In this representation the use of diagrammatic pertubation theory is possible.

$$\begin{aligned} \mathcal{C}_{\dot{P}\dot{P}}(\omega) &= \int_0^\infty dt e^{i\omega t} \mathcal{C}_{\dot{P}\dot{P}}(t) = \beta^{-1} \int_0^\infty dt e^{i\omega t} \int_0^\beta d\lambda \langle \dot{P}^\dagger(t) \dot{P}(0) \rangle \\ \Leftrightarrow \mathcal{C}_{\dot{P}\dot{P}}(\omega) &= \beta^{-1} \Phi_{\dot{P}\dot{P}}(\omega) = \frac{i\omega^{-1}}{\beta} \left[ \chi_{\dot{P}\dot{P}}(\omega) - \underbrace{\chi_{\dot{P}\dot{P}}(\omega=0)}_{=0} \right] \\ \Leftrightarrow \mathcal{C}_{\dot{P}\dot{P}}(\omega) &= -\frac{\omega^{-1}}{\beta} \int_0^\infty dt e^{i\omega t} \langle [\dot{P}(t), \dot{P}(0)] \rangle_0 \end{aligned} \quad (5.63)$$

### 5.3 The Formula of the Static Conductivity

The correlation function is transformed into time space and the definition of the scalar product (5.20) is used. This expression is equivalent to the Fourier transformed Kubo relaxation function. In frequency space, the Kubo relaxation function is connected with the susceptibility by relation (5.5). Since the time derivative of  $P$  is zero at  $t = 0$ , the static susceptibility vanishes. The susceptibility is again transformed into time space and the definition (5.2) is used.

Inserting this expression in our obtained equation for the static electrical conductivity, the final form of their is given by

$$\sigma_{\text{dc}} = \lim_{\omega \rightarrow 0} \frac{\omega |\chi_{\text{JP}}(\omega = 0)|^2}{\int_0^{\infty} dt e^{i\omega t} \left\langle \left[ \dot{P}(t), \dot{P}(0) \right] \right\rangle_0}, \quad (5.64)$$





## 6 Conclusion



# A Computation of the Damped Spin Density Propagator

In the present appendix, the propagator of damped spin density fluctuations is computed, considering the first order in perturbation theory. Our approach is separated in two parts. Firstly, the free spin density propagator is determined, using the equation of motion for Green functions, as suggested in [EG79] or many other textbooks. The damped propagator is then calculated, using the diagrammatic perturbation theory. The obtained propagator is transformed into Matsubara frequency space, since the computation of the conductivity is treated into there.

## A.1 Computation of the Free Propagator

Free propagators are easily computed, using the equation of motion of Green functions. The equation of motion is obtained, derivating the Green function with respect to the time  $t$ . In Fourier space the equation of motion is given by

$$\omega \langle \langle A; B \rangle \rangle_{\omega}^j = \langle [A, B]_{\eta} \rangle + \langle \langle [A, H]_{-}; B \rangle \rangle_{\omega}^j, \quad (\text{A.1})$$

where the typ of the Green function (retarded, advanced and causal) is denoted with  $j$  and the frequency dependence of the Green function is represented with an index  $\omega$ . The Green function itself is symbolized by double angle brackets. This equation is an algebraic equation or more precisely an infinite algebraic equation chain for Green functions. A new more complicated Green function appears on the right hand side. For this one exists a new equation chain with a more complicated Green function, and so on. Nevertheless, the equation chain is not infinity in the case of free propagators. The dynamic of free spin density waves is described by the Hamiltonian  $H_{\Phi}$  (see equation (3.5)). The operators  $A$  and  $B$  are replaced by bosonic field operators  $\Phi_{\mu}(\mathbf{k} + \mathbf{G}, t)$  and  $\Phi_{\mu}(-\mathbf{k} - \mathbf{G}, t)$ , respectively. During the computation, the abbreviation  $\langle \langle \Phi_{\mu}; \Phi_{\mu} \rangle \rangle_{\omega}$  is used, where the argument of the field operators is dropped. The first field operator is always considered with the momentum argument  $\mathbf{k} + \mathbf{G}$ , while the second one has opposite sign. The time argument is equal for both operators. The equation of motion is given by

$$\omega \langle \langle \Phi_{\mu}; \Phi_{\mu} \rangle \rangle_{\omega} = \langle [\Phi_{\mu}(\mathbf{k} + \mathbf{G}), \Phi_{\mu}(-\mathbf{k} - \mathbf{G})] \rangle + \langle \langle [\Phi_{\mu}(\mathbf{k} + \mathbf{G}), H_{\Phi}]; \Phi_{\mu} \rangle \rangle_{\omega} \quad (\text{A.2})$$

Both commutators are evaluated on the right hand side, using the bosonic commutator relations. The inhomogeneity is trivially zero, since the commutator relation is zero

per definition. The commutator, contained in the Green function, is given by

$$\begin{aligned}
 [\Phi_\mu(\mathbf{k} + \mathbf{G}, t), H_\Phi] &= -\frac{v_S^2}{2} \sum_\lambda \int_{\mathbf{p}} [\Phi_\mu(\mathbf{k} + \mathbf{G}, t), \pi_\lambda(\mathbf{p}, t) \pi_\lambda(-\mathbf{p}, t)] \\
 \Leftrightarrow [\Phi_\mu(\mathbf{k} + \mathbf{G}, t), H_\Phi] &= -\frac{v_S^2}{2} \sum_\lambda \int_{\mathbf{p}} \left[ \pi_\lambda(\mathbf{p}, t) [\Phi_\mu(\mathbf{k} + \mathbf{G}, t), \pi_\lambda(-\mathbf{p}, t)] \right. \\
 &\quad \left. + [\Phi_\mu(\mathbf{k} + \mathbf{G}, t), \pi_\lambda(\mathbf{p}, t)] \pi_\lambda(-\mathbf{p}, t) \right] \\
 \Leftrightarrow [\Phi_\mu(\mathbf{k} + \mathbf{G}, t), H_\Phi] &= -iv_S^2 \pi_\mu(\mathbf{k} + \mathbf{G}, t).
 \end{aligned} \tag{A.3}$$

The obtained result of the commutator is inserted in equation (A.2). This relation is the first term of the equation chain.

$$\omega \langle \langle \Phi_\mu; \Phi_\mu \rangle \rangle_\omega = -iv_S^2 \langle \langle \pi_\mu; \Phi_\mu \rangle \rangle_\omega \tag{A.4}$$

Equally to the initial Green function an algebraic equation chain is established for the Green function of the right hand side.

$$\omega \langle \langle \pi_\mu; \Phi_\mu \rangle \rangle_\omega = \langle [\pi_\mu(\mathbf{k} + \mathbf{G}, t), \Phi_\lambda(-\mathbf{k} - \mathbf{G}, t)] \rangle + \langle \langle [\pi_\mu(\mathbf{k} + \mathbf{G}, t), H_\Phi]; \Phi_\mu \rangle \rangle_\omega \tag{A.5}$$

The inhomogeneity is directly given by the commutator relations and yields  $-i$ . The commutator of the Green function is evaluated to  $[\pi_\mu(\mathbf{k} + \mathbf{G}, t), H_\Phi] = i((\mathbf{k} + \mathbf{G})^2 + r_0) \Phi_\mu(\mathbf{k} + \mathbf{G}, t)$ . Inserting our results in the (A.5), the initial Green function is obtained on the right hand side. This and (A.4) are an equation system, which is solved with respect to  $\langle \langle \Phi_\mu; \Phi_\mu \rangle \rangle_\omega$ .

$$\mathcal{D}_\mu^{(0)}(\mathbf{k}, \omega) := \langle \langle \Phi_\mu; \Phi_\mu \rangle \rangle_\omega = \sum_{\mathbf{G}} \frac{1}{(\mathbf{k} + \mathbf{G})^2 + r_0 - (flatfrac{\omega v_S}{\omega v_S})^{-2}} \tag{A.6}$$

## A.2 Consideration of Damping in the Spin Density Propagator

An interaction between electrons on different Fermi surfaces is considered in the spin-fermion-model. This interaction is originated by spin fluctuations and their damping is governed by the decay of partile-hole-excitations. The usual diagrammatic perturbation theory is used for considering the damping of the spin fluctuations. The full spin density wave propagator is given by

$$\mathcal{D}_\mu(\mathbf{k}, t - t') = -i \langle \mathcal{T}_t U(\infty, -\infty) \Phi_\mu(\mathbf{k} + \mathbf{G}, t) \Phi_\mu(-\mathbf{k} - \mathbf{G}, t') \rangle_0 \tag{A.7}$$

where  $\mathcal{T}_t$  is the time ordering operator. The index 0 denotes that the expectation value is performed with respect to the unpertubated Hamiltonian. The interaction is only incorporated through the time evolution operator  $U$ , which is given by

$$U(t, t') = \exp \left( -i \int_{t'}^t dt_1 H_{\text{int}}(t_1) \right). \tag{A.8}$$

## A.2 Consideration of Damping in the Spin Density Propagator

The full Green function  $\mathcal{D}_\mu$  is developed into a Dyson series, similar to the derivation of Landau's Fermi liquid theory illustrated in many textbooks about quantum field theory in condensed matter [Nol09]. The free propagator is denoted with an upper bracketed index 0. A new object  $\Pi$  is introduced, called the polarization operator. In general, this object is an infinite series, containing the interaction between spin fluctuation and fermions. The Dyson equation is solved using the geometric series.

$$\mathcal{D}_\mu = \mathcal{D}_\mu^{(0)} + \mathcal{D}_\mu^{(0)} \Pi_\mu \mathcal{D}_\mu \quad \Rightarrow \quad \mathcal{D}_\mu = \frac{1}{(\mathcal{D}_\mu^{(0)})^{-1} - \Pi_\mu} \quad (\text{A.9})$$

The polarization operator is separated into a real and imaginary part. The latter is interpreted as a lifetime, while the real part is an energy correction. In consequence of a finite lifetime the spin fluctuations are damped. Our next treatment is to identify the leading diagrams contained in the polarization operator.

Therefore, the time evolution operator is expanded up to the second order. The zeroth order yields the free propagator, calculated above, while the first order vanishes. One bosonic field operator is contained in the interaction Hamiltonian  $H_{\Psi\Phi}$  (3.6). Furthermore, two bosonic field operators are given by the definition of the Green function. An expectation value of three bosonic operators is generated in the first order. Wick's theorem yields that each expectation value of an odd number of operators is always zero.

The first correction to the free Green function is considered in the second order of series expansion. For the fermionic expectation values, Wick's theorem can not be used as simple as usual, since the fermionic field operators are connected via Pauli matrices. The fermionic expectation value is given in the following form:

$$\text{EV} := \left\langle \mathcal{T}_t \Psi_\alpha^\dagger(\mathbf{p}_4, t_2) \cdot \sigma_{\lambda'} \cdot \Psi_\beta(\mathbf{p}_3, t_2) \cdot \Psi_\gamma^\dagger(\mathbf{p}_2, t_1) \cdot \sigma_\lambda \cdot \Psi_\beta(\mathbf{p}_1, t_1) \right\rangle. \quad (\text{A.10})$$

Here  $\alpha, \beta, \gamma, \delta \in \{a, b\}$ , where two greek letters have to be an "a", while the other ones a "b". The quantum numbers of the field operators are denoted with  $\nu_i$ , where  $i = 1, 2, 3, 4$ . These kinds of expectation values are evaluated using Fierz identity. A product of two Pauli matrices are rewritten as the following relation, where  $\delta$  is the Kroncker symbol.

$$\sum_{\mu=1}^3 \sigma_{ij}^\mu \sigma_{kl}^\mu = 2\delta_{il}\delta_{jk} - \delta_{ij}\delta_{kl} \quad (\text{A.11})$$

For using Fierz identity the product of field operators and Pauli matrices is written in component representation. For reasons of clarity, the argument of the field operators are abbreviated by  $\nu_i$ ,  $i = 1, 2, 3, 4$ .

$$\begin{aligned} \text{EV}_F &= \sum_{\mu} \left\langle \left( \Psi_\alpha^\dagger(\nu_1) \right)_i \cdot \sigma_{ij}^\mu \cdot \left( \Psi_\beta(\nu_2) \right)_j \cdot \left( \Psi_\gamma^\dagger(\nu_3) \right)_k \cdot \sigma_{kl}^\mu \cdot \left( \Psi_\delta(\nu_4) \right)_l \right\rangle \\ \Leftrightarrow \text{EV}_F &= (2\delta_{il}\delta_{jk} - \delta_{ij}\delta_{kl}) \left\langle \left( \Psi_\alpha^\dagger(\nu_1) \right)_i \left( \Psi_\beta(\nu_2) \right)_j \left( \Psi_\gamma^\dagger(\nu_3) \right)_k \left( \Psi_\delta(\nu_4) \right)_l \right\rangle \end{aligned}$$

$$\Leftrightarrow \text{EV}_F = 2 \left\langle \Psi_\alpha^\dagger(\nu_1) \Psi_\delta(\nu_4) \Psi_\beta(\nu_2) \Psi_\gamma^\dagger(\nu_3) \right\rangle \delta_{\nu_3, \nu_4} - \left\langle \Psi_\alpha^\dagger(\nu_1) \Psi_\beta(\nu_2) \Psi_\gamma^\dagger(\nu_3) \Psi_\delta(\nu_4) \right\rangle \quad (\text{A.12})$$

The arising  $\delta$ -distribution is generated interchanging the field operators. In the next step, the remained expression is investigated under an explicitly choice of the greek letters. Two of the greek letters have to be always equal. Therefore only expectation values contribute, where one creation and one annihilation operator are dedicated by the same fermion species, a or b. Otherwise, the expectation value is zero. Equation (A.12) is used to express the obtained fermionic expectation values as (A.10). For using the definition of the Green function, the operators are sorted, that all annihilation operators are on the left side of the creation operators. A  $\delta$ -distribution is produced each time commuting a creation and an annihilation operator. The obtained expression for  $\mathcal{D}$  in second order perturbation theory is given by

$$\begin{aligned} \mathcal{D}_\mu^{(2)}(\mathbf{k}, \omega) &= (-i)^3 \lambda^2 \int_{-\infty}^{\infty} dt_1 dt_2 \int_{\mathbf{p}_1} \int_{\mathbf{p}_2} \\ &\times \left\langle \mathcal{T}_t \Phi_{\lambda'}(\mathbf{p}_2 - \mathbf{p}_1, t_2) \Phi_{\lambda}(\mathbf{p}_1 - \mathbf{p}_2, t_1) \Phi_{\mu}(\tilde{\mathbf{k}}, t) \Phi_{\mu}(-\tilde{\mathbf{k}}, t') \right\rangle_0 \\ &\times \left( \left\langle \mathcal{T}_t \Psi_a(\mathbf{p}_2, t_1) \Psi_a^\dagger(\mathbf{p}_2, t_2) \right\rangle_0 \left\langle \mathcal{T}_t \Psi_b(\mathbf{p}_1, t_2) \Psi_b^\dagger(\mathbf{p}_1, t_1) \right\rangle_0 \right. \\ &\left. + \left\langle \mathcal{T}_t \Psi_b(\mathbf{p}_2, t_1) \Psi_b^\dagger(\mathbf{p}_2, t_2) \right\rangle_0 \left\langle \mathcal{T}_t \Psi_a(\mathbf{p}_1, t_2) \Psi_a^\dagger(\mathbf{p}_1, t_1) \right\rangle_0 \right). \quad (\text{A.13}) \end{aligned}$$

For reasons of clarity, the momentum vectors are abbreviated as  $\tilde{\mathbf{k}} = \mathbf{k} + \mathbf{G}$ . Wick's theorem is now Utilized for the bosonic expectation value, which yields two possible contractions. All these obtained diagrams are of the same structure. These diagrams can be transfer to each other by interchange the acting point of the bosonic propagators or by interchange the fermionic propagators. Therefore all diagrams yield the same contribution and it is enough to compute one of them. This diagram is depicted in figure A.1 and is called bubble diagram. The bubble diagram is the lowest order of the full polarization operator. In the following this diagram is computed in detail. The first order of the polarization bubble is given by

$$\Pi_\mu^{(0)}(\mathbf{k}, \omega) = i \sum_{\mathbf{p}} \int_{|p| \leq p_F} \frac{d^2 \mathbf{p}}{(2\pi)^2} \int_{-\infty}^{\infty} \frac{d\epsilon}{2\pi} \mathcal{G}_a^{(0)}(\mathbf{p} + \frac{\mathbf{k}}{2}, \epsilon + \frac{\omega}{2}) \mathcal{G}_b^{(0)}(\mathbf{p} - \frac{\mathbf{k}}{2}, \epsilon - \frac{\omega}{2}). \quad (\text{A.14})$$

Here the outer momentum and frequency is shifted to symmetrize the argument of both fermionic Green functions. The Green function is given by

$$\mathcal{G}_\alpha^{(0)}(\mathbf{k}, \omega) := \langle \langle \Psi_\alpha; \Psi_\alpha^\dagger \rangle \rangle_\omega = \sum_{\mathbf{G}} \frac{1}{\omega - \epsilon_\alpha(\mathbf{k} + \mathbf{G})}, \quad (\text{A.15})$$

where the species of the corresponding fermions is indicated with the index  $\alpha = a, b$ . First of all, the dispersion relation of the fermions is investigated. Spin fluctuations

## A.2 Consideration of Damping in the Spin Density Propagator

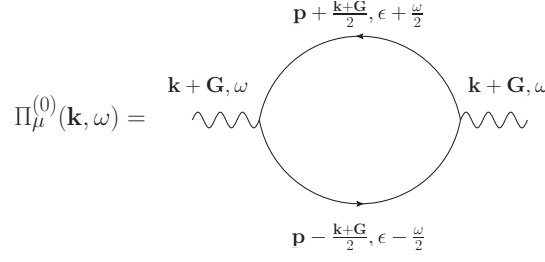


Figure A.1: This figure shows the first bubble diagram of the electronic polarization bubble caused by spin fluctuations. The momentum ( $\mathbf{k} + \mathbf{G}$ ) and frequency ( $\omega$ ) transfer, originated from spin fluctuations, is divided on both fermionic lines (continuous line).

interact only with fermions near the Fermi surface. Under this condition, the dispersion relation of the fermions of species a is expanded.

$$\begin{aligned}
 \epsilon_a(\mathbf{p} + \frac{\mathbf{k} + \mathbf{G}}{2}) &= \frac{(p_x + \frac{k_x + G_x}{2})^2}{2m_1} + \frac{(p_y + \frac{k_y + G_y}{2})^2}{2m_2} \\
 \Leftrightarrow \epsilon_a(\mathbf{p} + \frac{\mathbf{k} + \mathbf{G}}{2}) &= \frac{p_x^2}{2m_1} + \frac{1}{2} \frac{p_x}{m_1} (k_x + G_x) + \frac{(k_x + G_x)^2}{8m_1} \\
 &\quad + \frac{p_y^2}{2m_2} + \frac{1}{2} \frac{p_y}{m_2} (k_y + G_y) + \frac{(k_y + G_y)^2}{8m_2} \\
 \Leftrightarrow \epsilon_a(\mathbf{p} + \frac{\mathbf{k} + \mathbf{G}}{2}) &\approx \xi_a + \frac{1}{2} \mathbf{v}_{a,F}(\mathbf{k} + \mathbf{G}) + \mu
 \end{aligned} \tag{A.16}$$

where the quadratic term with respect to  $\mathbf{k}$  is neglected and  $\xi_a$  is the dispersion denoted in equation (3.9). Moreover, the velocity  $\mathbf{v}_a$  of the fermion of species a is introduced. Since only fermions near the Fermi surface are considered the velocity is assumed to be the Fermi velocity. The same procedure is valid for the fermions of species b. Finally, the normalized momentum vector  $\mathbf{n} = \frac{\mathbf{p}}{|\mathbf{p}|}$  is introduced. The Fermi velocity of fermions of species a is then given by  $\mathbf{v}_{a,F} = v_{a,F} \mathbf{n}$  and equally for b. The scalar product between the normalized momentum vector  $\mathbf{n}$  and the bosonic spin density wave vector  $\mathbf{k} + \mathbf{G}$  is rewritten as the magnitude multiplied with  $\cos(\vartheta)$ , where  $\vartheta$  is the angle between both.

In the investigated model, the points of interaction between the fermions caused by spin fluctuations are hot-spots (see chapter 3). These are certain points on the Fermi surface separated by the momentum vector  $\mathbf{Q}$ . The energy and the magnitudes of the Fermi velocities are equal on these points connected by  $\mathbf{Q}$ .

$$\xi := \xi_a = \xi_b \quad v_F := v_{a,F} = v_{b,F} \tag{A.17}$$

The direction of the velocities have to be unequal. Otherwise, the angle  $\vartheta$  is 0 or  $\pi$  and the imaginary part of  $\Pi_\mu$  is zero. Using these conversions and assumptions, the

polarization operator is given by

$$\begin{aligned} \Pi_{\mu}^{(0)}(\mathbf{k}, \omega) &= i\nu_F \int_0^{\pi} d\vartheta \int_{\xi \leq \xi_F} d\xi \int_{-\infty}^{\infty} \frac{d\epsilon}{2\pi} \\ &\quad \times \frac{1}{\epsilon + \frac{\omega}{2} - \xi - \frac{1}{2}v_F|\mathbf{k} + \mathbf{G}|\cos(\vartheta) + i\eta \operatorname{sign}(\epsilon + \frac{\omega}{2})} \\ &\quad \times \frac{1}{\epsilon - \frac{\omega}{2} - \xi + \frac{1}{2}v_F|\mathbf{k} + \mathbf{G}|\cos(\vartheta) + i\eta \operatorname{sign}(\epsilon - \frac{\omega}{2})}. \end{aligned} \quad (\text{A.18})$$

Here, the two dimensional momentum integral is firstly transformed in plane polar coordinates and then the  $k$ -integral is transformed into an energy integral over the density of states. The density of states is approximated with the value of the density of states at the Fermi surface,  $\nu_F := \nu(\xi_F)$ , since only fermions near the Fermi surface are considered. The energy integral is limited by the Fermi energy  $\xi_F$ .

The further treatment is started by computing the frequency integral. The integral over  $\epsilon$  is transformed into a complex contour integral, where the contour  $\Gamma$  is chosen in two different ways. According to the singularities of the integrand the contour is closed in the upper or lower half plane using a semicircle with radius infinity. In both cases the contribution of the semicircle is zero, since the integrand is proportional to  $1/\epsilon$ . The equality between the integral along the real axis and the complex contour integral is ensured due to the non-contributing of the semicircle. The investigated integrand has two singularities at

$$\epsilon_1 := \xi - \frac{1}{2}(\omega - v_F|\mathbf{k} + \mathbf{G}|\cos(\vartheta)) \quad \text{and} \quad \epsilon_2 := \xi + \frac{1}{2}(\omega - v_F|\mathbf{k} + \mathbf{G}|\cos(\vartheta)), \quad (\text{A.19})$$

where both singularities are of first order. The poles are located in the upper or lower plane, according to the signum function in the denominator. In total four different constitutions are possible. On the one hand, both singularities can be located in the lower or upper complex plane, which yield in both cases zero. On the other hand, one pole is sited in the upper plane, while the other one is sited in the lower plane, or vice versa, where both yield the same contribution

**1. case:**  $\operatorname{sign}(\epsilon + \frac{\omega}{2}) = \operatorname{sign}(\epsilon - \frac{\omega}{2})$

Both singularities are located in the upper or in the lower complex half plane. The contour is therefore closed in the upper or lower plane, respectively, enclosing both poles. In the first case the winding number is 1, since the pole is enclosed counterclockwise. Accordingly, the winding number is  $-1$  in the second case.

$$\begin{aligned} \mathcal{I}_{\omega}^e &:= i \oint_{\Gamma} \frac{d\omega}{2\pi i} \frac{1}{\omega - \omega_1 \mp i\eta} \cdot \frac{1}{\omega - \omega_2 \mp i\eta} \\ \Leftrightarrow \mathcal{I}_{\omega}^e &= \pm i \left[ \frac{1}{\omega_2 - \omega_1} + \frac{1}{\omega_1 - \omega_2} \right] = 0, \end{aligned} \quad (\text{A.20})$$



where the index "e" stands for even and means, that both poles are located in the same half plane.

**2. case:**  $\text{sign}(\epsilon + \frac{\omega}{2}) \neq \text{sign}(\epsilon - \frac{\omega}{2})$

The singularities are sited in different complex half planes, one in the upper and accordingly the other in the lower half plane. It is arbitrary in which half plane the contour is closed as long as one pole is enclosed. In the following computation the contour is closed in the upper half plane.

$$\begin{aligned} I_\omega^o &:= i \oint_\Gamma \frac{d\omega}{2\pi i} \frac{1}{\omega - \omega_1 \mp i\eta} \cdot \frac{1}{\omega - \omega_2 \pm i\eta} \\ \Leftrightarrow I_\omega^o &= \frac{\pm i}{\omega_2 - \omega_1 \pm i\eta} \end{aligned} \quad (\text{A.21})$$

where the index "o" stands for odd and mean, that both poles are located in opposite half planes.

After inserting both expressions for the singularities  $\omega_1$  and  $\omega_2$ , the integrand is independent with respect to  $\xi$ . The signum functions in (A.18) is equivalent to the signum functions  $\text{sign}(\xi \pm \frac{1}{2}v_F|\mathbf{k} + \mathbf{G}|\cos(\vartheta))$  in energy representation. The energy  $\xi$  is dropped, since the integrand is independent of  $\xi$ , and the constant positive factors are neglectable. Then, the signum function is expressed as  $\text{sign}[|\mathbf{k} + \mathbf{G}|\cos(\vartheta)]$ . Finally, the integrals limits are set to  $\pm \frac{1}{2}v_F|\mathbf{k} + \mathbf{G}|\cos(\vartheta)$ , which follows directly from the localization of both poles.  $\omega_1$  is assumed to be in the lower half plane, while  $\omega_2$  is then assumed in the opposite one. This implies that  $\epsilon + \frac{\omega}{2} > 0$  and  $\epsilon - \frac{\omega}{2} < 0$ , respectively. Transforming into energy representation the obtained expression yield the definition interval of  $\xi$ . The polarization operator is therefore given by

$$\Pi_\mu^{(0)}(\mathbf{k}, \omega) = i\nu_F \int_0^\pi d\vartheta \int_{-\xi_0}^{\xi_0} d\xi \frac{i \text{sign}(|\mathbf{k} + \mathbf{G}|\cos(\vartheta))}{\omega - v_F|\mathbf{k} + \mathbf{G}|\cos(\vartheta) + i\eta \text{sign}(|\mathbf{k} + \mathbf{G}|\cos(\vartheta))}, \quad (\text{A.22})$$

where the abbreviation  $\xi_0 = v_F|\mathbf{k} + \mathbf{G}|\cos(\vartheta)/2$  is introduced. The integration over  $\xi$  yields the factor  $v_F|\mathbf{k} + \mathbf{G}|\cos(\vartheta)$ . Subsequently the signum function is reexpressed in frequency representation corresponding to  $\text{sign}(\omega)$ . Since our interest is attracted to damping of the spin fluctuations, the imaginary part of the polarization operator is taken:

$$\text{Im}\left\{\Pi_\mu^{(0)}(\mathbf{k}, \omega)\right\} = \nu_F\pi \int_0^\pi d\vartheta v_F|\mathbf{k} + \mathbf{G}|\cos(\vartheta)\delta(\omega - v_F|\mathbf{k} + \mathbf{G}|\cos(\vartheta)). \quad (\text{A.23})$$

Here the formula  $\frac{1}{x \pm i\eta} = \text{P.V.}\frac{1}{x} \mp i\pi\delta(x)$  is used. The obtained  $\delta$ -distribution has a function  $g(\vartheta)$  as argument. Using formula

$$\delta(g(x)) = \sum_{i=1} \frac{\delta(x - x_{0,i})}{|g'(x_{0,i})|}, \quad (\text{A.24})$$

## A Computation of the Damped Spin Density Propagator

the  $\delta$ -distribution is rewritten as a sum over  $\delta$ -distributions with the zeros of  $g(\theta)$  as argument. In the above formula, the sum runs over all zeros of  $g(x)$ , which are denoted as  $x_{0,i}$ . The derivative with respect to  $x$  is labeled with a prime at  $g$  and is evaluated at the corresponding zero  $x_{0,i}$ .

In our observed case, the argument of  $\delta(g(\vartheta))$  contains only one zero at  $\vartheta_0 = \cos^{-1}(\omega/(v_F|\mathbf{k} + \mathbf{G}|))$  inside the integral boundaries. The  $\delta$ -distribution is rewritten as:

$$\begin{aligned} \delta(\omega - v_F|\mathbf{k} + \mathbf{G}|\cos(\vartheta)) &= \left(v_F|\mathbf{k} + \mathbf{G}| \cdot |\sin(\vartheta_0)|\right)^{-1} \delta(\vartheta - \vartheta_0) \\ \Rightarrow \delta(\omega - v_F|\mathbf{k} + \mathbf{G}|\cos(\vartheta)) &\approx \left(v_F|\mathbf{k} + \mathbf{G}|\right)^{-1} \delta(\vartheta - \vartheta_0). \end{aligned} \quad (\text{A.25})$$

In the second line the limit of small frequencies  $\omega$  is taken, which is valid in our observed low-energy theory in the spin fermion model. The integration over  $\vartheta$  is now performed and the imaginary part of the polarization operator is given by

$$\text{Im}\left\{\Pi_\mu^{(0)}(\mathbf{k}, \omega)\right\} = \frac{\nu_F \pi}{v_F|\mathbf{k} + \mathbf{G}|} \cdot \omega = \gamma\omega, \quad (\text{A.26})$$

where the damping parameter  $\gamma$  is introduced. As above demonstrated, the damped spin density propagator is determined by the Dyson equation (A.9). The polarization operator is separated into real and imaginary part. Inserting the free spin density propagator and the obtained result for  $\text{Im}\{\Pi_\mu\}$ , the damped spin density propagator is obtained to

$$\mathcal{D}_\mu(\mathbf{k}, \omega) = \sum_{\mathbf{G}} \frac{1}{(\mathbf{k} + \mathbf{G})^2 + r - (\omega/v_S)^{-2} - i\gamma\omega} \quad (\text{A.27})$$

where the abbreviation  $r = r_0 - \text{Re}\{\Pi_\mu(\mathbf{k}, \omega)\}$  is used. In the vicinity of the quantum critical point the real part of  $\Pi_\mu$  is canceled by  $r_0$ , since the correlations length is divergent and  $r = \xi^{-2}$ . In low-energy theory, the  $\omega^2$ -term is further neglectable.

### A.3 Transformation into Matsubara Frequency Space

The spin density wave propagator, obtained in the previous section, is a complex function of the real quantity  $\omega$ . In the following, the quantity  $\omega$  is transformed into an imaginary quantity  $i\omega_n$ , known as Matsubara frequencies. The real and imaginary part of the propagator  $\mathcal{D}_\mu(\mathbf{k}, i\omega_n)$  with respect to Matsubara frequencies is evaluated using the Kramers-Kronig relations [Sch08]. The propagator in (A.27) is separated into real and imaginary part, extending with the complex conjugated denominator.

$$\mathcal{D}_\mu(\mathbf{k}, \omega) = \sum_{\mathbf{G}} \left[ \frac{(\mathbf{k} + \mathbf{G})^2}{(\mathbf{k} + \mathbf{G})^4 + (\gamma\omega)^2} + i \frac{\gamma\omega}{(\mathbf{k} + \mathbf{G})^4 + (\gamma\omega)^2} \right], \quad (\text{A.28})$$

where  $r$  and  $\xi$  is set to zero. For the following treatment it is useful to investigate the symmetries of the real and imaginary part. The real part is a symmetric function and

the imaginary part is an antiymmetric function, with respect to  $\omega$ . The imaginary part of  $\mathcal{D}_\mu(\mathbf{k}, i\omega_n)$  is evaluated to zero, since its defined as the integral over the real part of  $\mathcal{D}_\mu(\mathbf{k}, \omega)$  divided by  $\omega$ . The integrand is therefore an odd function and the integral over all frequencies  $\omega$  is zero. In Matsubara frequency space, the damped propagator is given by its real part.

$$\mathcal{D}_\mu(\mathbf{k}, i\omega_n) = \text{Re}\{\mathcal{D}_\mu(\mathbf{k}, i\omega_n)\} = \frac{1}{\pi} \text{P.V.} \int_{-\infty}^{\infty} d\omega \frac{\text{Im}\{\mathcal{D}_\mu(\mathbf{k}, \omega)\}}{\omega - i\omega_n} \quad (\text{A.29})$$

where P.V. represents that the integrals is evaluated using the principal value. The integral is speperated into two parts. In the first one  $\omega$  is substituted by  $-\omega$  and the antismmetry of  $\text{Im}\{\mathcal{D}_\mu(\mathbf{k}, \omega)\}$  is utilized.

$$\begin{aligned} \mathcal{D}_\mu(\mathbf{k}, i\omega_n) &= \frac{1}{\pi} \int_0^{\infty} d\omega \text{Im}\{\mathcal{D}_\mu(\mathbf{k}, \omega)\} \left[ \frac{1}{\omega + i\omega_n} + \frac{1}{\omega - i\omega_n} \right] \\ \Leftrightarrow \mathcal{D}_\mu(\mathbf{k}, i\omega_n) &= \frac{2}{\pi} \sum_{\mathbf{G}} \int_0^{\infty} d\omega \frac{\gamma\omega}{(\mathbf{k} + \mathbf{G})^4 + (\gamma\omega)^2} \cdot \frac{\omega}{\omega^2 + \omega_n^2} \\ \Leftrightarrow \mathcal{D}_\mu(\mathbf{k}, i\omega_n) &= \sum_{\mathbf{G}} \frac{1}{(\mathbf{k} + \mathbf{G})^2 + \gamma|\omega_n|} \end{aligned} \quad (\text{A.30})$$

In the last step the integral formula

$$\int_0^{\infty} dx \frac{x}{a^2 + x^2} \cdot \frac{x}{y^2 + x^2} = \frac{\pi}{2} \frac{1}{a + |y|} \quad (\text{A.31})$$

is used, which can be shown by transforming into a complex contour integral.



## B Time Derivative of momentum P and current J

The time derivative of the momentum and current operator are designated for the case of non-perturbation and perturbation in chapter 3. In this appendix, the computation is outlined of them. Our further approach is to compute Hamiltonian, momentum and current operator, using the energy-momentum-tensor and current-tensor [Ili02]. The time derivative of momentum and current is then calculated, using the Heisenberg equation of motion. In the end, umklapp scattering is observed and the effect to momentum and current are discussed.

Our starting point is the Lagrangian  $\mathcal{L} = \mathcal{L}_\Psi + \mathcal{L}_\Phi + \mathcal{L}_{\Psi\Phi}$ , as suggested in [PS14] of the spin-fermion-model. In Matsubara time  $\tau = it$ , the single Lagrangians are given by

$$\mathcal{L}_\Psi = \Psi^\dagger(\mathbf{x}, \tau) \begin{pmatrix} \sigma_0(\partial_\tau + \mu_0 + \xi_a) & 0 \\ 0 & \sigma_0(\partial_\tau + \mu_0 + \xi_b) \end{pmatrix} \Psi(\mathbf{x}, \tau) \quad (\text{B.1})$$

$$\begin{aligned} \mathcal{L}_\Phi = & \frac{1}{2} [\partial_i \Phi_\mu(\mathbf{x}, \tau)] [\partial_i \Phi_\mu(\mathbf{x}, \tau)] + \frac{\epsilon}{2} [\partial_\tau \Phi_\mu(\mathbf{x}, \tau)] [\partial_\tau \Phi_\mu(\mathbf{x}, \tau)] \\ & + \frac{u}{6} \left[ \Phi_\mu(\mathbf{x}, \tau) \Phi_\mu(\mathbf{x}, \tau) + \frac{3}{g} \right]^2 \end{aligned} \quad (\text{B.2})$$

$$\mathcal{L}_{\Psi\Phi} = \lambda \Phi_\mu(\mathbf{x}, \tau) \left[ \Psi_a^\dagger(\mathbf{x}, \tau) \sigma_\mu \Psi_b(\mathbf{x}, \tau) + \Psi_b^\dagger(\mathbf{x}, \tau) \sigma_\mu \Psi_a(\mathbf{x}, \tau) \right] \quad (\text{B.3})$$

Here  $\Psi = (\Psi_a, \Psi_b)$  is a vector containing the two-component spinors  $\Psi_a, \Psi_b$ .  $\Phi_\mu$  is the three component bosonic field operator and describes the spin fluctuations in the spin-fermion-model. Since the spin fluctuations arise at the phase transition,  $\Phi_\mu$  is order parameter as well. The chemical potential is denoted with  $\mu_0$  and the Pauli matrix are labeled with  $\sigma_0$  and  $\sigma_\mu$ . The abbreviation  $\epsilon = v_S^{-2}$  is introduced, where  $v_S$  is the spin velocity. In the Lagrangian  $\mathcal{L}_\Phi$ , the term in the second line is neglectable in the low-energy theory of the spin fermion model. The anisotropic parabolical dispersion relations  $\xi_a$  and  $\xi_b$  are given by

$$\xi_a = \frac{\partial_x^2}{2m_1} + \frac{\partial_y^2}{2m_2} \quad \xi_b = \frac{\partial_x^2}{2m_2} + \frac{\partial_y^2}{2m_1} \quad (\text{B.4})$$

The Hamiltonian for umklapp scattering is assumed to be

$$\mathcal{H}_{\text{umklapp}} = J(\mathbf{R}) \Phi_\mu(\mathbf{x}, \tau) \Phi_\mu(\mathbf{x}, \tau) \quad (\text{B.5})$$

where  $J(\mathbf{R})$  is a coupling parameter and  $\mathbf{R}$  is a lattice vector. In a first step, the Hamiltonian for the unpertubated spin-fermion-model is calculated using the energy-momentum-tensor and current-tensor [Ili02].

$$\mathcal{T}_{\mu\nu} = \frac{1}{2} \sum_{\zeta_n} \left[ \left( \frac{\partial \mathcal{L}}{\partial(\partial_\mu \zeta_n)} \right) (\partial_\nu \zeta_n) + (\partial_\nu \zeta_n)^\dagger \left( \frac{\partial \mathcal{L}}{\partial(\partial_\mu \zeta_n)} \right)^\dagger \right] - \eta_{\mu\nu} \mathcal{L} \quad (\text{B.6})$$

$$\mathcal{J}_\mu = -i \sum_{\{\zeta_n\}} \epsilon(\zeta_n) \left[ \left( \frac{\partial \mathcal{L}}{\partial(\partial_\mu \zeta_n)} \right) \zeta_n - \zeta_n^\dagger \left( \frac{\partial \mathcal{L}}{\partial(\partial_\mu \zeta_n)} \right)^\dagger \right], \quad (\text{B.7})$$

Here,  $\zeta_n$  is the set of all contributing operator fields, which is in our case  $\{\Psi_a, \Psi_b, \Phi_\mu\}$ . The function  $\epsilon(\zeta_n)$  attains the values 0 or 1 in the case of real or complex fields, respectively.  $\eta_{\mu\nu}$  is the Minkowski metric, where the definition  $(1, -1, -1, -1)$  is used here. In chapter 3, the concept of hot spots is introduced. Fermions on different Fermi surfaces interact via spin fluctuations, described by  $\Phi_\mu$ . The bosonic field operators are supposed to be real quantities, since the interaction is assumed to be on the hot spots and not in a vicinity regime around them. Furthermore, the spatial derivative in  $\mathcal{L}_\Psi$  is rewritten. using relation  $\Psi^\dagger(\partial_i^2 \Psi) = -(\partial_i \Psi^\dagger)(\partial_i \Psi)$ . This relation is evaluated, integrating the left hand side by parts.

The (00)-component of the energy-momnetum-tensor represents the Hamiltonian of a system. This quantity is computed in the following.

$$\begin{aligned} \mathcal{H} &= \frac{1}{2} \sum_{\zeta_n} \left[ \left( \frac{\partial \mathcal{L}}{\partial(\partial_\tau \zeta_n)} \right) (\partial_\tau \zeta_n) - (\partial_\tau \zeta_n)^\dagger \left( \frac{\partial \mathcal{L}}{\partial(\partial_\tau \zeta_n)} \right)^\dagger \right] - \mathcal{L} \\ \Leftrightarrow \mathcal{H} &= \psi_a^\dagger (\partial_\tau \psi_a) + \psi_b^\dagger (\partial_\tau \psi_b) + \epsilon (\partial_\tau \Phi_\mu) (\partial_\tau \Phi_\mu) - \mathcal{L} \\ \Leftrightarrow \mathcal{H} &= -\psi_a^\dagger(\mathbf{x}, \tau) \left( \frac{\partial_x^2}{2m_1} + \frac{\partial_y^2}{2m_2} + \mu_0 \right) \psi_a(\mathbf{x}, \tau) \\ &\quad - \psi_b^\dagger(\mathbf{x}, \tau) \left( \frac{\partial_x^2}{2m_2} + \frac{\partial_y^2}{2m_1} + \mu_0 \right) \psi_b(\mathbf{x}, \tau) \\ &\quad - \frac{1}{2} (\partial_i \Phi_\mu(\mathbf{x}, \tau)) (\partial_i \Phi_\mu(\mathbf{x}, \tau)) + \frac{1}{2\epsilon} \pi_\mu(\mathbf{x}, \tau) \pi_\mu(\mathbf{x}, \tau) \\ &\quad - \lambda \Phi_\mu(\mathbf{x}, \tau) (\psi_a^\dagger(\mathbf{x}, \tau) \sigma_\mu \psi_b(\mathbf{x}, \tau) + \psi_b^\dagger(\mathbf{x}, \tau) \sigma_\mu \psi_a(\mathbf{x}, \tau)) \end{aligned} \quad (\text{B.8})$$

Here, the usual time derivative is transformed into the Matsubara time, using  $\partial_t = -i\partial_\tau$ . The Hermitain of the  $\tau$ -derivative is given by  $(\partial_\tau)^\dagger = -\partial_\tau$ , which is also used. The canonical momentum of  $\Phi_\mu$ , given by  $\pi_\mu(\mathbf{x}, \tau) = \epsilon \partial_\tau \Phi_\mu(\mathbf{x}, \tau)$ , is used in the last step. The  $\mathcal{T}_{0j}$ -component is identified with the  $j$ -component of the momentum operator, which is calculated as next.

$$\begin{aligned} \mathcal{P}_j &= \frac{-i}{2} \sum_{\zeta_n} \left[ \left( \frac{\partial \mathcal{L}}{\partial(\partial_\tau \zeta_n)} \right) (\partial_j \zeta_n) + (\partial_j \zeta_n)^\dagger \left( \frac{\partial \mathcal{L}}{\partial(\partial_\tau \zeta_n)} \right)^\dagger \right] - \eta_{0j} \mathcal{L} \\ \Leftrightarrow \mathcal{P}_j &= \frac{-i}{2} \left[ \psi_a^\dagger(\mathbf{x}, \tau) (\partial_j \psi_a(\mathbf{x}, \tau)) - (\partial_j \psi_a^\dagger(\mathbf{x}, \tau)) \psi_a(\mathbf{x}, \tau) \right. \end{aligned}$$

$$\begin{aligned}
& + \psi_b^\dagger(\mathbf{x}, \tau) (\partial_j \psi_b(\mathbf{x}, \tau)) - (\partial_j \psi_b^\dagger(\mathbf{x}, \tau)) \psi_b(\mathbf{x}, \tau) \Big] - i\pi_\mu(\mathbf{x}, \tau) (\partial_j \phi_\mu(\mathbf{x}, \tau)) \\
\Rightarrow \mathcal{P} = & \frac{-i}{2} \left[ \Psi^\dagger(\mathbf{x}, \tau) (\nabla \Psi(\mathbf{x}, \tau)) - (\nabla \Psi^\dagger(\mathbf{x}, \tau)) \Psi(\mathbf{x}, \tau) \right] - i\pi_\mu(\mathbf{x}, \tau) (\nabla \phi_\mu(\mathbf{x}, \tau))
\end{aligned} \tag{B.9}$$

The Hermitian of the  $\tau$ -derivative and the canonical momentum is again used at this computation. The two-component vector  $\Psi$  is inserted to write the vector components as vector. Now, the  $x$ -component of the current is calculated.

$$\begin{aligned}
\mathcal{J}_x = & -i \sum_{\zeta_n} \epsilon(\zeta_n) \left[ \left( \frac{\partial \mathcal{L}}{\partial (\partial_x \zeta_n)} \right) \zeta_n - \zeta_n^\dagger \left( \frac{\partial \mathcal{L}}{\partial (\partial_x \zeta_n)} \right)^\dagger \right] \\
\Leftrightarrow \mathcal{J}_x = & \frac{-i}{2} \left[ \frac{1}{m_1} \left[ (\partial_x \psi_a^\dagger(\mathbf{x}, \tau)) \psi_a(\mathbf{x}, \tau) - \psi_a^\dagger(\mathbf{x}, \tau) (\partial_x \psi_a(\mathbf{x}, \tau)) \right] \right. \\
& \left. + \frac{1}{m_2} \left[ (\partial_x \psi_b^\dagger(\mathbf{x}, \tau)) \psi_b(\mathbf{x}, \tau) - \psi_b^\dagger(\mathbf{x}, \tau) (\partial_x \psi_b(\mathbf{x}, \tau)) \right] \right]
\end{aligned} \tag{B.10}$$

The  $x$ -component of the current is computed analogical, where an interchange of the mass ( $m_1 \leftrightarrow m_2$ ) is the only difference. These three quantities are now transformed into momentum space, since all of them contains spatial derivatives. This is obstructive in the later calculation of the time derivative of  $\mathbf{P}$  and  $\mathbf{J}$ , since commutator relations of fermionic and bosonic fields are therefore used.

$$\begin{aligned}
\mathbf{H} = & \int_{\mathbf{k}} \left[ \sum_{\alpha} \epsilon_{\alpha}(\mathbf{k}) \psi_{\alpha}^\dagger(\mathbf{k}, \tau) \psi_{\alpha}(\mathbf{k}, \tau) - \frac{\mathbf{k}^2}{2} \Phi_{\mu}(\mathbf{k}, \tau) \Phi_{\mu}(-\mathbf{k}, \tau) + \frac{1}{2\epsilon} \pi_{\mu}(\mathbf{k}, \tau) \pi_{\mu}(-\mathbf{k}, \tau) \right. \\
& \left. - \lambda \int_{\mathbf{q}} \Phi_{\mu}(\mathbf{k} - \mathbf{q}, \tau) \left[ \psi_a^\dagger(\mathbf{k}, \tau) \sigma_{\mu} \psi_b(\mathbf{q}, \tau) + \psi_b^\dagger(\mathbf{k}, \tau) \sigma_{\mu} \psi_a(\mathbf{q}, \tau) \right] \right]
\end{aligned} \tag{B.11}$$

$$\mathbf{P}_j = \int_{\mathbf{k}} k_j \left[ \sum_{\alpha} \psi_{\alpha}^\dagger(\mathbf{k}, \tau) \psi_{\alpha}(\mathbf{k}, \tau) - \pi_{\mu}(\mathbf{k}, \tau) \Phi_{\mu}(-\mathbf{k}, \tau) \right] \tag{B.12}$$

$$\mathbf{J}_x = - \int_{\mathbf{k}} \left[ \frac{k_x}{m_1} \psi_a^\dagger(\mathbf{k}, \tau) \psi_a(\mathbf{k}, \tau) + \frac{k_x}{m_2} \psi_b^\dagger(\mathbf{k}, \tau) \psi_b(\mathbf{k}, \tau) \right] \tag{B.13}$$

The sum over  $\alpha$  summarizes over the two species of fermions  $a$  and  $b$ . Their dispersion relations are given by  $\epsilon_a(\mathbf{k}) = \frac{k_x^2}{2m_1} + \frac{k_y^2}{2m_2} - \mu_0$  und  $\epsilon_b(\mathbf{k}) = \frac{k_x^2}{2m_2} + \frac{k_y^2}{2m_1} - \mu_0$  in momentum space. All integrals are extended over the first Brillouin zone.

Now, the time derivative of momentum  $\mathbf{P}$  and current  $\mathbf{J}$  is computed. The Heisenberg equation of motion is the usual way to calculate the derivative of an operator in quantum mechanics. The simplicity of this method is, that only the commutator between

the Hamiltonian and the observed operator has to be computed. For the further approach, the commutator relations for bosonic and fermionic fields are required. Beside these two ones, all other commutator relations yield zero.

$$\left\{ \psi_\alpha(\mathbf{k}, \tau), \psi_\beta^\dagger(\mathbf{p}, \tau) \right\} = (2\pi)^2 \delta_{\alpha\beta} \delta(\mathbf{p} - \mathbf{k}) \quad (\text{B.14})$$

$$[\Phi_\mu(\mathbf{k}, \tau), \pi_\lambda(\mathbf{p}, \tau)] = (2\pi)^2 \delta_{\mu\lambda} \delta(\mathbf{p} + \mathbf{k}) \quad (\text{B.15})$$

At first the commutator between the Hamiltonian  $H$  and the  $x$ -component of  $P$  is computed. All integrals are extended over the first Brillouin zone, while the sums over greek letters runs over the fermionic species  $a$  and  $b$ . The condition  $\alpha \neq \beta$  means that in this case both greek latters has to be different. The commutator has to be transformed into component representation, if Pauli matrices  $\sigma_\mu$  connects to fermionic field operators. The above commutator relations are also valid in this representation.

$$\begin{aligned} [H, P_x] &= \int_{\mathbf{k}} \int_{\mathbf{p}} p_x \sum_{\alpha, \beta} \epsilon_\alpha(\mathbf{k}) \left[ \psi_\alpha^\dagger(\mathbf{k}, \tau) \psi_\alpha(\mathbf{k}, \tau), \psi_\beta^\dagger(\mathbf{k}, \tau) \psi_\beta(\mathbf{k}, \tau) \right] \\ &\quad + \int_{\mathbf{k}} \int_{\mathbf{p}} p_x \left[ \frac{k^2}{2} [\Phi_\mu(\mathbf{k}, \tau) \Phi_\mu(-\mathbf{k}, \tau), \pi_\lambda(\mathbf{p}, t) \Phi_\lambda(-\mathbf{p}, t)] \right. \\ &\quad \quad \left. - \frac{1}{2\epsilon} [\pi_\mu(\mathbf{k}, \tau) \pi_\mu(-\mathbf{k}, \tau), \pi_\lambda(\mathbf{p}, t) \Phi_\lambda(-\mathbf{p}, t)] \right] \\ &\quad - \lambda \int_{\mathbf{k}} \int_{\mathbf{p}} \int_{\mathbf{q}} p_x \Phi_\mu(\mathbf{k} - \mathbf{q}, \tau) \sum_{\alpha \neq \beta} \sum_{\gamma} \left[ \psi_\alpha^\dagger(\mathbf{k}, \tau) \sigma_\mu \psi_\beta(\mathbf{q}, \tau), \psi_\gamma^\dagger(\mathbf{p}, t) \psi_\gamma(\mathbf{p}, t) \right] \\ &\quad + \lambda \int_{\mathbf{k}} \int_{\mathbf{p}} \int_{\mathbf{q}} p_x \sum_{\alpha \neq \beta} \psi_\alpha^\dagger(\mathbf{k}, \tau) \sigma_\mu \psi_\beta(\mathbf{q}, \tau) [\Phi_\mu(\mathbf{k} - \mathbf{q}, \tau), \pi_\lambda(\mathbf{p}, t) \Phi_\lambda(-\mathbf{p}, t)] \\ &\Leftrightarrow [H, P_x] = -\lambda \int_{\mathbf{k}} \int_{\mathbf{q}} (q_x - k_x) \Phi_\mu(\mathbf{k} - \mathbf{q}, \tau) \sum_{\alpha \neq \beta} \psi_\alpha^\dagger(\mathbf{k}, \tau) \sigma_\mu \psi_\beta(\mathbf{q}, t) \\ &\quad + \lambda \int_{\mathbf{k}} \int_{\mathbf{q}} (q_x - k_x) \Phi_\mu(\mathbf{k} - \mathbf{q}, t) \sum_{\alpha \neq \beta} \psi_\alpha^\dagger(\mathbf{k}, \tau) \sigma_\mu \psi_\beta(\mathbf{q}, \tau) \\ &\Leftrightarrow [H, P_x] = 0 \end{aligned} \quad (\text{B.16})$$

This result is also obtained for the  $y$ -direction of the momentum. As consequence, the time derivative of momentum is zero,  $\dot{P} = 0$ . In the spin-fermion-model, described by the Hamiltonian  $H$ , momentum is a conserved quantity. This implies a unbroken translation symmetry. At next, the time derivative of the current in  $x$ -direction is calculated. The notation is equal to this used by the momentum above.

$$\begin{aligned} [H, J_x] &= \int_{\mathbf{k}} \int_{\mathbf{p}} \frac{p_x}{m_1} \sum_{\alpha} \epsilon_\alpha(\mathbf{k}) \left[ \psi_\alpha^\dagger(\mathbf{k}, \tau) \psi_\alpha(\mathbf{k}, \tau), \psi_a^\dagger(\mathbf{p}, \tau) \psi_a(\mathbf{p}, \tau) \right] \\ &\quad + \int_{\mathbf{k}} \int_{\mathbf{p}} \frac{p_x}{m_2} \sum_{\alpha} \epsilon_\alpha(\mathbf{k}) \left[ \psi_\alpha^\dagger(\mathbf{k}, \tau) \psi_\alpha(\mathbf{k}, \tau), \psi_b^\dagger(\mathbf{p}, \tau) \psi_b(\mathbf{p}, \tau) \right] \end{aligned}$$



$$\begin{aligned}
& + \lambda \int_{\mathbf{k}} \int_{\mathbf{p}} \int_{\mathbf{q}} \Phi_{\mu}(\mathbf{k} - \mathbf{q}, \tau) \frac{p_x}{m_1} \sum_{\alpha \neq \beta} \left[ \psi_{\alpha}^{\dagger}(\mathbf{k}, \tau) \sigma_{\mu} \psi_{\beta}(\mathbf{q}, t), \psi_{\mathbf{a}}^{\dagger}(\mathbf{p}, \tau) \psi_{\mathbf{a}}(\mathbf{p}, \tau) \right] \\
& + \lambda \int_{\mathbf{k}} \int_{\mathbf{p}} \int_{\mathbf{q}} \Phi_{\mu}(\mathbf{k} - \mathbf{q}, \tau) \frac{p_x}{m_2} \sum_{\alpha \neq \beta} \left[ \psi_{\alpha}^{\dagger}(\mathbf{k}, \tau) \sigma_{\mu} \psi_{\beta}(\mathbf{q}, t), \psi_{\mathbf{b}}^{\dagger}(\mathbf{p}, \tau) \psi_{\mathbf{b}}(\mathbf{p}, \tau) \right] \\
\Leftrightarrow [H, J_x] &= \lambda \int_{\mathbf{k}} \int_{\mathbf{q}} \Phi_{\mu}(\mathbf{k} - \mathbf{q}, \tau) \\
& \times \left[ \left( \frac{q_x}{m_1} - \frac{k_x}{m_2} \right) \psi_{\mathbf{b}}^{\dagger}(\mathbf{k}, \tau) \sigma_{\mu} \psi_{\mathbf{a}}(\mathbf{q}, \tau) + \left( \frac{q_x}{m_2} - \frac{k_x}{m_1} \right) \psi_{\mathbf{a}}^{\dagger}(\mathbf{k}, \tau) \sigma_{\mu} \psi_{\mathbf{b}}(\mathbf{q}, \tau) \right]
\end{aligned} \tag{B.17}$$

In the investigated spin-fermion-model, the time derivative of the current is non-zero and as a consequence the current is unconserved. This property of the model is important for the calculation of the static conductivity. The effect of umklapp scattering respective the time derivative of P and J is following computed. The Hamiltonian  $H_{\text{umklapp}}$  is given by

$$H_{\text{umklapp}} = \sum_{\mathbf{G}} J_{\mathbf{G}} \int_{\mathbf{k}} \Phi_{\mu}(\mathbf{k}, \tau) \Phi_{\mu}(-\mathbf{k} + \mathbf{G}, \tau) \tag{B.18}$$

in momentum space. The integral is extended over the first Brillouin zone and the sum runs over all reciprocal lattice vectors. The quantities P and J are not altered considering Umklapp scattering, since momentum and current only emerged, if the Hamiltonian possesses time or spatial derivatives, respectively. Both are not existing in the Hamiltonian  $H_{\text{umklapp}}$ . Nevertheless, the time derivative of P and J are possible modified. The contribution of umklapp scattering to the latter is zero. The field operators of the current are of fermionic nature, while these of the Hamiltonian  $H_{\text{umklapp}}$  are of bosonic nature. The time derivative of P is in contrast non-zero.

$$\begin{aligned}
\dot{P}_j &= -i \sum_{\mathbf{G}} J_{\mathbf{G}} \int_{\mathbf{k}} \int_{\mathbf{p}} p_j [\Phi_{\mu}(k) \Phi_{\mu}(-k + G), \pi_{\lambda}(p) \Phi_{\lambda}(-p)] \\
\dot{P}_j &= -i \sum_{\mathbf{G}} J_{\mathbf{G}} \int_{\mathbf{k}} \int_{\mathbf{p}} p_j \left[ \Phi_{\mu}(k) [\Phi_{\mu}(-k + G), \pi_{\lambda}(p)] \Phi_{\lambda}(-p) \right. \\
& \quad \left. + [\Phi_{\mu}(k), \pi_{\lambda}(p)] \Phi_{\mu}(-k + G) \Phi_{\lambda}(-p) \right] \\
\dot{P}_j &= -i \sum_{\mathbf{G}} J_{\mathbf{G}} \int_{\mathbf{k}} \left[ (k_j - G_j) \Phi_{\mu}(k) \Phi_{\mu}(-k + G) - k_j \Phi_{\mu}(-k + G) \Phi_{\mu}(k) \right] \\
\dot{P}_j &= i \sum_{\mathbf{G}} J_{\mathbf{G}} \int_{\mathbf{k}} G_j \Phi_{\mu}(k) \Phi_{\mu}(-k + G)
\end{aligned} \tag{B.19}$$

Considering umklapp scattering the time derivative of P is determined to an finite value. As a consequence the momentum is not conserved any longer. The characteristic of the considered perturbation to change momentum and leave current unchange is important for the computation of the static electrical conductivity.



## C Computation of the Static Susceptibility

In this appendix, the static susceptibility  $\chi_{JP}(\omega = 0)$  is explicitly calculated. The temperature dependence of  $\chi_{JP}$  is expected to be non-existent, since momentum and current are not explicitly time dependent. Using equation (5.31), the static susceptibility is directly proportional to the Kubo relaxation function (5.3) at  $t = 0$ .

$$\chi_{PJ}(\omega = 0) = \Phi_{PJ}(t = 0) = i \int_0^\infty dt' \langle [P_j(t'), J_j(0)] \rangle \quad (C.1)$$

In the formula above, the limit  $s \rightarrow 0$  is dropped, since the integral is assumed to be convergent. The spatial direction of P and J is signified by the index  $j$ . The integral is transformed into Matsubara time  $\tau = it$ , firstly. The Jacobi determinate is  $-i$  and the integral's limits is set to 0 and  $\beta$ . Observing only the zeroth order in perturbation theory the static susceptibility is given by

$$\chi_{PJ}(\omega = 0) = \int_0^\beta d\tau \langle \mathcal{T}_\tau P_j(\tau) J_j(0) \rangle_0. \quad (C.2)$$

The momentum and current operators are named in equation (3.10) and (3.11), respectively. Inserting them, expectation values are generated including four operators. Only if these operators are of the same species,  $\Phi_\mu$ ,  $\Psi_a$  or  $\Psi_b$ , the expectation values yield connected diagrams. This happens two times in the case of fermionic operators. Wick's theorem is used to separate the remaining two expectation values in terms of free Green functions. The contraction of operators with different time argument is generated the two bubble diagrams, depicted in figure C.1 The static susceptibility is given by

$$\chi_{PJ}(\omega = 0) = \int_0^\beta d\tau \int_{\mathbf{k}} k_j^2 \left[ \frac{1}{m_1} \mathcal{G}_a^{(0)}(\mathbf{k}, -\tau) \mathcal{G}_a^{(0)}(\mathbf{k}, \tau) + \frac{1}{m_2} \mathcal{G}_b^{(0)}(\mathbf{k}, -\tau) \mathcal{G}_b^{(0)}(\mathbf{k}, \tau) \right]. \quad (C.3)$$

Here the free fermionic propagator  $\mathcal{G}_\alpha^{(0)}(\mathbf{k}, \tau) = -\langle \mathcal{T}_\tau \Psi_\alpha(\mathbf{k}, \tau) \Psi_\alpha^\dagger(\mathbf{k}, 0) \rangle$  with  $\alpha \in \{a, b\}$  is inserted. Both fermionic Green functions are transformed into the Matsubara frequency space. The only  $\tau$ -dependence is thus given by the exponential functions. The  $\tau$ -integral is evaluated, using the definition of the  $\delta$ -distribution in Matsubara space,

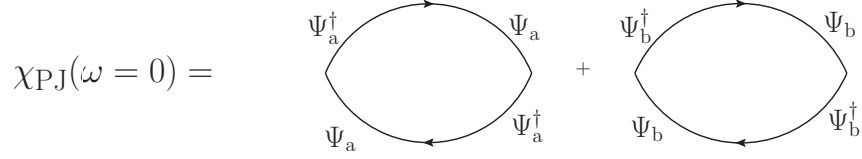


Figure C.1: This figure illustrated the two obtained fermionic bubble diagrams of zeroth order, considered in the calculation of the static susceptibility. The difference exists in the two fermionic species a and b. The diagrams have to be calculated apart since both fermions have a different dispersion relation.

$\int_0^\beta d\tau \exp(i(\omega_m - \omega_n)\tau) = \beta\delta(\omega_m - \omega_n)$ . One of the two sums over Matsubara frequencies is easily performed due to this  $\delta$ -distribution. The obtained expression is given by

$$\chi_{\text{PJ}}(\omega = 0) = \frac{1}{\hbar} \int_{\mathbf{k}} k_j^2 \left[ \frac{1}{m_1} S_a(\omega_n) + \frac{1}{m_2} S_b(\omega_n) \right]. \quad (\text{C.4})$$

The Matsubara sum  $S_\alpha(\omega_n) = \beta^{-1} \sum_{\omega_n} \mathcal{G}_\alpha^{(0)}(\mathbf{k}, \omega_n) \mathcal{G}_\alpha^{(0)}(\mathbf{k}, \omega_n)$ , where  $\alpha = a, b$ , is defined. This sum is transformed into a complex contour integral, offering the use of the usual complex analysis. The product of Green functions multiplied with the Fermi distribution are generated the integrand of this contour integral. The full transformation rule is given by

$$S = \frac{1}{\beta} \sum_{\omega_n} \mathcal{G}(\omega_n) = -\frac{1}{2\pi i} \oint_{\Gamma} dz n_F(z) \mathcal{G}(z). \quad (\text{C.5})$$

The choice of the contour is arbitrary beside one condition. All singularities of the Green functions are excluded in the contour, while the infinite poles  $\omega_n = (2n + 1)\pi/\beta$ , where  $n \in \mathbb{Z}$ , of the Fermi distribution are included in the contour. Our starting contour  $\Gamma$  is depicted on the left hand side in figure C.2.

The contour is generated by two paths along the imaginary axis, from  $i\infty$  to  $-i\infty$  and vice versa. Both paths are connected in plus and minus infinity and shifted infinitesimal aside the imaginary axis. This contour is now expanded to a circle with radius infinity, where always the singularities of the Green function is excluded. The obtained contour is depicted on the right hand side in figure C.2. The same magnitude with opposite sign is generated by the paths from infinity to the poles and vice versa. Therefore, the contour is separated into small circles around the poles of the Green functions and into one circle with infinite radius. The contribution of the latter is zero, since the Green function is proportional to  $1/z$ . In the remaining contour integrals the product of Green functions is now inserted, where the single free fermionic Green function is given by

$$\mathcal{G}_\alpha(\mathbf{k}, i\omega_n) = \frac{1}{i\omega_n - \epsilon_\alpha(\mathbf{k})}. \quad (\text{C.6})$$

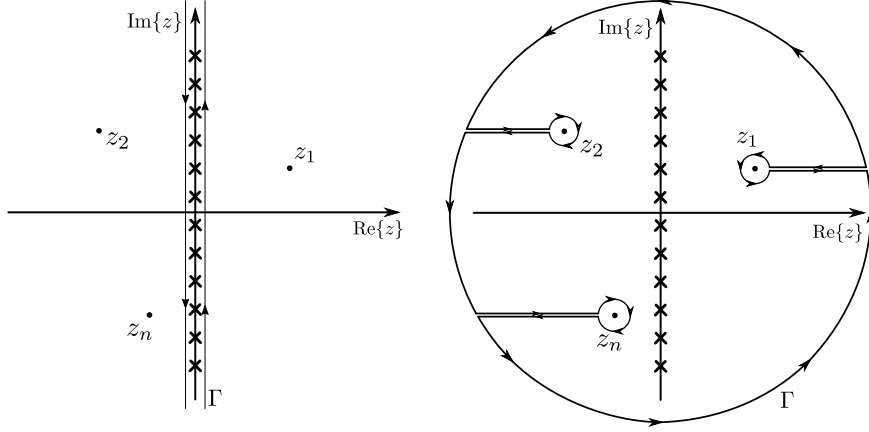


Figure C.2: The deformation of the contour of the determining complex contour integral is shown in this figure. The starting contour runs along the imaginary axis containing all singularities from the Fermi distribution, while the poles of the Green functions are excluded. This is depicted on the left hand side. The contour is expanded to a circle with infinite radius, but consider, the poles of the Green function are still excluded (right figure). The circle and the paths to small circles around the poles of the Green functions yields no contribution.

$\epsilon_\alpha(\mathbf{k})$ , where  $\alpha = a, b$ , is the fermion's dispersion and also the singularity of the Green function. The explicit expression is denoted in equation (3.9). Besides this singularity, the Green function is holomorphic in the whole complex plane. The contour integral is evaluated using the residue theorem, which yields

$$\chi_{\text{PJ}}(\omega = 0) = - \int_{\mathbf{k}} k_j^2 \left[ \frac{1}{m_1} \frac{dn_F(\epsilon_a(\mathbf{k}))}{d\epsilon_a(\mathbf{k})} + \frac{1}{m_2} \frac{dn_F(\epsilon_b(\mathbf{k}))}{d\epsilon_b(\mathbf{k})} \right] \quad (\text{C.7})$$

The derivatives of the distribution function with respect to the dispersion relation are generated, since the integrand has a singularity of second order at  $z_0 = \epsilon_\alpha(\mathbf{k})$ . These two obtained integrals are exactly solvable. Therefore the integrals are transformed into plane polar coordinates, where the transformation rule is given by  $(k_x, k_y) = (q\sqrt{2m_{1,2}}\cos(\phi), q\sqrt{2m_{2,1}}\sin(\phi))$ . Two types of transformation are used, since the dispersion relation of the two species of fermions differs in the contained mass terms. The only angular dependence is originated by the  $k_j^2$ -term. This term yields  $\cos^2(\phi)$  or  $\sin^2(\phi)$  for the  $x$ - or  $y$ -direction, respectively. Since the limits of the  $\phi$ -integral are 0 and  $2\pi$ , the contribution is  $\pi$  in both cases. The upper limit of the  $q$ -integral is set to infinity, since the integrand is decreasing fast to zero for large values of  $q$ .

$$\chi_{\text{PJ}}(\omega = 0) = \frac{8\beta\pi}{(2\pi)^2} \sqrt{m_1 m_2} \int_0^\infty dq q^3 \frac{e^{\beta(q^2 - \mu)}}{(e^{\beta(q^2 - \mu)} + 1)^2} \quad (\text{C.8})$$

### *C Computation of the Static Susceptibility*

The obtained integral is solved, substituting  $x = \beta(q^2 - \mu)$ . The first of the two obtained integrals is evaluated using integration by parts, while the derivative of the Fermi distribution with respect to  $x$  is originated in the second integral. Performing these integrals the static susceptibility of J and P is given by

$$\chi_{PJ}(\omega = 0) = \frac{\sqrt{m_1 m_2}}{\pi \beta} \ln(e^{\beta \mu} + 1) \quad (\text{C.9})$$

In the case of  $\mu \gg k_B T$ , the exponential function is large compared to 1 and neglectable. The static susceptibility is then temperature independent in the leading order and given by

$$\chi_{PJ}(\omega = 0) \rightarrow \frac{\mu \sqrt{m_1 m_2}}{\pi} \quad (T \rightarrow 0) \quad (\text{C.10})$$

## D Finite Conductivity because of Breaking the Translation Symmetry via Umklapp Scattering

The computation of the Green function  $\mathcal{G}_{\dot{\mathbf{p}}\dot{\mathbf{p}}}(\mathbf{k}, z)$  in (4.1) is displayed in detail in the following appendix. The Green function is given by equation (4.2). For using the diagrammatic technique the integral is transformed into Matsubara time  $\tau = it$ . The magnitude of the Jacobi determinate is  $-i$  and the upper limit is changed to  $\beta = T^{-1}$ . Each time derivative is further generated an imaginary unit  $i$ . The Green function is represented in Matsubara time as

$$\mathcal{G}_{\dot{\mathbf{p}}\dot{\mathbf{p}}}(\mathbf{k}, z) = i \int_0^\beta d\tau e^{z\tau} \left\langle \mathcal{T}_\tau \dot{\mathbf{P}}_j(\tau) \dot{\mathbf{P}}_j(0) \right\rangle_{\mathbf{H}}. \quad (\text{D.1})$$

$z$  is a complex frequency and the direction of the momentum is marked by the index  $j = x, y$ . The index  $H$  denotes, that the expectation value is evaluated with respect to Hamiltonian  $\mathbf{H} = \mathbf{H}_\Psi + \mathbf{H}_\Phi + mtH_{\Psi\Phi}$ , where the interaction between fermions and spin fluctuations is considered by the last term. In Matsubara interaction representation, the appearing time evolution operator is expanded up the the zeroth order. As a consequence, corrections of the Green function, caused by the fermion-spin fluctuation interaction, are neglected. Only the two time derivatives of momentum are therefore contained in the expectation value. This is the only origin, where the perturbation of umklapp scattering is considered. The Green function is given by

$$\mathcal{G}_{\dot{\mathbf{p}}\dot{\mathbf{p}}}(\mathbf{k}, z) = i \int_0^\beta d\tau e^{z\tau} \left\langle \mathcal{T}_\tau \dot{\mathbf{P}}_j(\tau) \dot{\mathbf{P}}_j(0) \right\rangle_{\mathbf{H}_0} \quad (\text{D.2})$$

where the expectation value is now evaluated with respect to the free Hamiltonian  $\mathbf{H}_0 = \mathbf{H}_\Psi + \mathbf{H}_\Phi$ . The time derivative of momentum is designated in equation (3.15). Inserting this expression,  $\mathcal{G}_{\dot{\mathbf{p}}\dot{\mathbf{p}}}(\mathbf{k}, z)$  is given by

$$\begin{aligned} \mathcal{G}_{\dot{\mathbf{p}}\dot{\mathbf{p}}}(\mathbf{k}, z) = & -i \sum_{\mu, \lambda} \sum_{\mathbf{G}_1, \mathbf{G}_2} \mathbf{J}_{\mathbf{G}_1} \mathbf{J}_{\mathbf{G}_2} \int_0^\beta d\tau e^{z\tau} \int_{\mathbf{k}_1} \int_{\mathbf{k}_2} G_{1,j} G_{2,j} \\ & \times \left\langle \mathcal{T}_\tau \Phi_\mu(\mathbf{k}_1, \tau) \Phi_\mu(-\mathbf{k}_1 - \mathbf{G}_1, \tau) \Phi_\lambda(\mathbf{k}_2, 0) \Phi_\lambda(-\mathbf{k}_2 - \mathbf{G}_2, 0) \right\rangle_{\mathbf{H}_0}. \end{aligned} \quad (\text{D.3})$$

Here, the moment integrals are extended over the first Brillouin zone, while the sum over  $\mathbf{G}_1$  and  $\mathbf{G}_2$  runs over all reciprocal lattice vectors.  $\mathbf{G}_i$ , where  $i = 1, 2$ , is the coupling parameter with respect to the reciprocal lattice vector. The sum over  $\mu$  and  $\lambda$  runs over the spatial direction of the three component bosonic field, while the direction of  $\mathbf{P}$  is indicated by  $j$ .

Wick's theorem is used to separate the expectation value in terms of free propagators. Three contraction are possible for a an expectation value, including four bosonic, real field operators. One of them is not contributed, since the operators to equal times are contracted. The remaining two diagrams are both bubble diagrams and topological equivalent. The diagram is depicted in figure 4.1.

Acting Wick's theorem in momentum representation, each interchange of the bosonic operators yields a  $\delta$ -distribution, or more presicely, the commutator relation. This signifies the momentum conservation at each vertex. One momentum integral one sum over reciprocal lattice vector and the sum over  $\lambda$  are therefore evaluated directly. The remaining vectors are renamed into  $\mathbf{k}$  and  $\mathbf{G}$  for the momentum and reciprocal lattice vector, respectively.

$$\begin{aligned} \mathcal{G}_{\dot{\mathbf{P}}\dot{\mathbf{P}}}(\mathbf{k}, z) = & -2 \sum_{\mathbf{G}} |\mathbf{J}_{\mathbf{G}}|^2 \int_0^\beta d\tau e^{z\tau} \int_{\mathbf{k}} G_j^2 \\ & \times \langle \mathcal{T}_\tau \Phi_\mu(\mathbf{k}, \tau) \Phi_\mu(-\mathbf{k}, 0) \rangle_{H_0} \langle \mathcal{T}_\tau \Phi_\mu(-\mathbf{k} - \mathbf{G}, \tau) \Phi_\mu(\mathbf{k} + \mathbf{G}, 0) \rangle_{H_0}, \end{aligned} \quad (\text{D.4})$$

The factor of 2 is originated by the sum over both identical diagrams. Furthermore, the relation  $\mathbf{J}_{-\mathbf{G}} = \mathbf{J}_{\mathbf{G}}^*$  is used, where the complex conjugated is denoted by the asterisk. The obtained expectation values are the free spin density propagtors  $\mathcal{D}_\mu^{(0)}(\mathbf{k}, \tau)$ . Both propagators are transformed into Matsubara frequency space, using the transformation rule

$$\mathcal{D}_\mu^{(0)}(\mathbf{k}, \tau) = \frac{1}{\beta} \sum_{\omega_n} e^{-i\omega_n \tau} \mathcal{D}_\mu^{(0)}(\mathbf{k}, i\omega_n) \quad (\text{D.5})$$

where the summation runs over all bosonic Matsubara frequencies  $\omega_n = 2n\pi/\beta$ , where  $n \in \mathbb{Z}$ . The frequency argument of the Green function is set to  $z = i\omega_l$ , since the Green function is now investigated onto the imaginary frequency axis. The exponential functions are generated the only  $\tau$ -dependence and the  $\tau$ -integral is evaluated to  $\beta\delta_{\omega_m+\omega_l-\omega_n}$ . One of the two sums over Matsubara frequencies is evaluated as well. The following expression is obtained:

$$\mathcal{G}_{\dot{\mathbf{P}}\dot{\mathbf{P}}}(\mathbf{k}, i\omega_l) = -2 \sum_{\mathbf{G}} |\mathbf{J}_{\mathbf{G}}|^2 \int_{\mathbf{k}} G_j^2 \frac{1}{\beta} \sum_{\omega_n} \mathcal{D}_\mu(\mathbf{k}, i\omega_n) \mathcal{D}_\mu(-\mathbf{k} - \mathbf{G}, i\omega_l - i\omega_n). \quad (\text{D.6})$$

In the following the Matsubara sum is evaluated. Therefore, the singularities of both propgators are observed. A discontinuity of the propagator, denoted in (3.7), is generated if the term of Matsubara frequencies in the denominator becomes to be zero. This type of singularity is called branch cut, since the whole horizontal line along



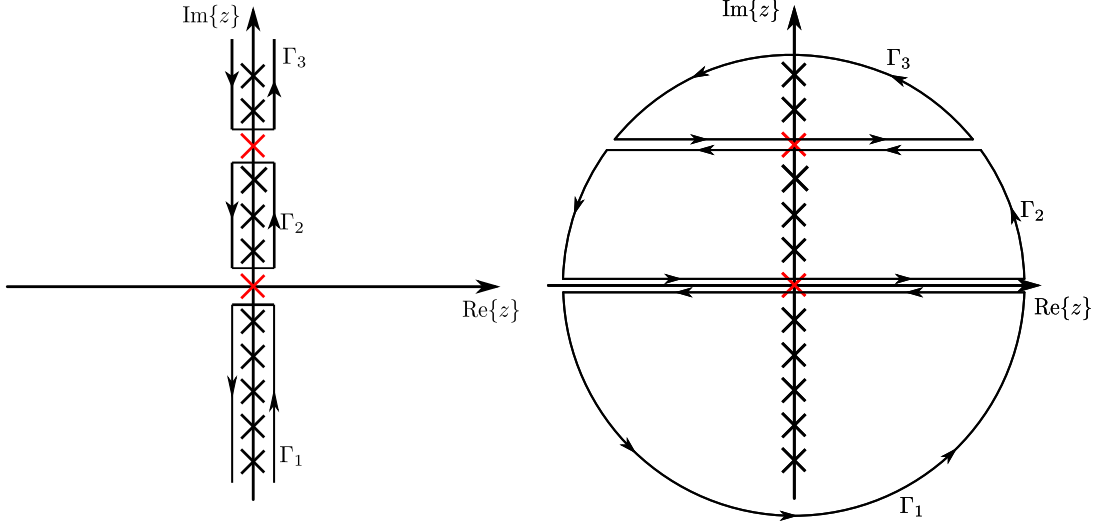


Figure D.1: This figure shows the starting contour of the complex integral appearing at the computation of the Green function  $\mathcal{G}_{\dot{\mathbf{p}}\dot{\mathbf{p}}}$ . The contour is separated into three parts due to the two discontinuities at 0 and  $\omega_l$  (red crosses) of the Green function, reflected as branch cuts in the complex plane. This is depicted on the left hand side. All three contours are expanded to infinity, depicted on the right hand side. The semicircles and the paths between both branches yield no contributions. The remaining paths are four ones, along each side of two branches.

the singularity is forbidden. In the investigated case, two singularity of them arise, where one is sited at  $\omega_n = 0$  and the other one is sited at  $\omega_n = \omega_l$ . To transform the Matsubara sum into a complex contour integral, both singularities are separated from the sum. For reasons of clarity the momentum argument of the second propagator is abbreviated by  $\mathbf{k}' = -\mathbf{k} - \mathbf{K}$  and the momentum arguments are written as a lower index.

$$\begin{aligned}
S(i\omega_l) &:= \frac{1}{\beta} \sum_{\omega_n} \mathcal{D}_{\mu,\mathbf{k}}(i\omega_n) \mathcal{D}_{\mu,\mathbf{k}'}(i\omega_l - i\omega_n) \\
\Leftrightarrow S(i\omega_l) &:= \frac{1}{\beta} \mathcal{D}_{\mu,\mathbf{k}}(0) \mathcal{D}_{\mu,\mathbf{k}'}(i\omega_l) + \frac{1}{\beta} \mathcal{D}_{\mu,\mathbf{k}}(i\omega_l) \mathcal{D}_{\mu,\mathbf{k}'}(0) \\
&\quad + \frac{1}{\beta} \sum_{\substack{n \neq 0 \\ n \neq l}} \mathcal{D}_{\mu,\mathbf{k}}(i\omega_n) \mathcal{D}_{\mu,\mathbf{k}'}(i\omega_l - i\omega_n)
\end{aligned} \tag{D.7}$$

The remaining sum, labeled with  $I_{MS}(\omega_l)$  in the following, is now transformed into a complex contour integral. All Matsubara frequencies are included into the contour  $\Gamma$ , beside the two separated frequencies. Similar to the case of simple poles, see C, the contour runs along the imaginary axis. The contour is closed infinitesimal above

and below the banches, since crossing of the branches is forbidden. The contour  $\Gamma$  is depicted on the left hand side in figure D.1. Since the spin propagators are bosonic, the Bose distribution  $n_B(z)$  is considered, transforming the sum into a contour integral.

$$I_{MS}(\omega_l) := \frac{1}{\beta} \sum_{\substack{n \neq 0 \\ n \neq l}} \mathcal{D}_{\mu, \mathbf{k}}(i\omega_n) \mathcal{D}_{\mu, \mathbf{k}'}(i\omega_l - i\omega_n) = \oint_{\Gamma} \frac{dz}{2\pi i} n_B(z) \mathcal{D}_{\mu, \mathbf{k}}(z) \mathcal{D}_{\mu, \mathbf{k}'}(i\omega_l - z) \quad (\text{D.8})$$

As shown in figure D.1  $\Gamma$  is seperated in three single contours, denoted as  $\Gamma_1$ ,  $\Gamma_2$  and  $\Gamma_3$ . These three contours are expanded to infity where the contour path is never allowed to cross the horizontal line at  $\omega_l$  or 0. The obtained contour is depicted on the right hand side in figure D.1.

The contour  $\Gamma_1$  is taken along the real axis in negative direction and is closed by a semi-circle with infinite radius in the lower complex plane.  $\Gamma_2$  is the contour between both branch cuts. The contour is started along the real axis in positive direction. At infinity the contour is performed up to the branch at  $\omega_n$ . The path is taken in oppsite direction to minus infinity and from there dwon to the starting point. The last contour  $\Gamma_3$  is taken along the  $\omega_n$ -axis in positive direction and is closed by a semi-circle with infinite radius in the upper complex plane. The contours parallel the real and  $\omega_n$ -axis is set infinitesimal beside these axis, which is indicated with the term  $\pm i\eta$ . The sign is chosen according to the corresponding contour.

Each one of these three contour integrals can be splitted in parts, where only the parts parallel to the real axis do not vanish. In all other segments the path is lying in infinity and, since the integrand is decreasing faster than  $1/z$  for  $z \rightarrow \infty$ , these part are zero. Only, the paths survive along the two branch cuts.

$$\begin{aligned} I_{MS}(\omega_l) = & \int_{-\infty}^{\infty} \frac{d\epsilon}{2\pi i} \mathcal{D}_{\mu, \mathbf{k}'}(i\omega_l - \epsilon) \left[ n_B(\epsilon - i\eta) \mathcal{D}_{\mu, \mathbf{k}}(\epsilon - i\eta) - n_B(\epsilon + i\eta) \mathcal{D}_{\mu, \mathbf{k}}(\epsilon + i\eta) \right] \\ & + \int_{-\infty}^{\infty} \frac{d\epsilon}{2\pi i} \mathcal{D}_{\mu, \mathbf{k}}(i\omega_l + \epsilon) \left[ n_B(i\omega_l + \epsilon - i\eta) \mathcal{D}_{\mu, \mathbf{k}'}(\epsilon - i\eta) \right. \\ & \quad \left. - n_B(i\omega_l + \epsilon + i\eta) \mathcal{D}_{\mu, \mathbf{k}'}(\epsilon + i\eta) \right] \end{aligned} \quad (\text{D.9})$$

The limit  $\eta \rightarrow 0^+$  is implied and the symmetry property with respect to the frequency is used. Now, the Bose distribution is simplified. Firstly the relation  $n_B(z + i\omega_l) = n_B(z)$  is used, which follows directly from the definition of the bosonic Matsubara frequencies  $\omega_n = 2n\pi/\beta$ , where  $n \in \mathbb{Z}$ . Inserting them into the Bose distribution, the exponential function is always evaluated to 1, since  $\exp(i2\pi) = 1$ . The Bose distribution is transformed onto the real axis using analytical continuation. The complex frequency  $z$  is expressed as  $\epsilon \pm i\eta$ , where the limit  $\eta \rightarrow 0^+$  is implied. The exponential function in  $n_B(\epsilon \pm i\eta)$  is expanded up the second order, since the first order is

chanceled.

$$n_B(\epsilon \pm i\eta) \approx \frac{\beta^{-1}}{\epsilon \pm i\eta} = \beta^{-1} \left( \text{P.V.} \frac{1}{\epsilon} \mp i\pi\delta(\epsilon) \right) \approx n_B(\epsilon) \mp i\pi\beta^{-1}\delta(\epsilon), \quad (\text{D.10})$$

The last equality is only valid for small frequencies. In equation (D.9), the Matsubara frequencies are eliminated in the argument of both Bose distributions. Both squared brackets under the integral are quite identical, beside the different momentum argument of the propagator. Our next approach is writing the Bose distribution and the propagators into real and imaginary parts. The real part of them are symmetric and the imaginary part of them is antisymmetric with respect to change  $\eta$  to  $-\eta$ . The following expression is obtained for the squared brackets in the first line of (D.9):

$$2i \left[ \text{Re}\{n_B(\epsilon + i\eta)\} \text{Im}\{\mathcal{D}_{\mu,\mathbf{k}}(\epsilon + i\eta)\} + \text{Im}\{n_B(\epsilon + i\eta)\} \text{Re}\{\mathcal{D}_{\mu,\mathbf{k}}(\epsilon + i\eta)\} \right]. \quad (\text{D.11})$$

An analogical expression is obtained for the squared brackets in the second line changing  $\mathbf{k}$  to  $\mathbf{k}'$  and vice versa. The second term of (D.11) is evaluated first. The imaginary part of the Bose distribution is given by equation (D.10). The equivalent procedure is performed for the second bracket in (D.9). Both relations are integrated with respect to  $\epsilon$ . Using relation  $\text{Re}\{\mathcal{D}_{\mu,\mathbf{k}}(0)\} = \mathcal{D}_{\mu,\mathbf{k}}(0)$ , the obtained expression is equivalent to the separated terms in equation (D.7), beside a minus sign.

$$-\frac{1}{\beta} \mathcal{D}_{\mu,\mathbf{k}'}(i\omega_l) \mathcal{D}_{\mu,\mathbf{k}}(0) - \frac{1}{\beta} \mathcal{D}_{\mu,\mathbf{k}}(i\omega_l) \mathcal{D}_{\mu,\mathbf{k}'}(0) \quad (\text{D.12})$$

These both terms are canceled the separated terms in (D.7). The remaining contributions of  $S(i\omega_l)$  are given by the first term of equation (D.11) and the corresponding term for the second squared brackets in (D.9). The real part of the Bose distribution  $n_B(\epsilon + i\eta)$  is the Bose distribution itself (see (D.10)). Since the imaginary part of  $\mathcal{D}_{\mu}$  is independent of the additional part  $i\eta$  the Matsubara sum is given by

$$S(i\omega_l) = \int_{-\infty}^{\infty} \frac{d\epsilon}{\pi} n_B(\epsilon) \left[ \mathcal{D}_{\mu,\mathbf{k}'}(i\omega_l - \epsilon) \text{Im}\{\mathcal{D}_{\mu,\mathbf{k}}(\epsilon)\} + \mathcal{D}_{\mu,\mathbf{k}}(i\omega_l + \epsilon) \text{Im}\{\mathcal{D}_{\mu,\mathbf{k}'}(\epsilon)\} \right] \quad (\text{D.13})$$

$S(i\omega_l)$  is now transformed on the real axis, using analytical continuation,  $i\omega_l = \omega + i\eta =: \tilde{\omega}$ . The Matsubara sum is given by

$$S(\omega) = \int_{-\infty}^{\infty} \frac{d\epsilon}{\pi} n_B(\epsilon) \left[ \mathcal{D}_{\mu,\mathbf{k}'}^*(\epsilon - \omega) \text{Im}\{\mathcal{D}_{\mu,\mathbf{k}}(\epsilon)\} + \mathcal{D}_{\mu,\mathbf{k}}(\epsilon + \omega) \text{Im}\{\mathcal{D}_{\mu,\mathbf{k}'}(\epsilon)\} \right] \quad (\text{D.14})$$

Here, relation  $\mathcal{D}_{\mu,\mathbf{k}'}(\omega - \epsilon) = \mathcal{D}_{\mu,\mathbf{k}'}^*(\epsilon - \omega)$  is used, following from equation (A.27). The frequency argument is shifted from  $\epsilon - \omega$  to  $\epsilon$  in the first term. The imaginary part of the retarded Green function is used in the calculation of the conductivity or resistance.

Considering equation (D.6), the Matsubara sum is the only observed complex quantity. The imaginary part of the Matsubara sum is given by

$$\text{Im}\{S(\omega)\} = \int_{-\infty}^{\infty} \frac{d\epsilon}{\pi} \left[ n_B(\epsilon) - n_B(\epsilon + \omega) \right] \text{Im}\{\mathcal{D}_\mu(-\mathbf{k} - \mathbf{G}, \epsilon)\} \text{Im}\{\mathcal{D}_\mu(\mathbf{k}, \epsilon + \omega)\} \quad (\text{D.15})$$

where  $\text{Im}\{\mathcal{D}^*\} = -\text{Im}\{\mathcal{D}\}$  is used. The imaginary part of the retarded Green function is obtained by inserting the expression for  $\text{Im}\{S(\omega)\}$ .

$$\begin{aligned} \text{Im}\{\mathcal{G}_{\text{PP}}^{\text{ret}}(\omega)\} &= -2 \sum_{\mathbf{G}} |\mathbf{J}_{\mathbf{G}}|^2 \int_{-\infty}^{\infty} \frac{d\epsilon}{\pi} \left[ n_B(\epsilon) - n_B(\epsilon + \omega) \right] \\ &\quad \times \int_{\mathbf{k}} G_j^2 \text{Im}\{\mathcal{D}_\mu(-\mathbf{k} - \mathbf{G}, \epsilon)\} \text{Im}\{\mathcal{D}_\mu(\mathbf{k}, \epsilon + \omega)\}, \end{aligned} \quad (\text{D.16})$$

The imaginary part of the spin propagator is denoted in equation (A.28). Small frequencies  $\omega$  are considered, since our interest is based on the static electrical conductivity. Spin propagators and Bose distributions are investigated separately in this limit. The latter is expanded up to the first order, since the zeroth order vanishes. In the case of spin propagators,  $\omega$  is simply set to zero. The first derivative of the Bose distribution and both spin propagators are even function with respect to  $\epsilon$ . Therefore, the lower boundary of the integral is set to zero and the integral is multiplied by 2. Inserting the explicit expressions for the imaginary parts of the propagators, the imaginary part of the retarded Green function is obtained.

$$\begin{aligned} \text{Im}\{\mathcal{G}_{\text{PP}}^{\text{ret}}(\omega)\} &= -\frac{4\gamma^2\beta\omega}{\pi} \sum_{\mathbf{Q}_1, \mathbf{Q}_2} \sum_{\mathbf{G}} |\mathbf{J}_{\mathbf{G}}|^2 \int_0^{\infty} d\epsilon \frac{\epsilon^2 e^{\beta\epsilon}}{(e^{\beta\epsilon} - 1)^2} \\ &\quad \times \int_{\mathbf{k}} G_j^2 \cdot \frac{1}{(\mathbf{k} + \mathbf{G} - \mathbf{Q}_1)^4 + \gamma^2\epsilon^2} \cdot \frac{1}{(\mathbf{k} + \mathbf{Q}_2)^4 + \gamma^2\epsilon^2} \end{aligned} \quad (\text{D.17})$$

## E Properties of the Kubo Relaxation Function

The Kubo relaxation function

$$\Phi_{AB}(t) = \frac{i}{\hbar} \lim_{s \rightarrow 0} \int_t^\infty d\tau \langle [A_I(\tau), B_I(0)] \rangle_0 e^{-s\tau}. \quad (\text{E.1})$$

is introduced in section 5.1 and the three relations below are still supposed.

$$1. \quad \chi_{AB}(t) = -\Theta(t) \frac{d}{dt} \Phi_{AB}(t) \quad (\text{E.2})$$

$$2. \quad \Phi_{AB}(t=0) = \chi_{AB}(\omega=0) \quad (\text{E.3})$$

$$3. \quad \Phi_{AB}(\omega) = \frac{1}{i\omega} [\chi_{AB}(\omega) - \chi_{AB}(\omega=0)]. \quad (\text{E.4})$$

The evidence of these three relation is proven in this appendix. The Kubo relaxation function is derivated with respect to the time  $t$ . This yields immediatly the first relation, comparing the obtained derivative with the definition of the dynamical susceptibility (5.2).

$$-\Theta(t) \frac{d}{dt} \Phi_{AB}(t) = \frac{i}{\hbar} \Theta(t) \langle [A_I(t), B_I(0)] \rangle_0 = \chi_{AB}(t) \quad (\text{E.5})$$

For the evidence of the second relation, the kubo relaxation function is evaluated for the time  $t=0$ . The limit  $\lim_{\omega \rightarrow 0} \exp(i\omega\tau)$  is inserted and the lower limit of the integral is set to minus infinity, introducing the  $\theta$ -distribution  $\theta(\tau)$ . In the last step equation (E.5) and the Laplace transformation are used.

$$\begin{aligned} \Phi_{AB}(t=0) &= \frac{i}{\hbar} \lim_{s \rightarrow 0} \int_0^\infty d\tau \langle [A_I(\tau), B_I(0)] \rangle_0 e^{-s\tau} \\ \Leftrightarrow \Phi_{AB}(t=0) &= \frac{i}{\hbar} \lim_{\substack{s \rightarrow 0 \\ \omega \rightarrow 0}} \int_{-\infty}^\infty d\tau \Theta(\tau) \langle [A_I(\tau), B_I(0)] \rangle_0 e^{i\omega\tau} e^{-s\tau} \\ \Leftrightarrow \Phi_{AB}(t=0) &= \lim_{\omega \rightarrow 0} \int_{-\infty}^\infty d\tau \chi_{AB}(\tau) e^{i\omega\tau} = \chi_{AB}(\omega=0) \end{aligned} \quad (\text{E.6})$$

## *E Properties of the Kubo Relaxation Function*

Furthermore, the susceptibility is assumed to be good function in the sence of convergence and the limit respective to  $s$  is hence taken with no doubt. The thrird relation follows in combination of the first and second relation Relation one is multiplied by  $\exp(i\omega t)$  and is intgrated with respect to time  $t$  from 0 to  $\infty$ . The definition of the Laplace transformation and integration by parts is used on the left and right hand side, respectively.

$$\begin{aligned}
 \int_0^{\infty} dt \chi_{AB}(t) e^{i\omega t} &= - \int_0^{\infty} dt e^{i\omega t} \frac{d}{dt} \Phi_{AB}(t) \\
 \stackrel{\text{PI}}{\Leftrightarrow} \chi_{AB}(\omega) &= -e^{i\omega t} \Phi_{AB}(t) \Big|_0^{\infty} + i\omega \int_0^{\infty} dt e^{i\omega t} \Phi_{AB}(t) \\
 \Leftrightarrow \Phi_{AB}(\omega) &= \frac{1}{i\omega} [\chi_{AB}(\omega) - \chi_{AB}(\omega = 0)] \tag{E.7}
 \end{aligned}$$

## Todo list

right or wrong? . . . . . 18





# Bibliography

- [Dru00] P. Drude. „Zur Elektronentheorie der Metalle“. In: *Annalen der Physik* 306.3 (1900), pp. 566–613. DOI: [10.1002/andp.19003060312](https://doi.org/10.1002/andp.19003060312).
- [BF10] H. Bruus and K. Flensberg. *Many-body quantum theory in condensed matter physics: an introduction*. Repr. Oxford Univ. Press, 2010. ISBN: 978-0-19-856633-5.
- [Bab37] W. G. Baber. „The Contribution to the Electrical Resistance of Metals from Collisions between Electrons“. In: *Proceedings of the Royal Society of London. Series A, Mathematical and Physical Sciences* 158.894 (1937), pp. 383–396. ISSN: 00804630. URL: <http://www.jstor.org/stable/96825>.
- [PYM12] H. K. Pal, V. I. Yudson, and D. L. Maslov. „Resistivity of non-Galilean-invariant Fermi- and non-Fermi liquids“. In: *Lithuanian Journal of Physics and Technical Sciences* 52 (2012), pp. 142–164. DOI: [10.3952/lithjphys.52207](https://doi.org/10.3952/lithjphys.52207). arXiv: [1204.3591](https://arxiv.org/abs/1204.3591) [cond-mat.str-el].
- [Alt+80] B. L. Altshuler et al. „Magnetoresistance and Hall effect in a disordered two-dimensional electron gas“. In: *Phys. Rev. B* 22 (11 Dec. 1980), pp. 5142–5153. DOI: [10.1103/PhysRevB.22.5142](https://doi.org/10.1103/PhysRevB.22.5142).
- [Kon64] J. Kondo. „Resistance Minimum in Dilute Magnetic Alloys“. In: *Progress of Theoretical Physics* 32.1 (1964), pp. 37–49. DOI: [10.1143/PTP.32.37](https://doi.org/10.1143/PTP.32.37). URL: <http://dx.doi.org/10.1143/PTP.32.37>.
- [KG01] L. Kouwenhoven and L. Glazman. „Revival of the Kondo effect“. In: *eprint arXiv:cond-mat/0104100* (Apr. 2001). eprint: [cond-mat/0104100](https://arxiv.org/abs/cond-mat/0104100).
- [Löh+07] H. v. Löhneysen et al. „Fermi-liquid instabilities at magnetic quantum phase transitions“. In: *Rev. Mod. Phys.* 79 (3 Aug. 2007), pp. 1015–1075. DOI: [10.1103/RevModPhys.79.1015](https://doi.org/10.1103/RevModPhys.79.1015). URL: <https://link.aps.org/doi/10.1103/RevModPhys.79.1015>.
- [Mor65] H. Mori. „Transport, Collective Motion, and Brownian Motion“. In: *Progress of Theoretical Physics* 33.3 (1965), pp. 423–455. DOI: [10.1143/PTP.33.423](https://doi.org/10.1143/PTP.33.423).
- [Czy17] G. Czycholl. *Theoretische Festkörperphysik Band 2 : Anwendungen: Nichtgleichgewicht, Verhalten in äußeren Feldern, kollektive Phänomene*. 4. Aufl. 2017. SpringerLink : Bücher, 2017. ISBN: 978-3-662-53701-5.
- [GM14] R. Gross and A. Marx. *Festkörperphysik*. 2., aktualisierte Aufl. De Gruyter Oldenbourg, 2014. ISBN: 978-3-11-035870-4; 978-3-11-039687-4.

- [ACS03] A. Abanov, A. V. Chubukov, and J. Schmalian. „Quantum-Critical Theory of the Spin-Fermion Model and its Application to Cuprates: Normal State Analysis“. In: *Advances in Physics* 52.3 (2003), pp. 119–218. DOI: [10.1080/0001873021000057123](https://doi.org/10.1080/0001873021000057123).
- [Sac11] S. Sachdev. *Quantum phase transitions*. 2. ed., 1. publ. Cambridge Univ. Press, 2011. ISBN: 978-0-521-51468-2; 0-521-51468-1.
- [PS14] A. A. Patel and S. Sachdev. „DC Resistivity at the Onset of Spin Density Wave Order in Two-Dimensional Metals“. In: *Phys. Rev. B* 90 (16 2014), p. 165146. DOI: [10.1103/PhysRevB.90.165146](https://doi.org/10.1103/PhysRevB.90.165146).
- [Wei15] P. Weiß. „Interference of quantum critical excitations and soft diffusive modes in a disordered antiferromagnetic metal“. masterthesis. Karlsruhe institut of technology (KIT), 2015.
- [Ili02] B. Z. Iliev. „On the Action Principle in Quantum Field Theory“. In: *ArXiv High Energy Physics - Theory e-prints* (2002). URL: [arXiv:hep-th/0204003](https://arxiv.org/abs/hep-th/0204003).
- [For90] D. Forster. *Hydrodynamic, Fluctuations, Broken Symmetry, and Correlation Functions*. 1990.
- [Sch08] F. Schwabl. *Advanced Quantum Mechanics*. 4. ed. 2008.
- [Sch06] F. Schwabl. *Statistische Mechanik*. 3., aktualisierte Aufl. 2006.
- [Aud05] J. Audretsch. *Verschränkte Systeme: die Quantenphysik auf neuen Wegen*. Wiley-VCH, 2005. ISBN: 3-527-40452-X; 978-3-527-40452-0978-325-40452-0.
- [Jun07] P. Jung. „Transport and Approximate Conservation Laws in Low Dimensional Systems“. dissertation. Universität zu Kön, 2007.
- [EG79] K. Elk and W. Gasser. *Die Methode der Greenschen Funktionen in der Festkörperphysik*. Akademie-Verl., 1979.
- [Nol09] W. Nolting. *Fundamentals of many-body physics : principles and methods*. Springer, 2009. ISBN: 978-3-540-71930-4.